



NTNU – Trondheim
Norwegian University of
Science and Technology

Producing Gas-Oil Ratio Performance of Conventional and Unconventional Reservoirs

Guowen Lei

Petroleum Engineering

Submission date: June 2012

Supervisor: Curtis Hays Whitson, IPT

Norwegian University of Science and Technology

Department of Petroleum Engineering and Applied Geophysics

Abstract

This study presents a detailed analysis of producing gas-oil ratio performance characteristics from conventional reservoir to unconventional reservoir. Numerical simulations of various reservoir fluid systems are included for comparison.

In a wide sense of the word, the term of unconventional reservoir is including tight gas sand, coal bed methane, gas hydrate deposits, heavy oil gas shale and etc. In this study we specify the unconventional reservoir to only mean the low and ultra low permeability reservoir, which is including tight or shale reservoir. As an emerging research topic in the E&P industry, shale reservoir's long-term well performance characteristics are generally not well understood (Anderson et al. 2010). Research methods and techniques for conventional reservoir are usually directly used in this unconventional reservoir analysis. These methods, however, have proven to be too pessimistic (Anderson et al., 2010). Fit-for-purpose approaches or solutions should be introduced in this new topic. Recently, hydraulic fracturing treatment is commonly used in the low matrix permeability reservoir to attain an economic production rate. The difference of well production performance between conventional reservoir and unconventional reservoir is not well known. In this study, we are trying to give a quantitative analysis in order to answer this question.

In this study, a "generic" reservoir from field data with constant reserves and size were assumed. This reservoir model is homogeneous and of constant porosity, permeability and initial water saturation. In order to compare the production performance, fluid systems are varied from volatile oil to near critical oil, to gas condensate and to wet gas. The permeability of the reservoir model is also designed from high (conventional reservoir) to ultra low (unconventional), which ranges from 10^1 to 10^{-5} mD. Influence from fracture is especially considered because fractures in the low permeability reservoir provide a high conductivity that connects the reservoir matrix to the horizontal well. Fractures in the model are designed with identical

geometrical characteristics (length, thickness) and of inner homogeneous properties (porosity, permeability).

A black-oil model is used for each reservoir, and its PVT properties are generated with a 31 components EOS model using Whitson-Torp procedure (Whitson et al., 1983). Reservoir fluid systems equilibrium calculation in the black-oil model is done using the initial gas-oil ratio. We have compared the well's production performance for each fluid system.

Based on the industry experience, two standards are used in reservoir simulation control: gas production rate and cumulative revenue. The gas production rate with 10×10^6 ft³/day in the first 10 days or the cumulative revenue equal to 5×10^5 USD from the first 10 days is set as the standard for the commercial well rate. All of these simulations are run under the control of these two types which have just been mentioned.

A case of liquid rich gas reservoir is analyzed systematically, to compare its production performance when reservoir permeability is changed from high to low. We are interested in how much oil or gas condensate can be extracted from the "reservoir" if same initial fluids in the reservoir but of a different permeability. This study is useful and practical, particularly for the industry in the era of "high" oil price and "low" gas price in North America.

The simulation results show that we can extract more liquid from the reservoir if the matrix permeability is higher, particularly for the reservoir with initially large oil contents (volatile oil reservoir, near critical reservoir and gas condensate reservoir). Fracturing treatment in unconventional reservoir is required to attain an economic production rate. We also realize that for the required number of fractures and reservoir's matrix permeability, there exists linear correlation in log-log plot in the low-permeability reservoir.

In this study, the unique optimization software *Pipe-It* and reservoir simulator *SENSOR* are used. Optimal simulation results of permeability combination are obtained by the module *Optimizer* in *Pipe-It*.

Acknowledgement

I want to thank my supervisor: Professor Curtis Hays Whitson. Thanks to him for giving me the chance to work with him from the beginning of 2011. His excellent academic and professional guidance lead me to start working as an engineer. It was my great honour to work with him and his group.

I also would like to thank Dr. Nan Cheng at Statoil Research Centre in Trondheim. He, together with Curtis, introduced this interesting topic to me. And the comments and advice from him always gave new ideas in my thesis. I greatly enjoyed discussing with him.

Thanks to the staff from *PERA* and *PETROSTREAMZ*: Dr. Mohammad Faizul Hoda, Dr. Kameshwar Singh, Snjezana Sunjerga, Dr. Aleksander Juell, Oleksandr Iakovliev, Hans Jørgen Grimstad and Dr. Silvyia Dewi Rahmawati. Thank you for helping me on the software usage and studies; they always give me support on my thesis.

Sincere thanks to all staff in the Department of Petroleum Engineering and Applied Geophysics. I appreciate all the helps from them.

Finally, I would like to thank my dear wife Wei Huang whom is still waiting for me in China. Without her understanding, it would not have been possible for me to accomplish this.

Trondheim, June, 2012

Guowen Lei

Table of Contents

| | |
|---|-----------|
| Abstract..... | I |
| Acknowledgment..... | III |
| Table of Contents..... | V |
| List Of Tables..... | VII |
| List Of Figures..... | IX |
| List Of Symbols..... | XIII |
| Chapter 1—Introduction..... | 1 |
| Chapter 2—Simulation Model Description | 5 |
| 1. 1 Simulation Area | 5 |
| 1. 2 Simulation Gridding System..... | 6 |
| 1. 3 Reservoir Properties..... | 9 |
| 1. 4 Fluid Properties..... | 9 |
| 1. 5 Relative Permeability Model | 13 |
| 1. 6 Simulation Constraints..... | 13 |
| 1. 7 Simulation Cases Definition | 14 |
| Chapter 3—Gas Production Control | 17 |
| 2. 1 Cases Of $GOR_i=1,000$ Scf/STB..... | 18 |
| 2. 2 Cases Of $GOR_i=3,000$ Scf/STB..... | 21 |
| 2. 3 Cases Of $GOR_i=4,587$ Scf/STB..... | 23 |
| 2. 4 Cases Of $GOR_i=10,000$ Scf/STB..... | 26 |
| 2. 5 Gas Production Control Summary | 28 |
| Chapter 4—Revenue Control..... | 31 |
| 3. 1 Cases Of $GOR_i=1,000$ Scf/STB..... | 32 |
| 3. 2 Cases Of $GOR_i=3,000$ Scf/STB..... | 36 |
| 3. 3 Cases Of $GOR_i=4,587$ Scf/STB..... | 39 |

| | |
|---|-----------|
| 3. 4 Cases Of $GOR_i=10,000$ Scf/STB..... | 43 |
| 3. 5 Cases Of $GOR_i=100,000$ Scf/STB..... | 46 |
| 3. 6 Revenue Control Summary..... | 50 |
| Chapter 5—Fractures Number And Reservoir Permeability Relation | 53 |
| 4. 1 Gas Rate Control..... | 53 |
| 4. 2 Revenue Control | 55 |
| Chapter 6—Production Performance Trends Study | 59 |
| Chapter 7—Conclusion..... | 65 |
| References..... | 67 |
| Appendix A—SENSOR Input Deck..... | 69 |
| Appendix B—Simulation Oscillation Problem Analysis | 75 |

List of Tables

| | |
|--|----|
| Table 2.1—Reservoir properties | 9 |
| Table 2.2—Reference fluid sample contains | 11 |
| Table 2.3—Parameters of the 31-component SRK EOS model | 12 |
| Table 2.4—Simulation cases list..... | 15 |
| Table 3.1—Simulation model size of different..... | 17 |
| Table 3.2—Simulation optimal results by gas rate control, $GOR_i=1,000$ scf/STB | 19 |
| Table 3.3—Simulation optimal results by gas rate control, $GOR_i=3,000$ scf/STB | 21 |
| Table 3.4—Simulation optimal results by gas rate control, $GOR_i=4,587$ scf/STB | 24 |
| Table 3.5—Simulation optimal results by gas rate control, $GOR_i=10,000$ scf/STB | 26 |
| Table 4.1—Revenue calculation assumption..... | 31 |
| Table 4.2—Simulation optimal results by revenue control, $GOR_i=1,000$ scf/STB..... | 32 |
| Table 4.3—Simulation optimal results by revenue control, $GOR_i=3,000$ scf/STB..... | 36 |
| Table 4.4—Simulation optimal results by revenue control, $GOR_i=4,587$ scf/STB..... | 40 |
| Table 4.5—Simulation optimal results by revenue control, $GOR_i=10,000$ scf/STB..... | 43 |
| Table 4.6—Simulation optimal results by revenue control, $GOR_i=100,000$ scf/STB..... | 47 |
| Table 5.1—Relation between fractures number and reservoir permeability by gas rate control, $k_f=100,000$ mD | 53 |
| Table 5.2—Calculation results of fractures number request by generated equation, gas rate control | 55 |
| Table 5.3—Relation between fractures number and reservoir permeability by revenue control, $k_f=100,000$ mD | 55 |
| Table 5.4—Calculation results of fractures number request by generated equation, revenue control..... | 57 |
| Table 6.1—Simulation optimal results of case, $GOR_i=4,587$ scf/STB | 60 |

List of Figures

| | |
|---|----|
| Fig. 2.1—Illustration of the planar model simulation segment and its relation to the number of fractures, 1: background area; 2: fracture perpendicular area | 6 |
| Fig. 2.2—Reservoir model grid system of one fracture shale reservoir, the area of simulation segment in model is 320 acres, 5,280 ft×2,640 ft, and half length of hydraulic fracture is 200 ft..... | 8 |
| Fig. 2.3—The area of pressure depletion in one fracture reservoir model after 10 days of production, the red colour indicates the initial reservoir pressure: 4,800 psia. | 8 |
| Fig. 2.4—Solution oil/gas ratios for reservoir oils, $1/R_s$ and inverse solution gas/oil ratio for reservoir gases, r_s as a function of pressure. | 12 |
| Fig. 2.5—Gas-oil relative permeability curves used in simulations..... | 13 |
| Fig. 2.6—Simulation cases definition with different reservoir permeability combinations in specified initial gas-oil ratio (gor_i) in simulator..... | 15 |
| Fig. 3.1—Simulation well gas production profile of 7 cases, $GOR_i=1,000$ scf/STB. . | 19 |
| Fig. 3.2—Reservoir model producing gas-oil ratio profile of 7 cases, $GOR_i=1,000$ scf/STB. | 20 |
| Fig. 3.3—Reservoir model producing oil-gas ratio profile of 7 cases,..... | 20 |
| Fig. 3.4—Simulation well gas production profile of 7 cases, $GOR_i=3,000$ scf/STB. . | 22 |
| Fig. 3.5—Reservoir model producing gas-oil ratio profile of 7 cases,..... | 22 |
| Fig. 3.6—Reservoir model producing oil-gas ratio profile of 7 cases,..... | 23 |
| Fig. 3.7—Simulation well gas production profile of 7 cases, $GOR_i=4,587$ scf/STB. . | 24 |
| Fig. 3.8—Reservoir model producing gas-oil ratio profile of 7 cases,..... | 25 |
| Fig. 3.9—Reservoir model producing oil-gas ratio profile of 7 cases,..... | 25 |
| Fig. 3.10—Simulation well gas production profile of 7 cases,..... | 27 |
| Fig. 3.11—Reservoir model producing gas-oil ratio profile of 7 cases,..... | 27 |
| Fig. 3.12—Reservoir model producing oil-gas ratio profile of 7 cases, $r_s=100$ stb/MMcf ($GOR_i=10,000$ scf/STB). | 28 |
| Fig. 3.13—Relation between gor_i and reservoir permeability of critical case, no fracture is required and uniform permeability in reservoir | 29 |
| Fig. 4.1—Simulation well cumulative revenue of 50 years production of 7 cases, $GOR_i=1,000$ scf/STB. | 33 |
| Fig. 4.2—Simulation well oil production profile of 7 cases by total revenue control, $GOR_i=1,000$ scf/STB. | 34 |

| | |
|---|----|
| Fig. 4.3—Simulation well gas production profile of 7 cases by total revenue control, $GOR_i=1,000$ scf/STB..... | 34 |
| Fig. 4.4—Reservoir model producing gas-oil ratio profile of 7 cases by total revenue control, $GOR_i=1,000$ scf/STB..... | 35 |
| Fig. 4.5—Reservoir model producing oil-gas ratio profile of 7 cases by total revenue control, $r_s=1000$ STB/MMcf ($GOR_i=1,000$ scf/STB)..... | 35 |
| Fig. 4.6—Simulation well cumulative revenue of 50 years production of 7 cases, $GOR_i=3,000$ scf/STB..... | 37 |
| Fig. 4.7—Simulation well oil production profile of 7 cases by total revenue control, $GOR_i=3,000$ scf/STB..... | 37 |
| Fig. 4.8—Simulation well gas production profile of 7 cases by total revenue control, $GOR_i=3,000$ scf/STB..... | 38 |
| Fig. 4.9—Reservoir model producing gas-oil ratio profile of 7 cases by total revenue control, $GOR_i=3,000$ scf/STB..... | 38 |
| Fig. 4.10—Reservoir model producing oil-gas ratio profile of 7 cases by total revenue control, $r_s=333$ STB/MMcf ($GOR_i=3,000$ scf/STB)..... | 39 |
| Fig. 4.11—Simulation well cumulative revenue of 50 years production of 7 cases, $GOR_i=4,587$ scf/STB..... | 40 |
| Fig. 4.12—Simulation well oil production profile of 7 cases by total revenue control, $GOR_i=4,587$ scf/STB..... | 41 |
| Fig. 4.13—Simulation well gas production profile of 7 cases by total revenue control, $GOR_i=4,587$ scf/STB..... | 41 |
| Fig. 4.14—Reservoir model producing gas-oil ratio profile of 7 cases by total revenue control, $GOR_i=4,587$ scf/STB..... | 42 |
| Fig. 4.15—Reservoir model producing oil-gas ratio profile of 7 cases by total revenue control, $r_s=218$ STB/MMcf($GOR_i=4,587$ scf/STB)..... | 42 |
| Fig. 4.16—Simulation well cumulative revenue of 50 years production of 7 cases, $GOR_i=10,000$ scf/STB..... | 44 |
| Fig. 4.17—Simulation well oil production profile of 7 cases by total revenue control, $GOR_i=10,000$ scf/STB..... | 44 |
| Fig. 4.18—Simulation well gas production profile of 7 case by total revenue control, $GOR_i=10,000$ scf/STB..... | 45 |
| Fig. 4.19—Reservoir model producing oil-gas ratio profile of 7 cases by total revenue control, $GOR_i=10,000$ scf/STB..... | 45 |
| Fig. 4.20—Reservoir model producing oil-gas ratio profile of 7 cases by total revenue control, $r_s=100$ STB/MMcf($GOR_i=10,000$ scf/STB)..... | 46 |
| Fig. 4.21—Simulation well cumulative revenue of 50 years production of 7 cases, $GOR_i=100,000$ scf/STB..... | 47 |
| Fig. 4.22—Simulation well oil production profile of 7 cases by total revenue control, $GOR_i=100,000$ scf/STB..... | 48 |

| | |
|---|----|
| Fig. 4.23—Simulation well gas production profile of 7 cases by total revenue control, $GOR_i=100,000$ scf/STB. | 48 |
| Fig. 4.24—Reservoir model producing gas-oil ratio profile of 7 cases by total revenue control, $GOR_i=100,000$ scf/STB. | 49 |
| Fig. 4.25—Reservoir model producing oil-gas ratio profile of 7 cases by total revenue control, $r_s=21,135$ STB/MMcf($GOR_i=100,000$ scf/STB). | 49 |
| Fig. 4.26—Relation between reservoir permeability and initial gas-oil ratio, cases controlled by total revenue. | 50 |
| Fig. 4.27—Oil contribution to total revenue of the first 10 days in different initial gas-oil ratio. | 51 |
| Fig. 5.1—Plot of fractures number in the function of reservoir matrix permeability, gas production control. | 54 |
| Fig. 5.2—Plot of fractures number in the function of reservoir matrix permeability, total revenue control. | 56 |
| Fig. 5.3—Plot of fractures number and reservoir permeability when the fracture permeability fix to 100,000 md and cumulative revenue of 5×10^5 USD. | 57 |
| Fig. 6.1—Producing oil-gas ratio versus time, $r_s= 218$ STB/MMcf ($GOR_i=4,587$ scf/STB). | 61 |
| Fig. 6.2—Producing oil-gas ratio versus reservoir average pressure, $r_s= 218$ STB/MMcf ($GOR_i=4,587$ scf/STB). | 62 |
| Fig. 6.3— r_s/r_p versus reservoir matrix permeability, and reservoir classification. | 63 |

List of Symbols

| | | |
|--------------------|---|---|
| Δx_i | = | Grid size of i grid in x direction, Cartesian grid system |
| Δy_i | = | Grid size of i grid in y direction, Cartesian grid system |
| Δz_i | = | Grid size of i grid in z direction, Cartesian grid system |
| x_e | = | Model size in x direction, Cartesian grid system |
| y_e | = | Model size in y direction, Cartesian grid system |
| y_f | = | Half length or wing of hydraulic fracture, ft |
| ε_x | = | logarithmic spacing grids ratio in x direction |
| ε_{yf} | = | logarithmic spacing grids ratio in fracture perpendicular area, y direction |
| ε_{yb} | = | logarithmic spacing grids ratio in background area, y direction |
| N_x | = | Grids number in model's x direction, Cartesian grid system |
| N_{yf} | = | Grids number in model's y direction of fracture perpendicular part |
| N_{yb} | = | Grids number in model's y direction of background area |
| N_f | = | Fractures number along horizontal well |
| h | = | Thickness of simulation model, ft |
| w_f | = | Width of fracture, ft |
| k_m | = | Reservoir matrix permeability, mD |
| k_f | = | Fracture permeability, mD |
| GOR | = | Gas-oil-ratio, scf/STB |
| GOR_i | = | Initial gas-oil-ratio, scf/STB |
| q_o | = | Well oil production, STB |
| q_g | = | Well gas production, Mscf |
| P_o | = | Price of oil product, USD/STB |
| P_g | = | Price of gas product, USD/Mscf |
| G | = | Fracture geometry factor |
| Con | = | Simulation constraint, either gas rate or total revenue |
| R_p | = | Producing gas-oil ratio, scf/STB |
| r_p | = | Producing oil-gas ratio, STB/MMcf |
| r_s | = | Initial oil-gas ratio in reservoir, STB/MMcf |
| PVT | = | Pressure/Volume/Temperature |
| BHP | = | Bottom-hole flowing pressure |
| USD | = | United states dollar |

Chapter 1

Introduction

Shale-gas reservoir has become an important part in North American gas supply and its development has opened a new era of oil and gas production worldwide (Fazlipour, 2010; Cipolla et al, 2009). The technology of hydraulic fracturing treatment is widely used in the development of unconventional reservoir (extremely low permeability reservoir), particularly for tight gas and shale gas reservoir (Ghassemi et al, 2011). Hydraulic fracturing treatment stimulates the extremely low-permeability reservoir and connects the matrix to the wellbore, helping the well to attain a commercial production rate (Cipolla et al, 2009). As a new emerging type of reservoir, we still do not fully understand its performance characteristics compared to the performance characteristics of a conventional reservoir. This study is interested in the comparison of the production performance between these two, or the gradually variation trends from high-permeability reservoirs to ultra low-permeability reservoirs.

Numerical simulation is a versatile tool for this study, and all conclusions are based on the simulation results. A “Generic” reservoir of homogenous properties was designed, and an identical number of cells are applied in all simulation segments. In order to meet the constraint in the simulator, the fracture with high conductivity is designed in the low permeability reservoir as a positive factor. The fracture is also used in the high-permeability reservoir to limit well’s production. The geometry of fracture is the same and with inner identical properties. Based on a uniform production rate or revenue of the first 10 days, production performance is compared among reservoirs with different permeability.

This study also shows that more fractures are required to obtain a commercial production rate if reservoir permeability is reduced. There is a linear correlation between the number of fractures and matrix permeability in the log-log plot. The equation can be generated for different reservoir fluid systems if the fracture geometry, fracture’s conductivity and simulation controls have been specified before.

Section 1 outlines the description of the reservoir simulation model, including all parts of simulation input: grid system, rock and fluid properties, equilibrium initialization and simulation constraints. Only half of the entire fracture drainage space is used as simulation model in order to reduce the simulation CPU-time of computer. It also describes the various reservoir fluid systems which are used in this study.

Section 2 presents the simulation results under gas production control. The daily gas production: $10 \times 10^6 \text{ ft}^3$ in the first 10 days is used to control the well production in all simulation cases. The comparison is based on each reservoir fluid system. Production performances of daily gas rate, ratio of gas-oil and oil-gas are compared for the reservoir with different permeability.

Section 3 shows the simulation results under revenue control. The revenue from the production of gas and oil is added to meet the limitation of 5×10^5 USD of the first 10 days. The comparison is based on different reservoir fluid system: from volatile oil to critical fluid, to gas condensate and to wet gas. Production performances of daily gas and oil rate are compared for the reservoir with different permeability. And the comparison of producing ratios of gas-oil and oil-gas is also addressed in this section.

Section 4 mainly introduces the relation between the number of fractures and the reservoir matrix permeability, which is under gas rate control or revenue control. A general equation was obtained, and can be used in the calculation of the number of fractures. But this equation is imperfect and relies on the simulation results. Furthermore, the required number of fractures in shale reservoir is calculated by using the generated equation. The calculated value depends on the standard of commercial well.

Section 5 presents the variation trends of producing oil-gas ratio for a liquid rich reservoir ($\text{GOR}_i=4,587 \text{ scf/STB}$). Based on the assumption that the reservoir has the same initial fluids underground and geometry size, the reservoir is developed by pressure depletion. Cumulative revenue in the first 10 days equal to 5×10^5 USD is used to control the reservoir simulation. The producing oil-gas ratio is compared from conventional reservoir to unconventional reservoir. Simulation results indicate that production from the same 'reservoir' will vary with reservoir matrix permeability. High permeability reservoir will produce more liquid products (oil, condensate), while

low permeability reservoir will produce less. This is important when oil is more profitable compared to gas.

Chapter 2

Simulation Model Description

In this part, the simulation model is described and all simulation input sections are included: simulation area, grid system/structure, PVT model/Fluid model, rock properties and well constraint.

2.1 Simulation Area

First, the area of interest in the simulation or the definition of a proper reservoir model is described. A planar model, the simplest reservoir model for a horizontal well with fractures, is used in this study. The fracture system is assumed to be created solely by hydraulic fracturing, giving pure planar fractures (Knudsen, 2011). We also suppose that the reservoir is homogeneous and of constant matrix permeability, porosity and initial water saturation. The model is fixed to 1 mile \times 1 mile (640 acres) in planar spacing area and 200 ft in thickness. One horizontal well with one or more than one fracture is designed as producer in the fixed area, and hydraulic fracturing treatment will be used if the reservoir permeability is low. Required numbers of fracture in the reservoir will vary if the reservoir's matrix permeability is changed. In geometry, the fracture is perpendicular to the horizontal wellbore and penetrates 200 ft to each side from the wellbore.

The simulation model is homogeneous and symmetrical, indicating that it is possible to simulate half of the indicated grid. In this study, simulation segment is half of the entire fracture's drainage area. The area of simulation segment is designed to decrease if more fractures go perpendicular on the horizontal well. For example, in single fracture model, only half of the spacing area is used in the simulation model, which is 320 acres. If fractures number increased to 2, the area of simulation segment reduces

to one quarter of the entire spacing area, which is 160 acres. The simulate segment and its relation with the number of fractures is shown in **Fig. 2.1**.

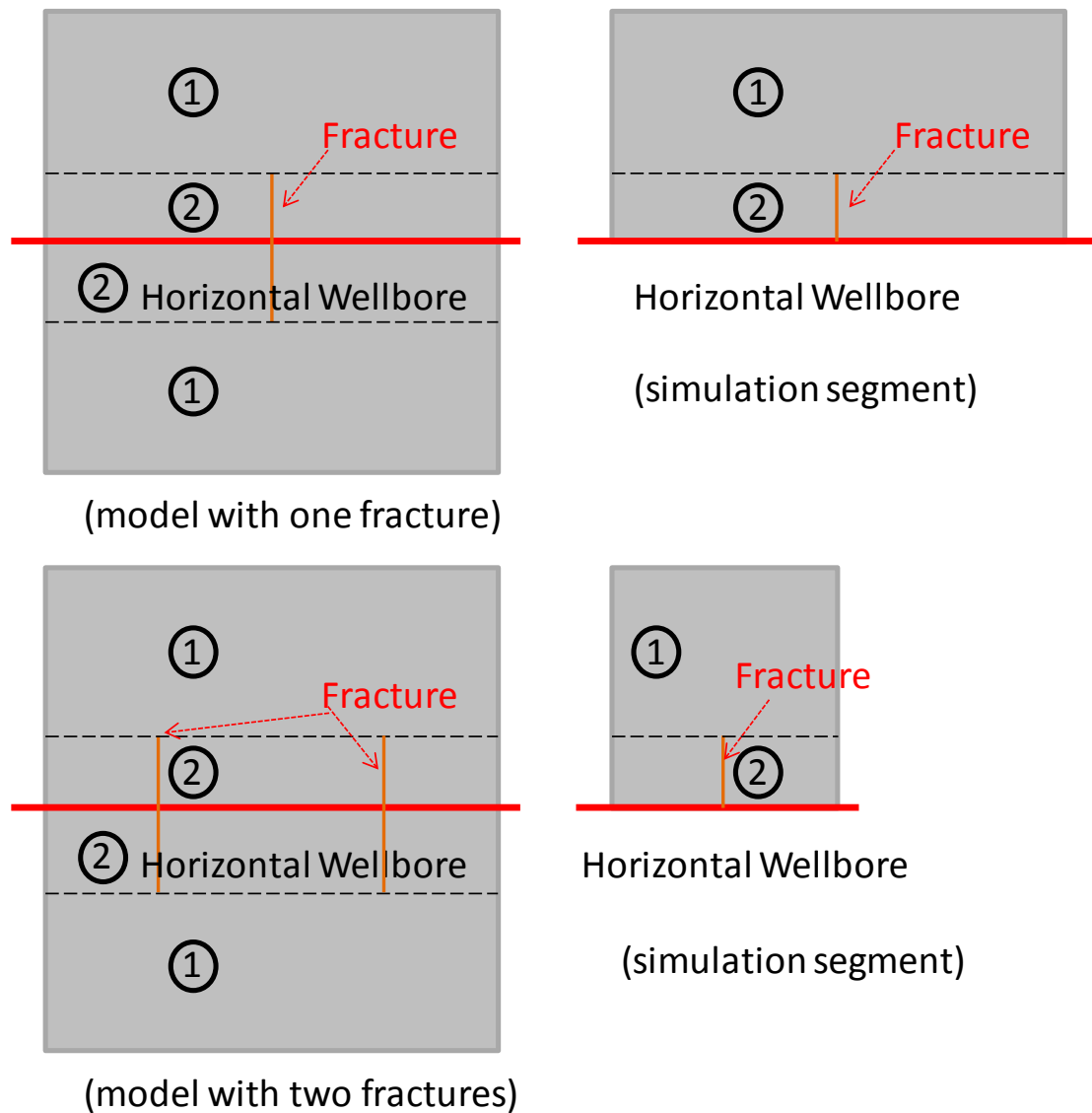


Fig. 2.1—Illustration of the planar model simulation segment and its relation to the number of fractures, 1: Background area; 2: Fracture perpendicular area

2.2 Simulation Gridding System

Cartesian grid geometry is used in this study. Multistage hydraulic-fracturing treatment creates a complex fracture grid structure. Unlike a common conventional gridding system of the same grid size in the whole simulation model, a fit-for-purpose grids geometry is introduced in this study. The new gridding structure is developed to reflect the shale gas reservoir production mechanism. Its typical feature is that the

sizes of the grids gradually grow as well as the model's length in x direction is increased at the same time.

The simulation grid system of one fracture reservoir model is shown in **Fig. 2.2**. In x direction, the smallest cell is close to the fracture and the sizes of grids increase as their distance from the fracture increases, too. In y direction, the smallest grids are the grids nearby fracture tip¹ and the sizes of grids increasing either toward or away from the well bore in y direction. The grids number is constant of 81×74×1 with one layer in vertical direction. The grids in y direction are fixed to 20 (N_{yf}) in the fracture perpendicular area and 54 (N_{yb}) in the background area. The number of grids in x direction is 81, including 1 grid representing the fracture. The total number of the grids in the simulation model is 5,994. The block size of both grids in x direction and in y direction follows the logarithm scale spacing rule (Eq. 2.1—2.3):

$$\varepsilon_x = \frac{\Delta x_{i+1}}{\Delta x_i} = \left(\frac{x_e/2}{\Delta x_1} \right)^{(2/N_x)} \quad (2.1)$$

$$\varepsilon_{yf} = \frac{\Delta y_{fi+1}}{\Delta y_{fi}} = \left(\frac{y_f}{\Delta y_{f1}} \right)^{(1/N_{yf})} \quad (2.2)$$

$$\varepsilon_{yb} = \frac{\Delta y_{bi+1}}{\Delta y_{bi}} = \left(\frac{y_e - y_f}{\Delta y_{b1}} \right)^{(1/N_{yb})} \quad (2.3)$$

Where Δx_1 , Δy_{f1} and Δy_{b1} represent the smallest grid and are close to the fracture in x direction, fracture perpendicular part and background area, respectively. x_e is the model length in x direction and will be changed if more fractures goes perpendicular to the horizontal well, y_f and y_e is the fracture's half length and total length in y direction respectively. Note that the block size of grids in x direction will change if different number of fractures exists in the horizontal well, however the grids block size in y direction remains unchanged in all cases.

¹ Fracture tip is the end/tail of fracture, the place of fracture end, 200 ft from the horizontal well bore

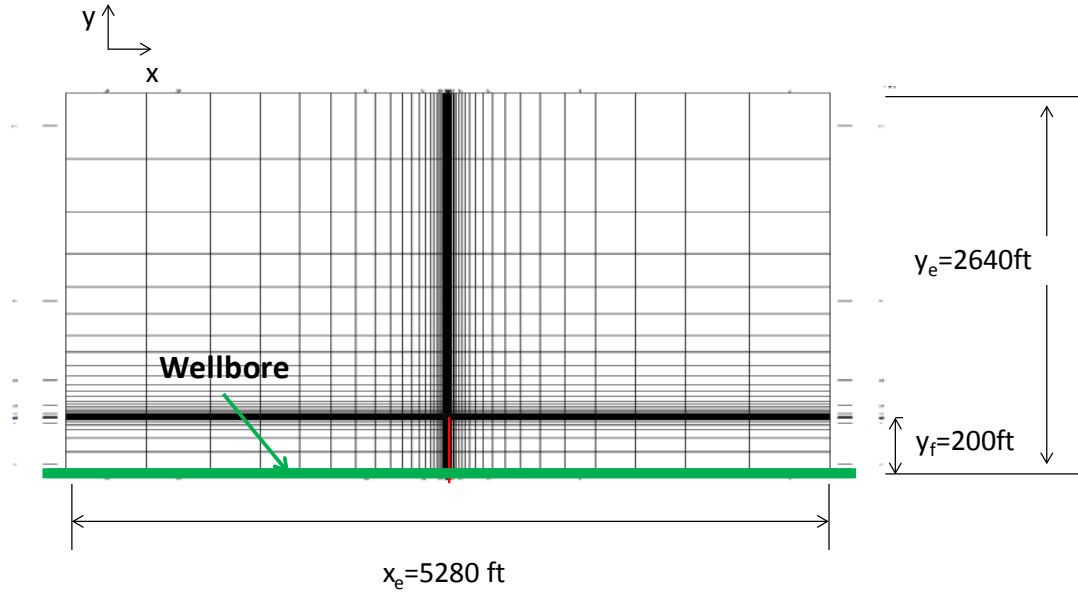


Fig. 2.2—Reservoir model grid system of one fracture shale reservoir, the area of simulation segment in model is 320 acres, 5,280 ft×2,640 ft, and half length of hydraulic fracture is 200 ft.

The grid geometry setting represents a reasonable grid for fluid flow character in the low permeability reservoir: refined grids nearby fracture capture the high pressure gradient. In low permeability reservoir and shale layer, rocks are impermeable without fracture. With the stimulate fracture, fluids which nearby fracture is able to flow from the matrix to the horizontal well. **Fig. 2.3** shows the pressure depletion in one fracture reservoir model after 10 days’ production. The pressure depletion area is confined in a small space of the whole model.

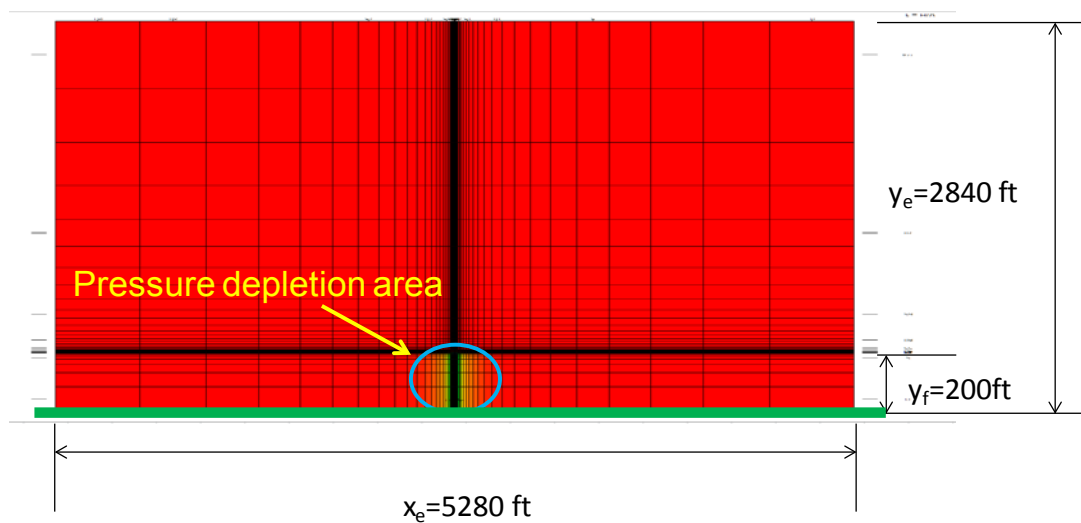


Fig. 2.3—The area of pressure depletion in one fracture reservoir model after 10 days of production, the red colour indicates the initial reservoir pressure: 4,800 psia.

2.3 Reservoir Properties

Reservoir properties such as reservoir porosity, thickness, well data etc, are from real field data of shale gas fields in North America. A ‘generic’ reservoir was assumed based on the real field data. The reservoir’s parameter values which have been used in the simulation model are given in **Table 2.1**. The method of hydraulic-fracturing treatment creates fractures with high conductivity. A good fracture conductivity ($k_f \cdot w_f = 100$ mD-ft) and a constant fracture width of 0.01 ft are assumed in this study (Golan and Whitson, 1985). Fracture permeability is calculated to 100,000 mD and used as a regular value in low permeability reservoir. Because of the hydraulic fracturing treatment, the porosity in fracture increased from 5.9% to 30% as well.

| | |
|---------------------------------------|---------|
| Depth (ft): | 10,000 |
| Horizontal length (ft): | 5,280 |
| Spacing area, arce | 640 |
| Initial reservoir pressure (psia): | 4,800 |
| Reservoir temperature (°F): | 250 |
| Casing diameter OD (in): | 4.5 |
| Open hole (in): | 5 |
| h net (ft): | 200 |
| Reservoir porosity: | 0.059 |
| y_f , half length of fracture (ft): | 200 |
| k_f^* (mD) | 100,000 |
| w_f , Fracture width (ft) | 0.01 |
| Fracture porosity: | 0.30 |
| Fracture conductivity (mD.ft) | 1,000 |

2.4 Fluid Properties

The black-oil model is used in this study. Black-oil PVT properties have been generated by a 31-component SRK equation of state model (EOS) using the Whitson-Torp procedure (Whitson et al, 1983). The mole-fraction of each component is shown

in **Table 2.2**. **Table 2.3** provides the fluid characterization of the 31-component EOS. In order to compare production performances, different fluid systems are used for the given “reservoir”. The type of reservoir fluids is varied if different initial gas oil ratio (GOR_i) is entered in the simulator. The fluid systems include:

- Volatile oil fluid system A, $GOR_i = 1,000$ scf/STB.
- Volatile oil fluid system B, $GOR_i = 3,000$ scf/STB.
- Near critical oil fluid system, $GOR_i = 4,587$ scf/STB.
- Gas condensate fluid system, $GOR_i = 10,000$ scf/STB
- Wet gas fluid system, $GOR_i = 100,000$ scf/STB

The relation between r_s , $1/R_s$ and saturation pressures is shown in **Fig. 2.4**. Reservoir fluid parameters were calculated with the help of the PVT analysis software *PhazeComp*. In simulation, the specified initial gas oil ratio (GOR_i) at depth 10,000 ft is used to define the type of the reservoir fluids. In this way, 5 different reservoir fluid systems were used out of the single compositional calculation.

Table 2.2—REFERENCE FLUID SAMPLE CONTAINS

| Nc | Composition mole-fraction |
|---------------------------|------------------------------|
| H2S | 0.0000000 |
| N2 | 0.00009032 |
| CO2 | 0.00028785 |
| C1 | 0.72443534 |
| C2 | 0.09995367 |
| C3 | 0.04329560 |
| I-C4 | 0.01200208 |
| N-C4 | 0.01612318 |
| I-C5 | 0.00799159 |
| N-C5 | 0.00604448 |
| C6 | 0.01486822 |
| C7 | 0.01338211 |
| C8 | 0.01085318 |
| C9 | 0.00878513 |
| C10 | 0.00723370 |
| C11 | 0.00595599 |
| C12 | 0.00490595 |
| C13 | 0.00404363 |
| C14 | 0.00333555 |
| C15 | 0.00275400 |
| C16 | 0.00227619 |
| C17 | 0.00188340 |
| C18 | 0.00156027 |
| C19 | 0.00129424 |
| C20 | 0.00107500 |
| C21 | 0.00089414 |
| C22 | 0.00074477 |
| C23 | 0.00062126 |
| C24 | 0.00051899 |
| C25 | 0.00043420 |
| C26+ | 0.00235598 |
| Depth, TVD, ft | 10,000 |
| Pressure, psia | 4,800 |
| Saturation pressure, psia | 4,800 |
| Temperature, °F | 250 |

Table 2.3—PARAMETERS OF THE 31-COMPONENT SRK EOS MODEL

| PSAT psia | BO rb/STB | RS scf/STB | VISO cp | rs STB/MMcf | BG rb/scf | VISG cp | IFT dyne/cm |
|--------------|--------------|---------------|------------|----------------|--------------|------------|----------------|
| 100 | 1.0976 | 11.4 | 0.347 | 57.8224 | 0.037307 | 0.0127 | 12.7740 |
| 500 | 1.1867 | 125.0 | 0.223 | 27.2592 | 0.007022 | 0.0134 | 8.8271 |
| 1000 | 1.3063 | 305.7 | 0.172 | 21.2774 | 0.003383 | 0.0142 | 5.8335 |
| 1200 | 1.3557 | 384.2 | 0.158 | 21.1350 | 0.002790 | 0.0146 | 4.9039 |
| 1400 | 1.4070 | 467.3 | 0.146 | 21.6758 | 0.002372 | 0.0150 | 4.0930 |
| 1600 | 1.4604 | 555.2 | 0.136 | 22.7574 | 0.002062 | 0.0156 | 3.3877 |
| 1800 | 1.5164 | 648.3 | 0.127 | 24.3051 | 0.001824 | 0.0162 | 2.7776 |
| 2000 | 1.5752 | 747.2 | 0.119 | 26.2822 | 0.001637 | 0.0168 | 2.2532 |
| 2200 | 1.6374 | 852.6 | 0.112 | 28.6755 | 0.001487 | 0.0176 | 1.8059 |
| 2400 | 1.7035 | 965.4 | 0.105 | 31.4883 | 0.001364 | 0.0184 | 1.4280 |
| 2600 | 1.7743 | 1086.6 | 0.099 | 34.7371 | 0.001262 | 0.0193 | 1.1118 |
| 2800 | 1.8506 | 1217.8 | 0.094 | 38.4510 | 0.001177 | 0.0204 | 0.8501 |
| 2900 | 1.8912 | 1287.6 | 0.091 | 40.4952 | 0.001140 | 0.0209 | 0.7377 |
| 3000 | 1.9336 | 1360.5 | 0.089 | 42.6730 | 0.001106 | 0.0214 | 0.6364 |
| 3100 | 1.9780 | 1436.9 | 0.087 | 44.9926 | 0.001074 | 0.0220 | 0.5456 |
| 3200 | 2.0246 | 1517.1 | 0.084 | 47.4634 | 0.001045 | 0.0226 | 0.4644 |
| 3300 | 2.0737 | 1601.5 | 0.082 | 50.0967 | 0.001018 | 0.0233 | 0.3923 |
| 3400 | 2.1256 | 1690.6 | 0.080 | 52.9060 | 0.000993 | 0.0239 | 0.3284 |
| 3600 | 2.2392 | 1884.9 | 0.076 | 59.1189 | 0.000949 | 0.0253 | 0.2231 |
| 3800 | 2.3690 | 2105.9 | 0.072 | 66.2752 | 0.000911 | 0.0269 | 0.1436 |
| 4000 | 2.5210 | 2362.4 | 0.068 | 74.6424 | 0.000880 | 0.0286 | 0.0858 |
| 4200 | 2.7049 | 2669.4 | 0.064 | 84.6738 | 0.000853 | 0.0305 | 0.0457 |
| 4400 | 2.9399 | 3055.3 | 0.060 | 97.2489 | 0.000832 | 0.0327 | 0.0200 |
| 4600 | 3.2733 | 3589.2 | 0.055 | 114.5335 | 0.000817 | 0.0356 | 0.0056 |
| 4800 | 3.9266 | 4587.7 | 0.049 | 146.5819 | 0.000814 | 0.0402 | 0.0002 |
| 4821 | 4.0742 | 4804.7 | 0.048 | 153.5214 | 0.000816 | 0.0412 | 0.0001 |

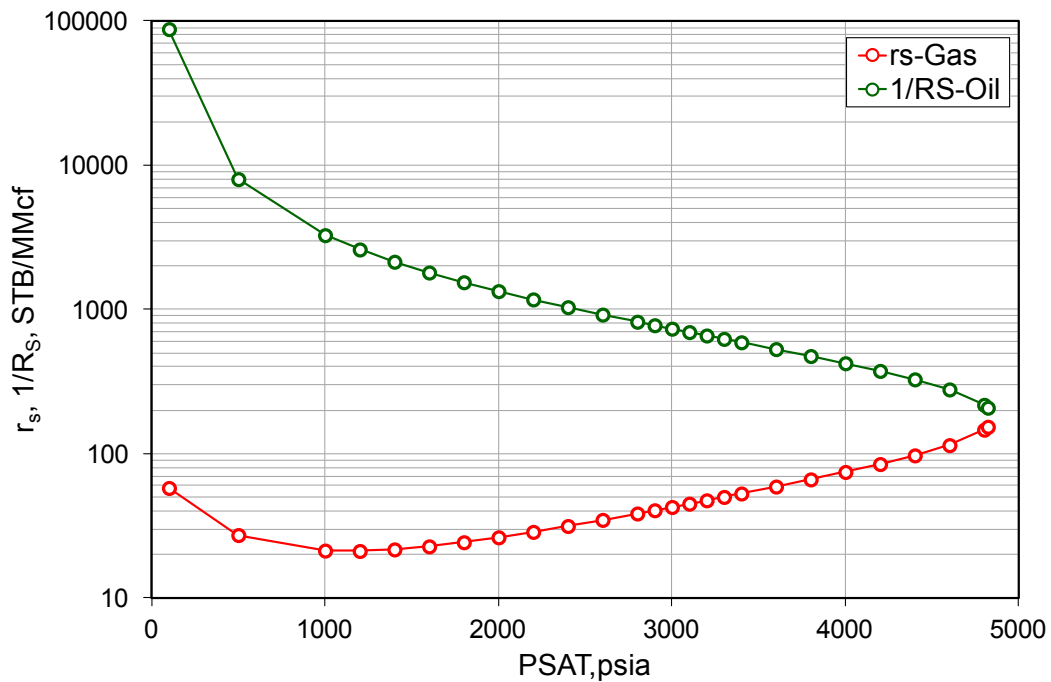


Fig. 2.4—Solution oil/gas ratios for reservoir oils, $1/R_S$ and inverse solution gas/oil ratio for reservoir gases, r_s as a function of pressure.

2.5 Relative Permeability Model

The relative permeability curve used in this simulation study is shown in **Fig. 2.5**. The initial water saturation (S_{wc}) is setting to 0.2, the residual oil saturation to water (S_{orw}) is 0.2, residual oil saturation to gas (S_{org}) is 0.2, and the critical gas saturation is setting to 0.1.

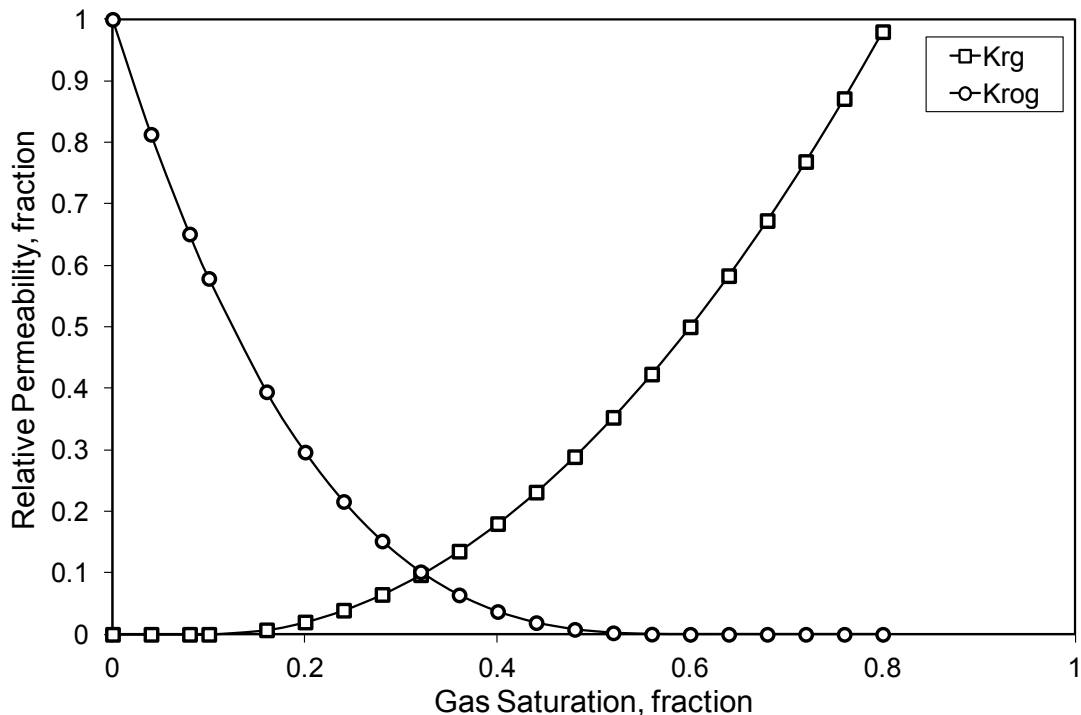


Fig. 2.5—Gas-Oil relative permeability curves used in simulations.

2.6 Simulation Constraints

A horizontal well is placed in the centre of the reservoir model as a producer, and the grid at the joint of horizontal wellbore and fracture ($X=41$, $Y=1$, $Z=1$) is perforated. The well is always run to 500 psia bottom-hole flowing pressure (BHP) or a specified model rate, whichever ever occurred first. The two types of production constraint used in this study is the daily gas rate or total revenue of the first 10 days.

Concerning gas rate control, daily well production of 10×10^6 ft³/day is assigned as the simulation constraint of the first 10 days. Note that the gas rate constraint in the simulation model will change if more fractures were designed in the reservoir. For

example, if the number of fractures (N_f) is 10, the gas constraint in the simulator is reduce to 500 Mscf/day because only 1/20 of the entire reservoir is simulated in the model.

Concerning the revenue control, total revenues of 50,000 USD from the first 10 days production is used in the simulation control. The revenues of simulation segment will also change if different amounts of fractures are set in the reservoir.

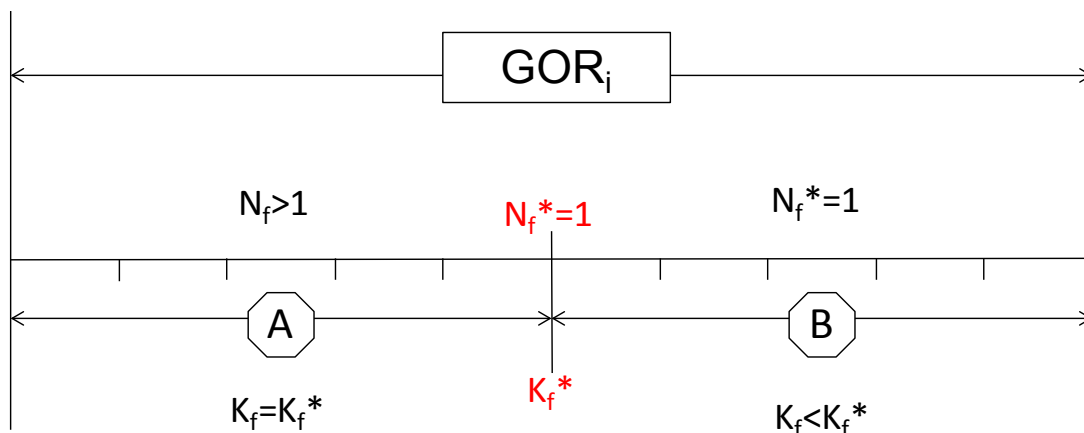
2.7 Simulation Cases Definition

This section presents the definition of simulation cases in this study. The simulation cases were designed with different reservoir fluid systems, which range from volatile oil, near critical oil, gas condensate to wet gas. The reservoir fluid systems are specified by setting the initial gas oil ratio (GOR_i) in simulator.

With the purpose of studying the performance trends of well production from conventional reservoir (high permeability) to unconventional reservoir (low permeability), reservoir permeability is designed in the range from 10^1 mD to 10^{-5} mD. In order to obtain the objective production rate/revenue in the early stage, the number of fractures in the horizontal well will increase if the reservoirs vary from conventional reservoir to unconventional reservoir. Since it is based on an identical fracture geometry and conductivity, production from single fracture segment will decrease in the low permeability reservoir. Finally, the optimal results of the combination of reservoir permeability and fracture numbers are given and their comparisons of well performance among different cases are shown. The relation between the number of fractures and reservoir permeability are established based on the numerical simulation results. Generated equations are used in the fracture design.

Fig. 2.6 shows the running simulation cases definition. Reservoirs with different fluid systems (GOR_i) and permeability were designed to run reservoir simulation. In low permeability case, more fractures ($N_f > 1$) are designed to meet the target of gas rate or cumulative revenue of the first 10 days. The fracture permeability is fixed to 100,000 mD when fracture play as a positive factor to stimulate fluids flow from reservoir to well. On the condition of fracture permeability (k_f) equal to reservoir matrix

permeability (k_m), no fracture will be required for stimulation or restriction. The case with identical reservoir permeability ($k_m=k_f$) is named as ‘critical case’ in this study. On the condition where matrix permeability is higher than the permeability in ‘critical case’, the permeability of fracture is limited ($k_f < k_m$) to reach either the objective production rate or total revenue. All simulation cases are list in **Table. 2.4**.



K_f^* : 100,000 mD
 N_f^* : 1

Fig. 2.6—Simulation cases definition with different reservoir permeability combinations in specified initial gas-oil ratio (GOR_i) in simulator.

| Table 2.4—SIMULATION CASES LIST | | |
|--|-----------------|-------------------|
| Simulation Constraint | GOR_i | Fluid System |
| Well daly gas rate of : 10×10^6 ft ³ /day | 1,000 scf/STB | Volatile Oil |
| | 3,000 scf/STB | Volatile Oil |
| | 4,587 scf/STB | Near Critical Oil |
| | 10,000 scf/STB | Gas Condensate |
| Cumulative revenue of: 50,000 USD/first10 days | 1,000 scf/STB | Volatile Oil |
| | 3,000 scf/STB | Volatile Oil |
| | 4,587 scf/STB | Near Critical Oil |
| | 10,000 scf/STB | Gas Condensate |
| | 100,000 scf/STB | Wet Gas |

In all cases, reservoir is developed by pressure depletion, which means there is no gas injection or alternative treatment to modify the production schedule. The production from reservoir is driven by its natural energy.

Chapter 3

Gas Production Control

This section presents the simulation results under the gas production control. Simulation is controlled by the specified well gas production. The gas production rate, 10×10^6 ft³/day, is assumed to be the objective gas rate in simulation of the first 10 days. In other word, gas production of well is in plateau of 10×10^6 ft³/day in the first 10 days. From the industry experience, one well with this amount of gas production is considered to be a commercial production rate which can create profit.

As introduced in the simulation area part, simulation segment is only half of the entire fracture drainage area. The cut of simulation area can save the CPU-time, and lead to faster simulator running. The constraint gas rate in simulation will change if different amount of fractures was designed in the entire reservoir area (1 mile \times 1 mile). **Table 3.1** shows the size of the simulation model with different number of fractures when the fracture play as a positive factor. The size includes the value in x, y, z direction and its spacing area. The model's length in x direction, along the horizontal wellbore, will decrease if more fractures were designed in the well. The model's length in y direction, along the fracture penetration direction, was however fixed to 2,640 ft. The thickness of the model is fixed to 200 ft as well.

| Fracture-Number | xe-model ft | ye-model ft | ze-model ft | Spacing-model acre |
|-----------------|----------------|----------------|----------------|-----------------------|
| 1 | 5280 | 2640 | 200 | 320 |
| 2 | 2640 | 2640 | 200 | 160 |
| 10 | 528 | 2640 | 200 | 32 |
| 20 | 264 | 2640 | 200 | 16 |

* xe-model: length perpendicular fracture of simulation model
ye-model: length along fracture direction of simulation model
ze-model: thickness of model in vertical direction

In addition to these four cases, two cases with high reservoir matrix permeability (5 mD and 10 mD) were designed, and their corresponding fracture permeability was optimized to match the gas rate constraint in simulation. Fracture in these cases, with low conductivity, is implemented as a damage factor in well production.

In addition, ‘critical case’ with identical reservoir permeability is designed. The fracture is not required to stimulate or restrict the production on this condition. However, maintaining the fracture in the model is for the purpose of having same gridding structure as other cases and to make it easy to compare. The fracture in this model plays as neither positive nor negative factor for well’s production.

The simulated production performance is systematic analyzed for a variety of reservoir fluid systems which range from volatile oil to near critical oil, and to gas condensate.

3.1 Cases of $GOR_i=1,000$ scf/STB

Gas-oil ratio equal to 1,000 scf/STB indicates the reservoir fluid type of volatile oil. 7 simulation cases of volatile oil reservoir were designed, and run to a 20-years-production period. **Table 3.2** shows the simulation optimal results that matched the gas production constraint, daily production of 10×10^6 ft³/day in the first ten days. The reservoir matrix permeability is ranging from 10 mD to 0.0043 mD. On the case of $k_f=k_m=2.2158$ mD, critical condition, no fracture was required to reach this production target. When the matrix permeability is higher than 2.2158 mD, the permeability in fracture is limited to meet the gas rate control. In such case, fracture plays as a damage factor.

All daily gas production profiles are shown in **Fig. 3.1**. Daily gas production in the first 10 days is the same, 10×10^6 ft³/day. However, there is significant difference after the first 10 days. In low reservoir permeability cases, the gas production dropped rapidly. While in high permeability cases, production will carry on a long period of high rate.

The producing gas-oil ratio (GOR) and oil-gas ratio (OGR) are shown in **Figs. 3.2 – 3.3**. The greatest difference in yield is their variation range over the duration of 20 years' production, ratio in low permeability case is keeping stable from the beginning to the end.

| Table 3.2—SIMULATION OPTIMAL RESULTS BY GAS RATE CONTROL, $GOR_i=1,000$ scf/STB | | | |
|---|-----------------|-------------|-------------|
| Case No. | Fracture-Number | k_m mD | k_f mD |
| 1 | 1 | 0.9245 | 100000 |
| 2 | 2 | 0.3000 | 100000 |
| 3 | 10 | 0.0165 | 100000 |
| 4 | 20 | 0.0043 | 100000 |
| 5* | 1 | 2.2158 | 2.2158 |
| 6 | 1 | 5.0000 | 0.8965 |
| 7 | 1 | 10.0000 | 0.8080 |

* $k_m=k_f$, fractures are not required to get 10 MMcf/day for the first 10 days

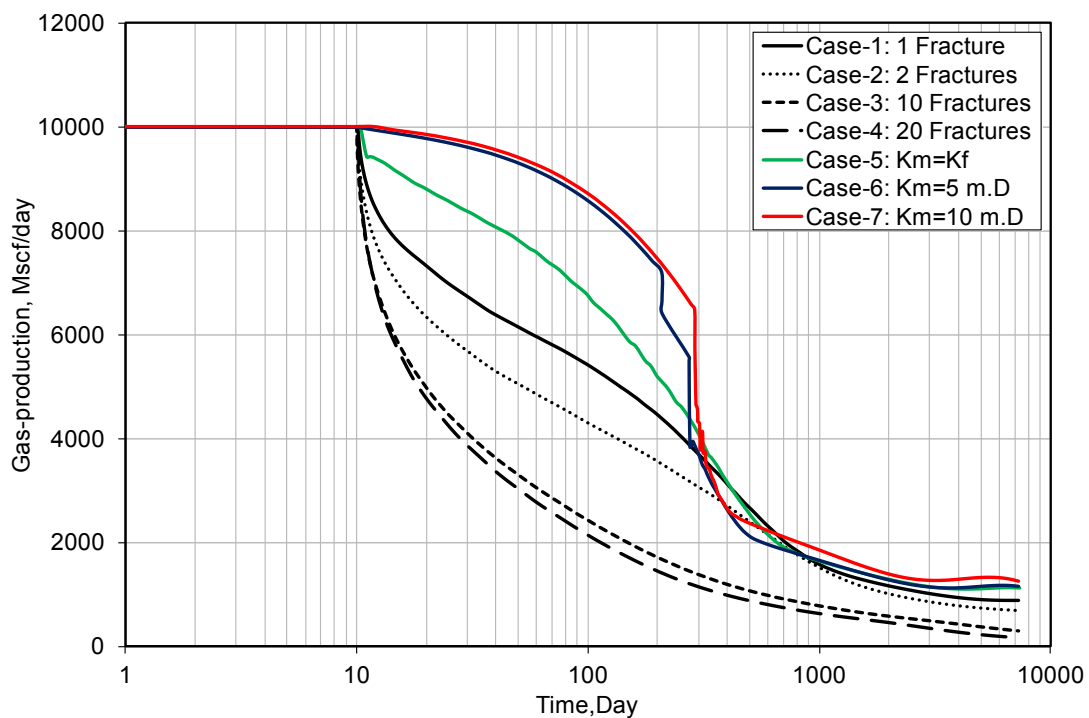


Fig. 3.1—Simulation well gas production profile of 7 cases, $GOR_i=1,000$ scf/STB.

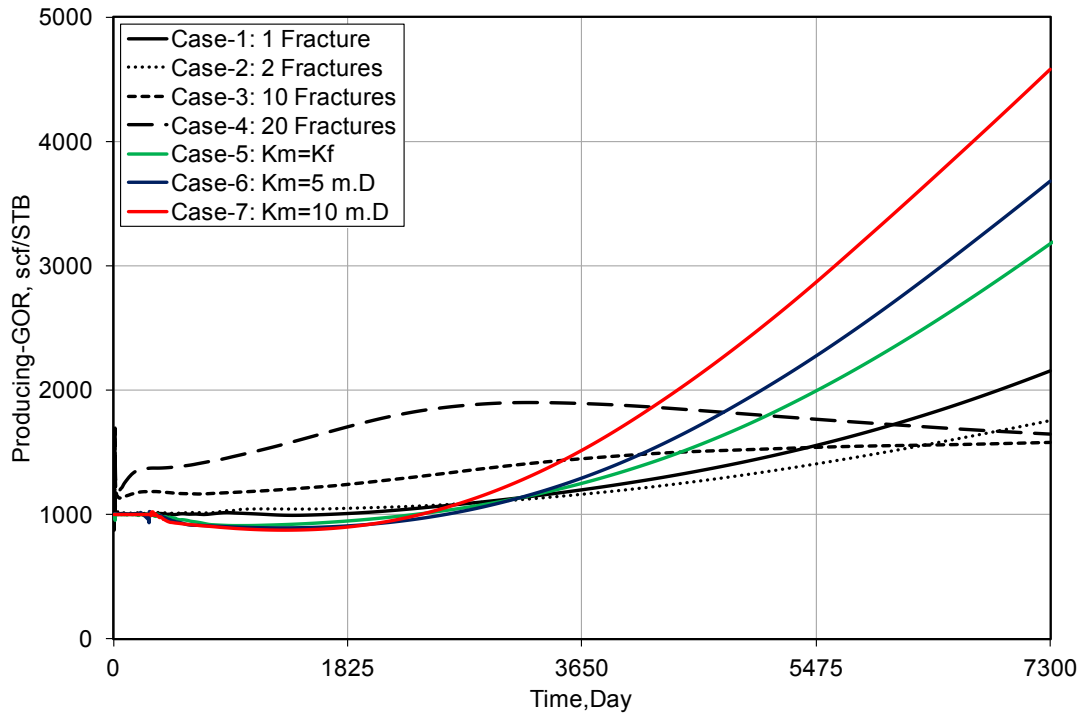


Fig. 3.2—Reservoir model producing gas-oil ratio profile of 7 cases, $GOR_i=1,000$ scf/STB.

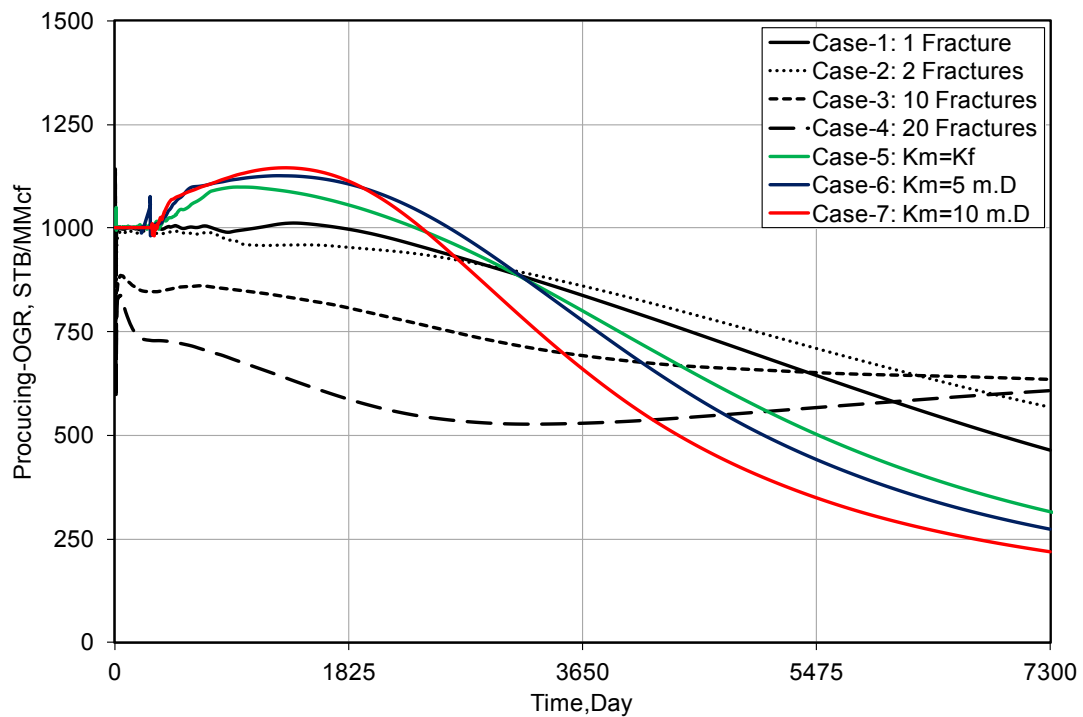


Fig. 3.3—Reservoir model producing oil-gas ratio profile of 7 cases, $r_s=1000$ STB/MMcf ($GOR_i=1,000$ scf/STB).

3.2 Cases of $GOR_i=3,000$ scf/STB

Gas-oil ratio of 3,000 scf/STB indicates a reservoir fluid type of lean volatile oil. 7 cases of lean volatile oil are set up and run to 20 years production duration. **Table 3.3** shows the optimal results of each model which is under the gas production control: daily gas rate with 10×10^6 ft³/day of the first 10 days. The reservoir matrix permeability ranges from 10 mD to 0.0008 mD. If the lowest matrix permeability of reservoir is reduced to 0.0008 mD, 20 fractures in reservoir are required to attain the plateau rate of 10 days.

| Table 3.3—SIMULATION OPTIMAL RESULTS BY GAS RATE CONTROL, $GOR_i=3,000$ scf/STB | | | |
|---|-----------------|-------------|-------------|
| Case No. | Fracture-Number | k_m mD | k_f mD |
| 1 | 1 | 0.2690 | 100000 |
| 2 | 2 | 0.0710 | 100000 |
| 3 | 10 | 0.0030 | 100000 |
| 4 | 20 | 0.0008 | 100000 |
| 5* | 1 | 1.5412 | 1.5412 |
| 6 | 1 | 5.0000 | 0.1972 |
| 7 | 1 | 10.0000 | 0.1923 |

* $k_m=k_f$, fractures are not required to get 10 MMcf/day for the first 10 days

Fig. 3.4 shows the well gas rate profile of these 7 simulation cases. All cases have the same gas production rate in the first 10 days, but present different performance after this period. The gas rate in the ultra low matrix permeability ($k_m=0.0008$ mD) case drops to 2×10^6 ft³/day after 100 days, while the gas rate in high matrix permeability is around 9.5×10^6 ft³/day at the same time. The oscillation problem in simulation appears in the cases with high permeability ($k_m=5$ mD and 10 mD), particularly in the case of $k_m=5$ mD. A detailed analysis is shown in **Appendix B**.

The producing gas-oil ratio and oil-gas ratio profile of 7 cases are shown in **Figs. 3.5–3.6**. Ratio profiles will change with different permeability, and the ratio in low permeability case was remaining relative stable over the 20-year simulation period.

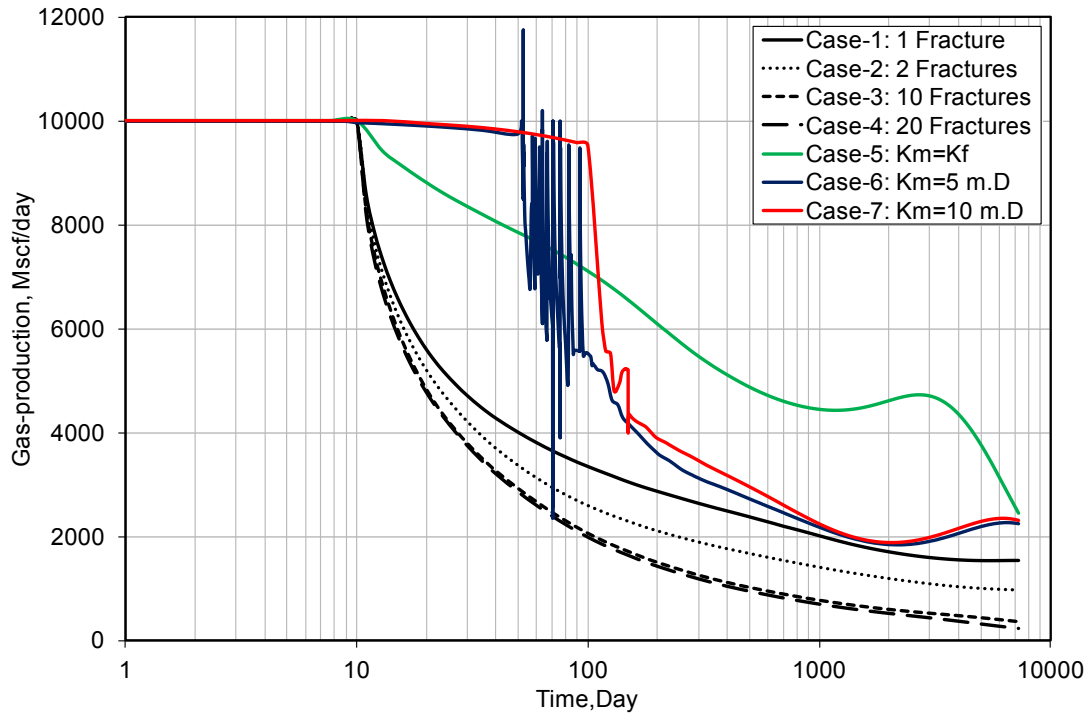


Fig. 3.4—Simulation well gas production profile of 7 cases, $GOR_i=3,000$ scf/STB.

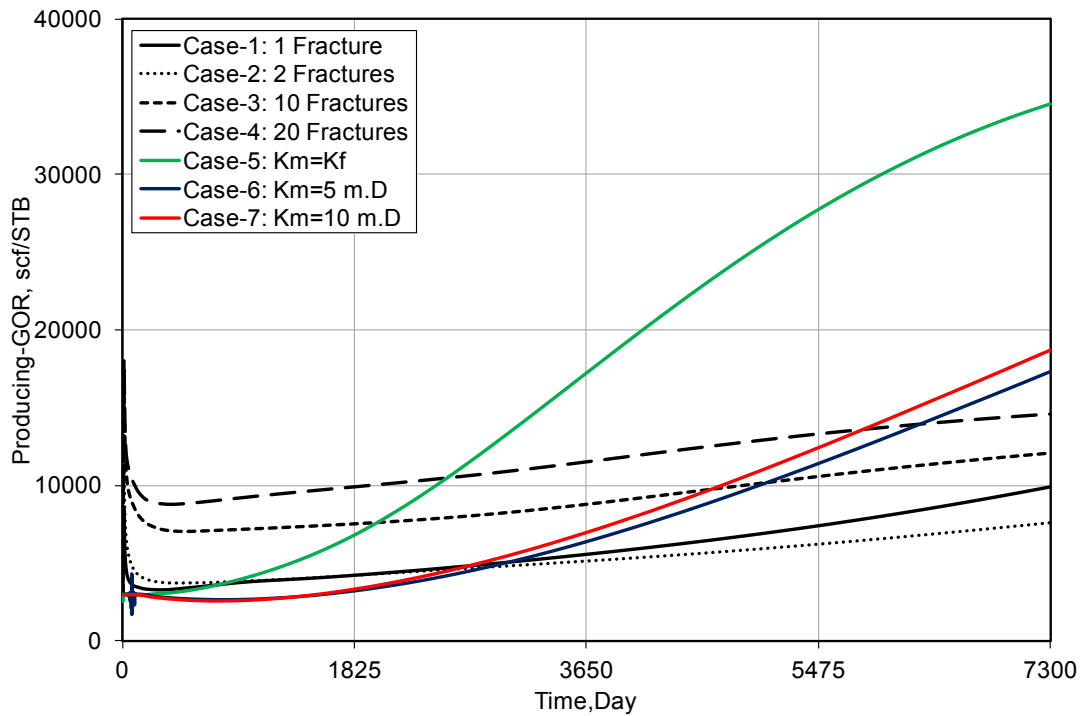


Fig. 3.5—Reservoir model producing gas-oil ratio profile of 7 cases, $GOR_i=3,000$ scf/STB.

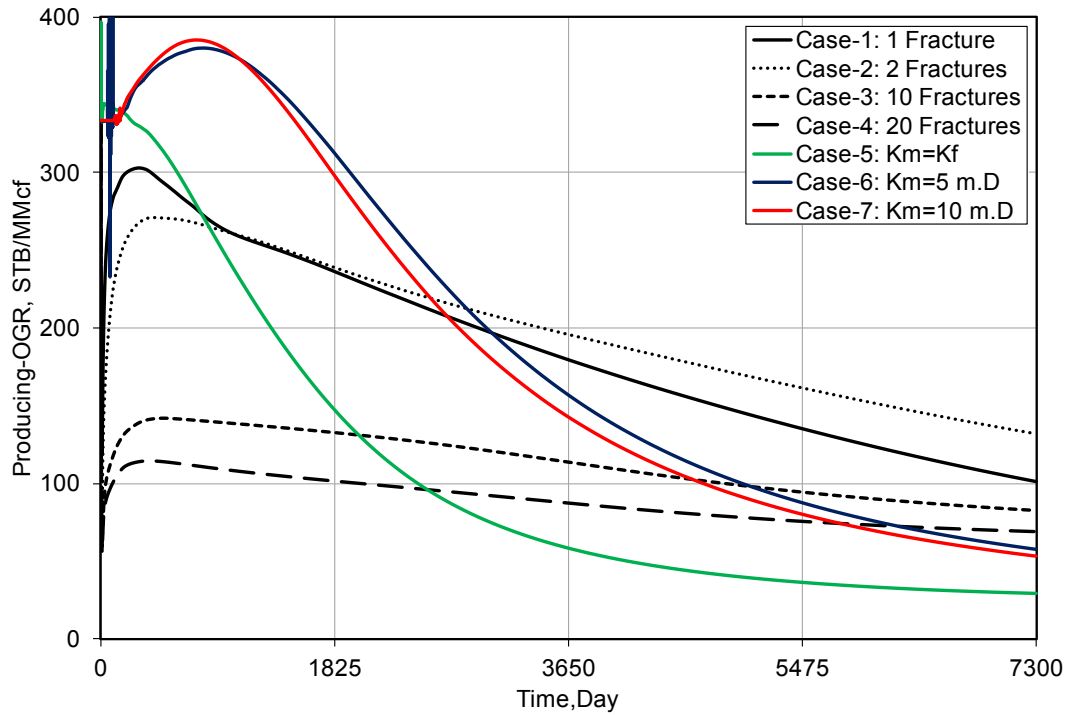


Fig. 3.6—Reservoir model producing oil-gas ratio profile of 7 cases, $r_s=333$ STB/MMcf($GOR_i=3,000$ scf/STB).

3.3 Cases of $GOR_i=4,587$ scf/STB

The gas-oil ratio of 4,587 scf/STB suggests the fluids type of near critical oil. 7 cases with GOR_i of 4,587 scf/STB are designed to study. **Table 3.4** shows the optimal results that reach the gas rate control: daily production of 10×10^6 ft³/day in the first 10 days. The optimal results of matrix permeability range from 10 mD to 0.0003 mD.

Fig. 3.7 shows the well gas rate profile over the duration of 50 years production. The gas rate is same in all cases of the first 10 days. However, it becomes different after this period. The gas production in the model of low matrix permeability reduces rapidly after the first 10 days. While, the gas production in high matrix permeability cases ($k_m=5$ mD and 10 mD) is remaining in a high rate level to 7 years. **Figs. 3.8 –3.9** show the producing gas-oil ratio (R_p) and oil-gas ratio (r_p) of each case. In the low permeability cases ($k_m=0.02$ mD, 0.0011 mD and 0.0003 mD), these two ratios keep in a stable level over 50 years of production.

| Table 3.4—SIMULATION OPTIMAL RESULTS BY GAS RATE CONTROL: $GOR_i=4,587$ scf/STB | | | |
|--|-----------------|-------------|-------------|
| Case No. | Fracture-Number | k_m mD | k_f mD |
| 1 | 1 | 0.1100 | 100000 |
| 2 | 2 | 0.0298 | 100000 |
| 3 | 10 | 0.0011 | 100000 |
| 4 | 20 | 0.0003 | 100000 |
| 5* | 1 | 1.0088 | 1.0088 |
| 6 | 1 | 5.0000 | 0.7100 |
| 7 | 1 | 10.0000 | 0.6720 |

* $k_m=k_f$, fractures are not required to get 10 MMcf/day for the first 10 days

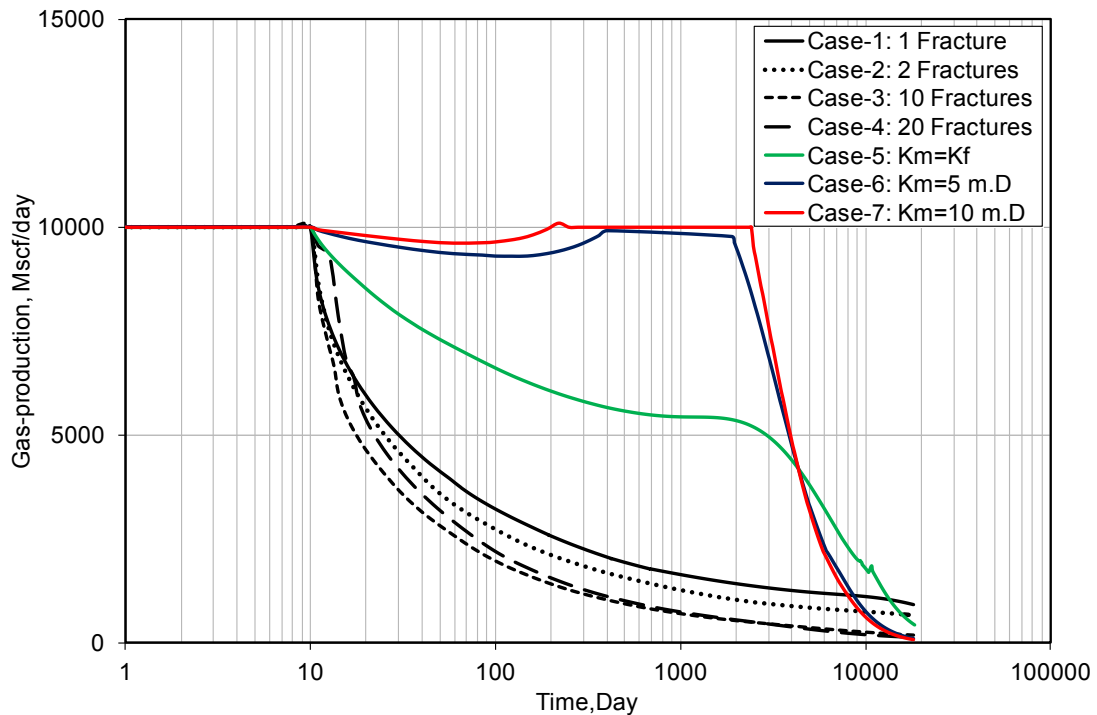


Fig. 3.7—Simulation well gas production profile of 7 cases, $GOR_i=4,587$ scf/STB.

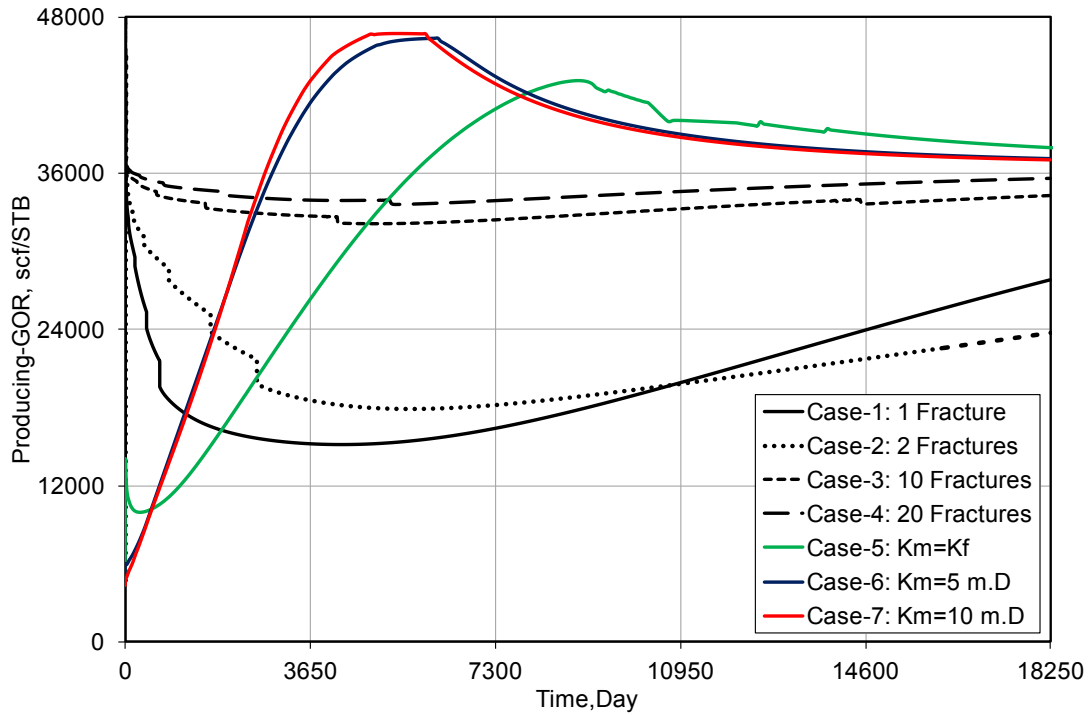


Fig. 3.8—Reservoir model producing gas-oil ratio profile of 7 cases, $GOR_i=4,587$ scf/STB.

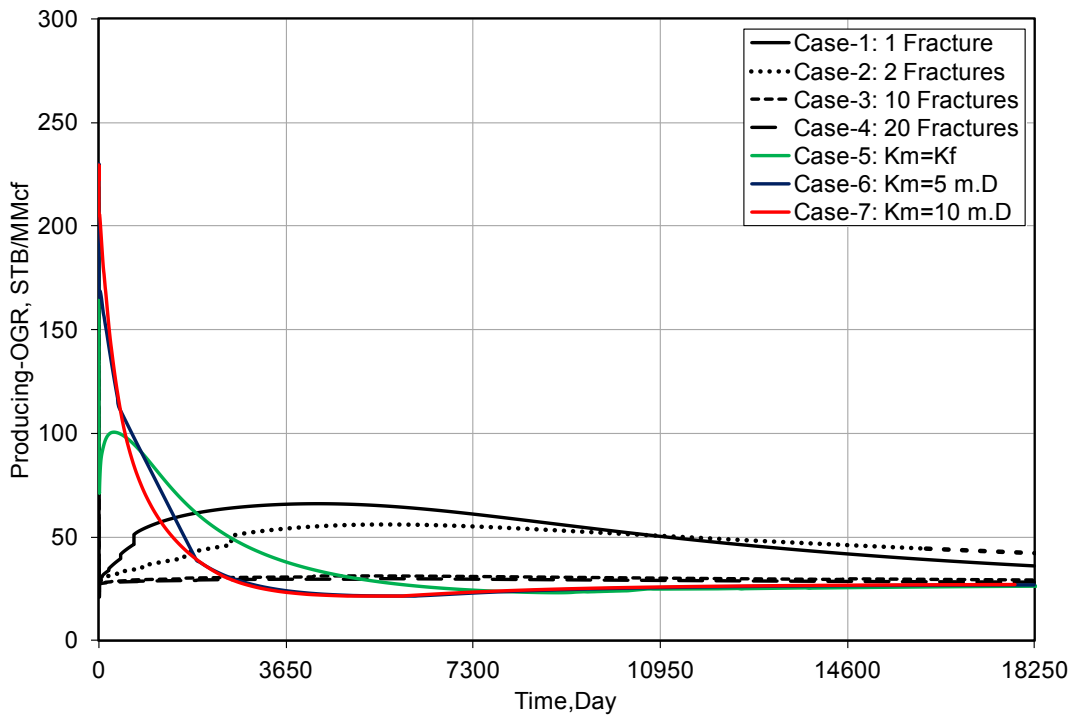


Fig. 3.9—Reservoir model producing oil-gas ratio profile of 7 cases, $r_s=218$ STB/MMcf ($GOR_i=4,587$ scf/STB).

3.4 Cases of $GOR_i=10,000$ scf/STB

A reservoir with initial gas-oil ratio of 10,000 scf/STB represents a gas condensate reservoir with 100 STB/MMcf liquid contents. The optimal results are shown in **Table 3.5**, which summarize the combination of fractures number and reservoir permeability. Each model with the combination is run to reach the gas production constraint of the first 10 days. **Fig. 3.10** shows the gas production profile over the duration of production period (50 years), the daily gas rate is equal to 10 MMcf/day in the first 10 days. Their corresponding plots of producing gas-oil ratio and oil-gas ratio are shown in **Figs. 3.11 –3.12**. The ratio in low permeability cases performs rather stable, which almost no changes over the 50 years production.

| Table 3.5—SIMULATION OPTIMAL RESULTS BY GAS RATE | | | |
|---|-----------------|-------------|-------------|
| CONTROL: $GOR_i=10,000$ scf/STB | | | |
| Case No. | Fracture-Number | k_m mD | k_f mD |
| 1 | 1 | 0.04400 | 100000 |
| 2 | 2 | 0.01200 | 100000 |
| 3 | 10 | 0.00051 | 100000 |
| 4 | 20 | 0.00013 | 100000 |
| 5* | 1 | 0.4820 | 0.4820 |
| 6 | 1 | 5.0000 | 0.0907 |
| 7 | 1 | 10.0000 | 0.0893 |

* $k_m=k_f$, fractures are not required to get 10 MMcf/day for the first 10 days

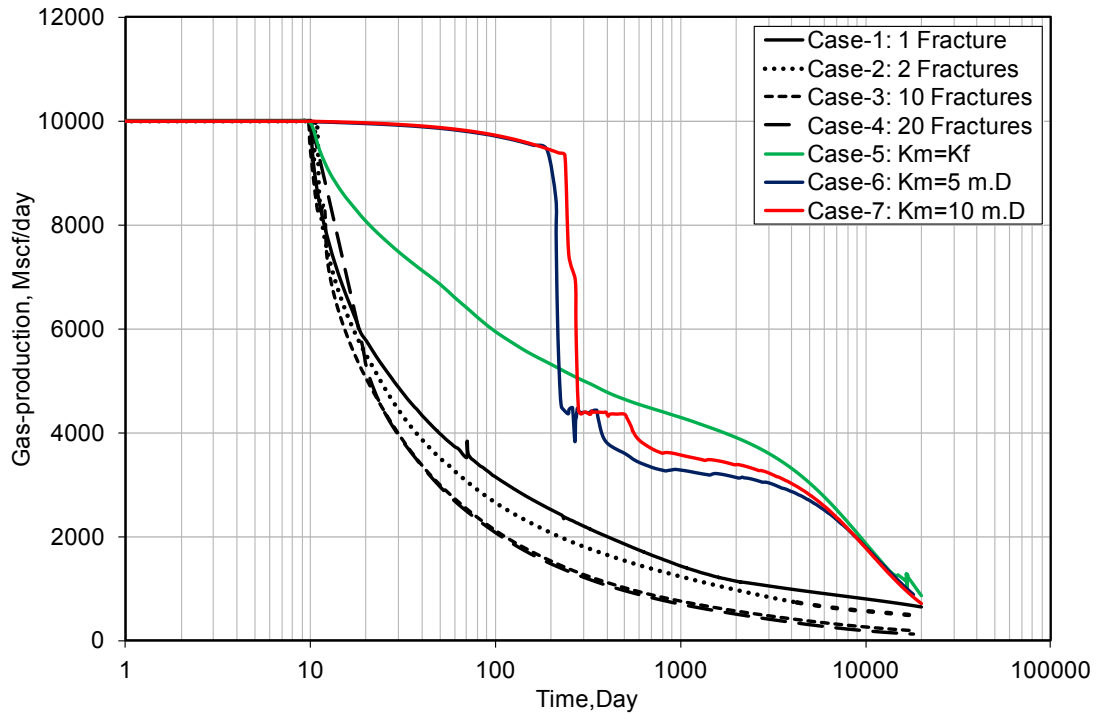


Fig. 3.10—Simulation well gas production profile of 7 cases, $GOR_i=10,000$ scf/STB.

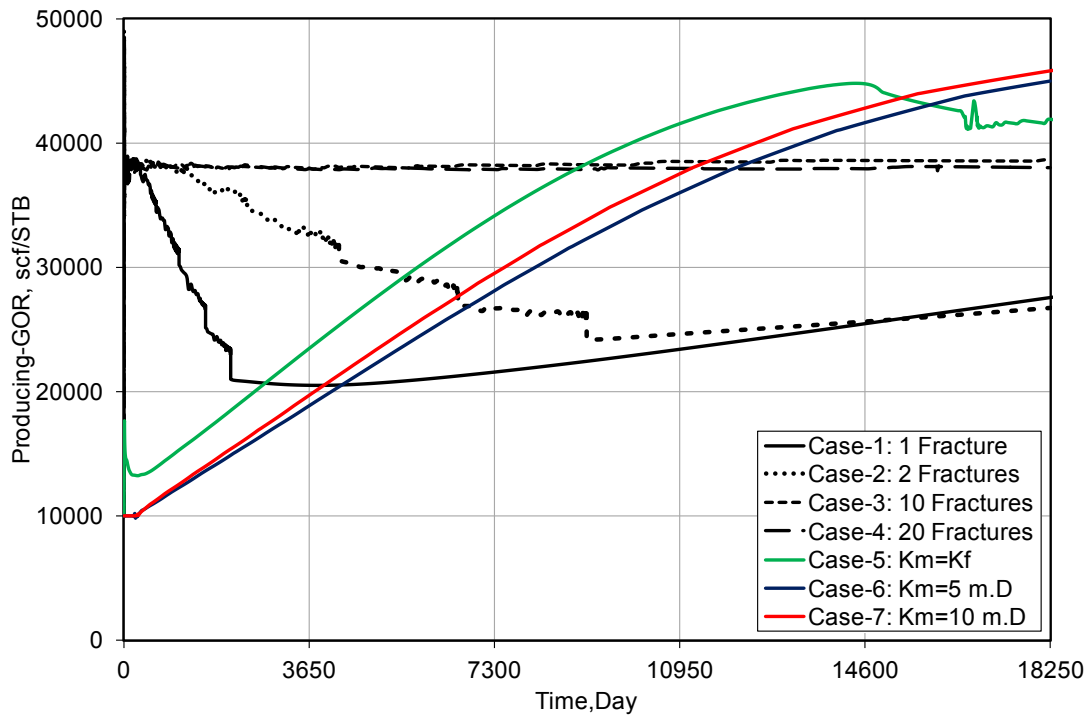


Fig. 3.11—Reservoir model producing gas-oil ratio profile of 7 cases, $GOR_i=10,000$ scf/STB

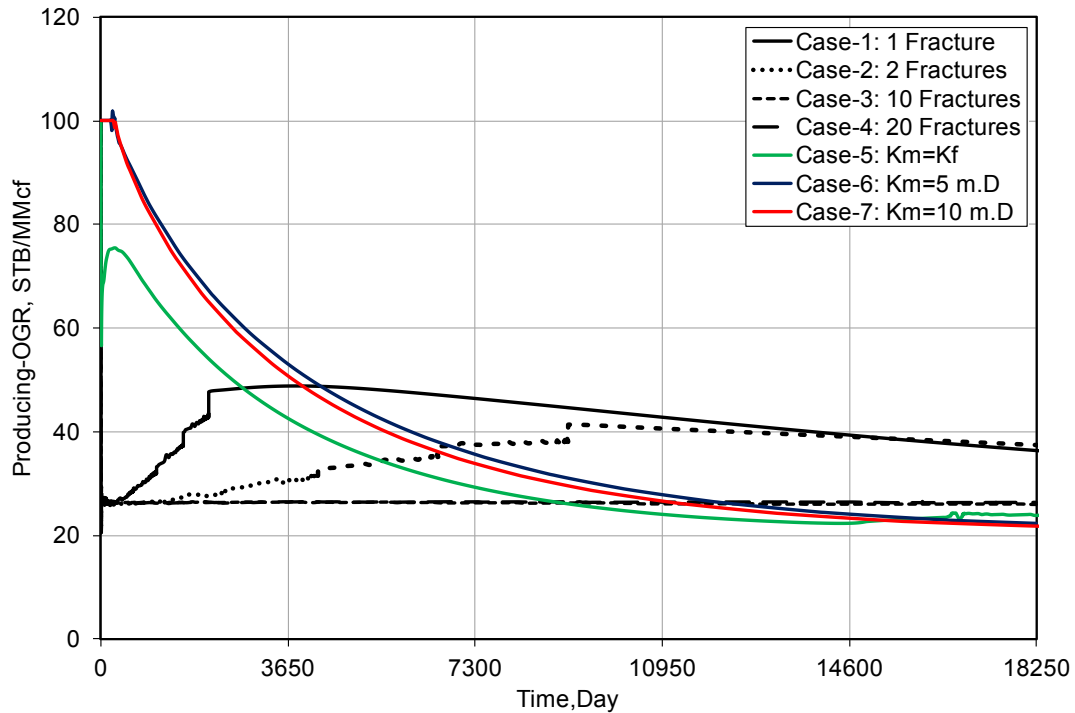


Fig. 3.12—Reservoir model producing oil-gas ratio profile of 7 cases, $r_s=100$ STB/MMcf ($GOR_i=10,000$ scf/STB).

3.5 Gas Production Control Summary

This section summarizes the most important conclusion from the simulation controlled by gas rate. With numerical simulation studies, some significant phenomenon of well's production performance are obtained.

To obtain a same gas rate of the first 10 days, more fractures are needed if the matrix permeability is decreased. In addition, gas production in the low permeability model drops rapidly after the first 10 days. On the condition of high matrix permeability, the fracture conductivity is limited to obtain the objective gas rate. The fracture plays as a positive factor in the low permeability reservoir, while performs as a negative factor in the high permeability reservoir.

Fig. 3.13 shows the relation between the reservoir permeability and the initial gas-oil ratio of critical cases. In the critical case, the fracture is not required to limit or increase the conductivity from reservoir matrix to horizontal wellbore. Inverse correlation exists between the initial gas-oil ratio (GOR_i) and the reservoir matrix

permeability (k_m). This means more gas will produce if the initial gas-oil ratio is in a large value.

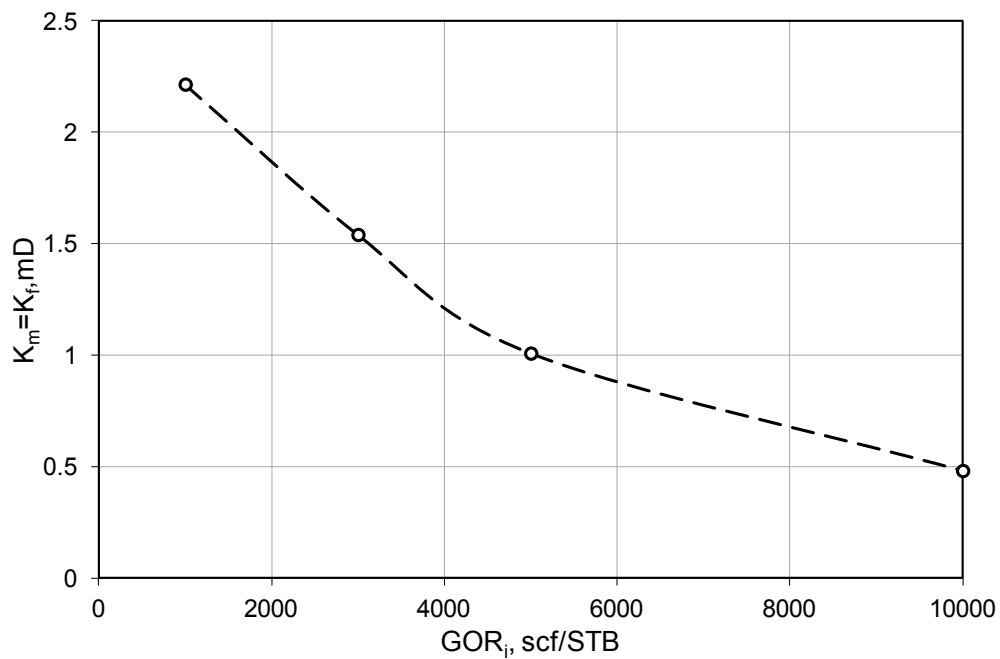


Fig. 3.13—Relation between GOR_i and reservoir permeability of critical case, no fracture is required and uniform permeability in reservoir

The simulation oscillation problem is shown in some model of high matrix permeability, including these cases of $k_m=5$ mD or 10 mD When $GOR_i=3,000$ scf/STB and the case of $k_m=5$ mD when $GOR_i=10,000$ scf/STB. The simulation oscillation problem is caused by the model's gridding geometry. A detailed analysis is described in **Appendix B**.

Chapter 4

Revenue Control

In the gas production control, reservoir simulation only considers the well production from gas. This is true for the dry gas or wet gas reservoir, which contain a small amount of liquid. However, concerning the reservoir of low initial gas-oil ratio, such as volatile oil reservoir, near critical oil reservoir and gas condensate reservoir, large amounts of revenue is come from liquid part. At a time when oil price is keeping in high level and gas prices is cheap, it is more reasonable and appropriates to use well's total revenue as the constrain in simulation. Revenue both from gas production and oil production will be considered if the simulation is controlled by the total revenue.

The revenue calculation of well's production is based on both of the production rate and the price of the products. **Table 4.1** shows the assumption of products price, and the total revenue of the well's production is calculated by equation (4.1):

$$\text{Revenue}_{\text{total}} = q_o \times P_o + q_g \times P_g \quad (4.1)$$

| Table 4.1—REVENUE CALCULATION ASSUMPTION | | | |
|--|-------|-----|---------|
| Oil-price | P_o | 100 | \$/STB |
| Gas-price | P_g | 4 | \$/Mscf |

Based on the E&P industry experience, cumulative revenue of 500,000 USD in the first 10 days is set as the criterion of a commercial well. All simulation cases in this section will be optimized to match this standard.

In order to compare the well performance between the conventional reservoir and the unconventional reservoir, reservoir's matrix permeability is set in the range from 10 mD to 10^{-5} mD. The comparisons are analyzed of each fluid system. In all simulation cases, two of them are conventional reservoirs with a high matrix permeability ($k_m=1$

mD, 10 mD), one of them is critical case of an identical permeability and the others are low permeability reservoirs with a high fracture conductivity ($k_f=100,000$ mD).

The fracture conductivity is high in the low permeability reservoir, while it will be reduced to restrict the fluid flow from reservoir matrix to fracture in high permeability reservoirs. Neither the fracture plays as a positive or a negative factor in the critical case, which has identical permeability.

4.1 Cases of $GOR_i=1,000$ scf/STB

7 cases with initial gas-oil ratio of 1,000 scf/STB are set to run, and their optimal results are listed in the **Table 4.2**. The matrix permeability ranges from 10 mD to 1.2×10^{-5} mD. Comparing the optimal results of simulation controlled by gas rate, the matrix permeability is lower in the reservoir with same fracture conductivity.

| Table 4.2—SIMULATION OPTIMAL RESULTS BY REVENUE CONTROL, $GOR_i=1,000$ scf/STB | | | | |
|--|-----------------|-------------|-------------|--|
| Case No. | Fracture-Number | k_m mD | k_f mD | |
| 1 | 1 | 0.004440 | 100000 | |
| 2 | 2 | 0.001166 | 100000 | |
| 3 | 10 | 0.000048 | 100000 | |
| 4 | 20 | 0.000012 | 100000 | |
| 5* | 1 | 0.051518 | 0.051518 | |
| 6 | 1 | 1 | 0.035916 | |
| 7 | 1 | 10 | 0.034990 | |

* $k_m=k_f$, fractures are not required to get 10 MMcf/day for the first 10 days cumulative production

Fig. 4.1 shows the total revenue of 7 different cases over the duration of a 50 years simulation. All of these cases have the same cumulative revenue of the first 10 days. However, the reservoir with high matrix permeability yields more revenue after 50 years of production. The producing total revenue is 10 times as much between the highest permeability reservoir ($k_m=10$ mD) and the lowest permeability reservoir ($k_m=1.2 \times 10^{-5}$ mD) after 50 years.

Figs. 4.2 – 4.3 show the 50-year profile of gas production and oil production. As seen in these two figures, the greatest difference is the production variation range over the 50 years production period. The production from low permeability model is high in the early stage and starts to decline after a short time. However, the production from the high permeability model stays at a stable level for the first 30 years. There is large difference in rate between the early stage and the late stage of the low permeability reservoir.

Figs. 4.4 –4.5 show the plot of gas-oil ratio and oil-gas ratio respectively. The simulation oscillation problem occurs in the critical cases with identical permeability ($k_m=k_f=0.051518$ mD). This problem is caused by the gridding structure in the simulation model, and a detailed analysis is shown in **Appendix B**.

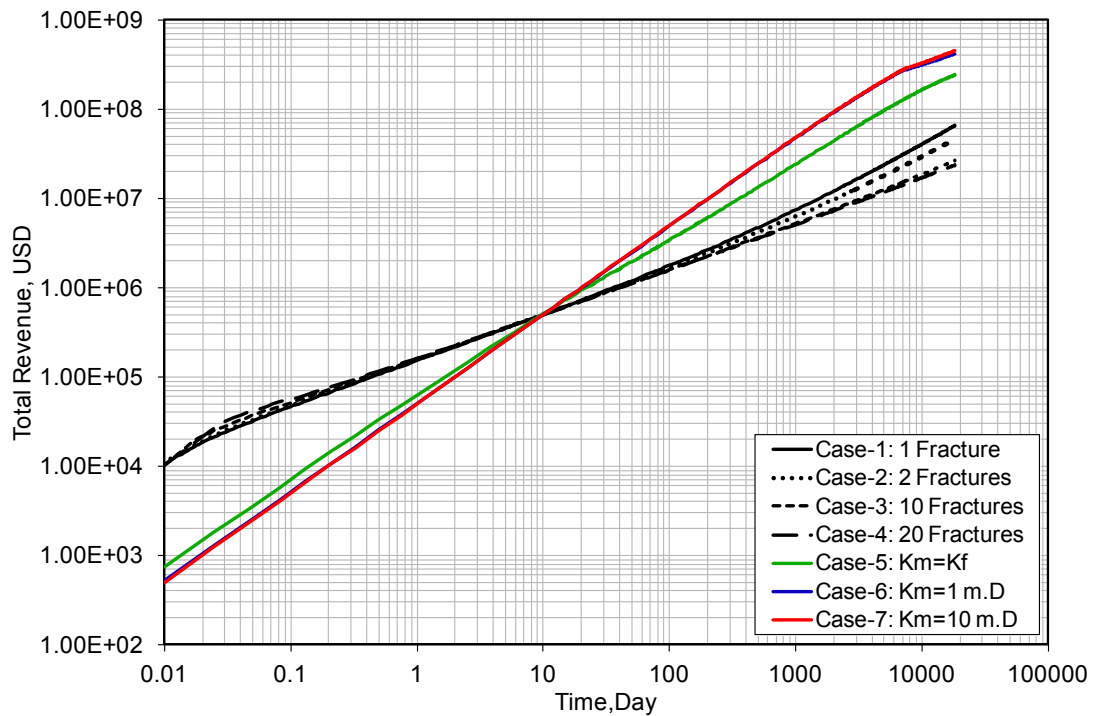


Fig. 4.1—Simulation well cumulative revenue of 50 years production of 7 cases, $GOR_i=1,000$ scf/STB.

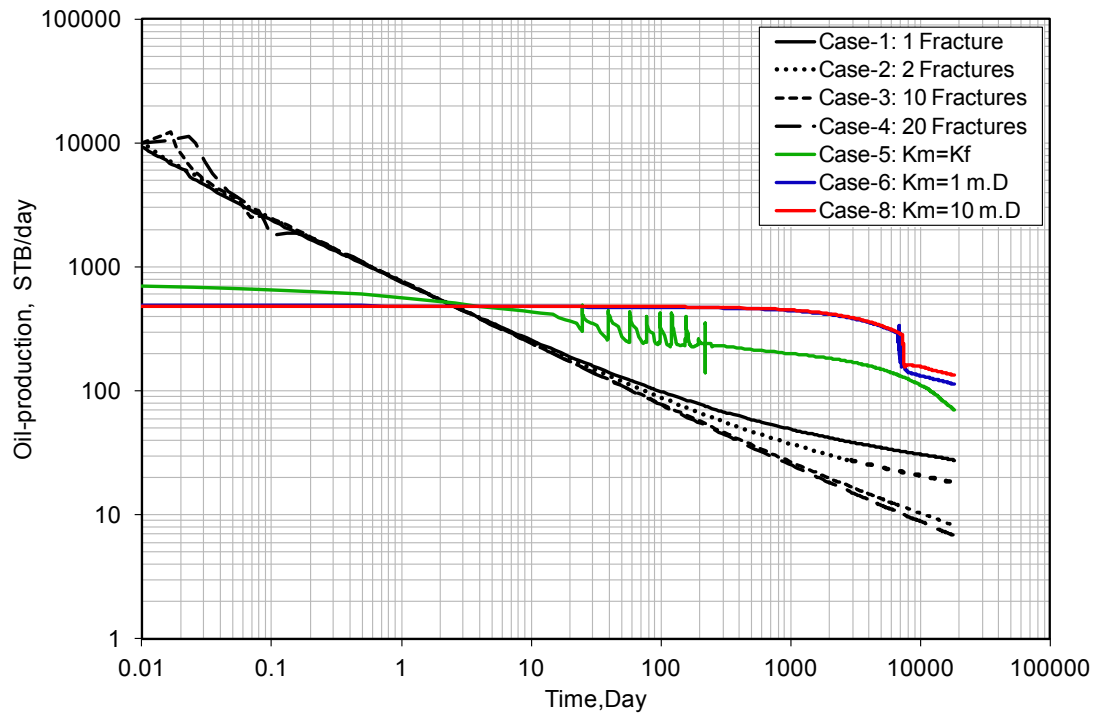


Fig. 4.2—Simulation well oil production profile of 7 cases by total revenue control, $GOR_i=1,000 \text{ scf/STB}$.

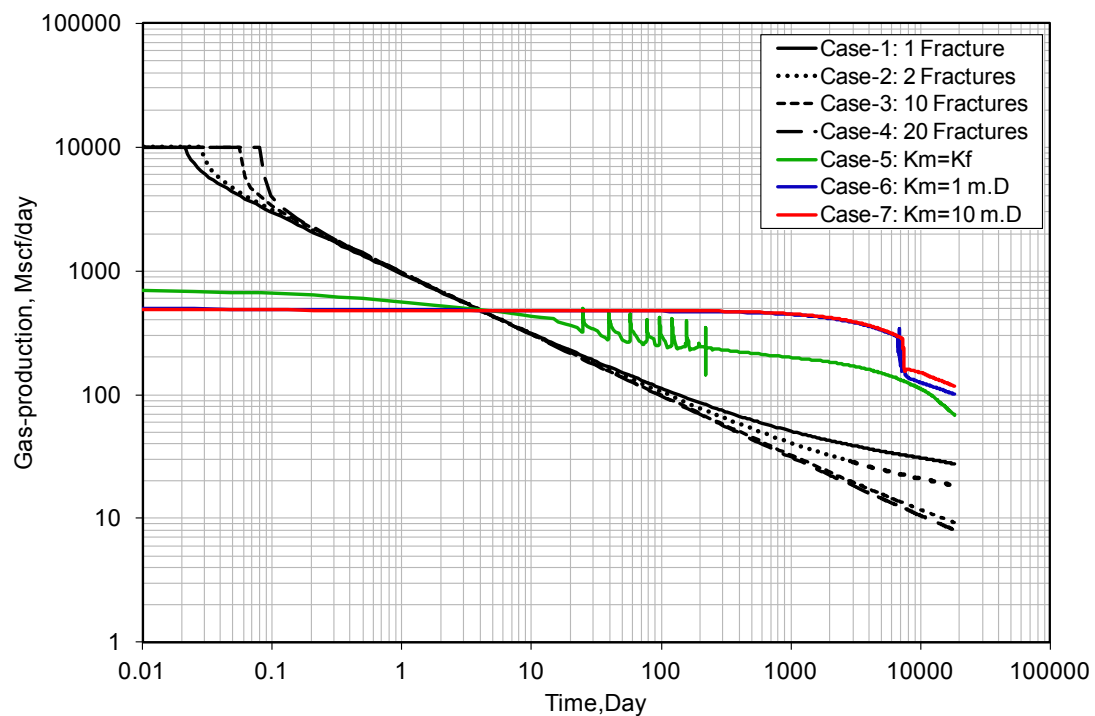


Fig. 4.3—Simulation well gas production profile of 7 cases by total revenue control, $GOR_i=1,000 \text{ scf/STB}$.

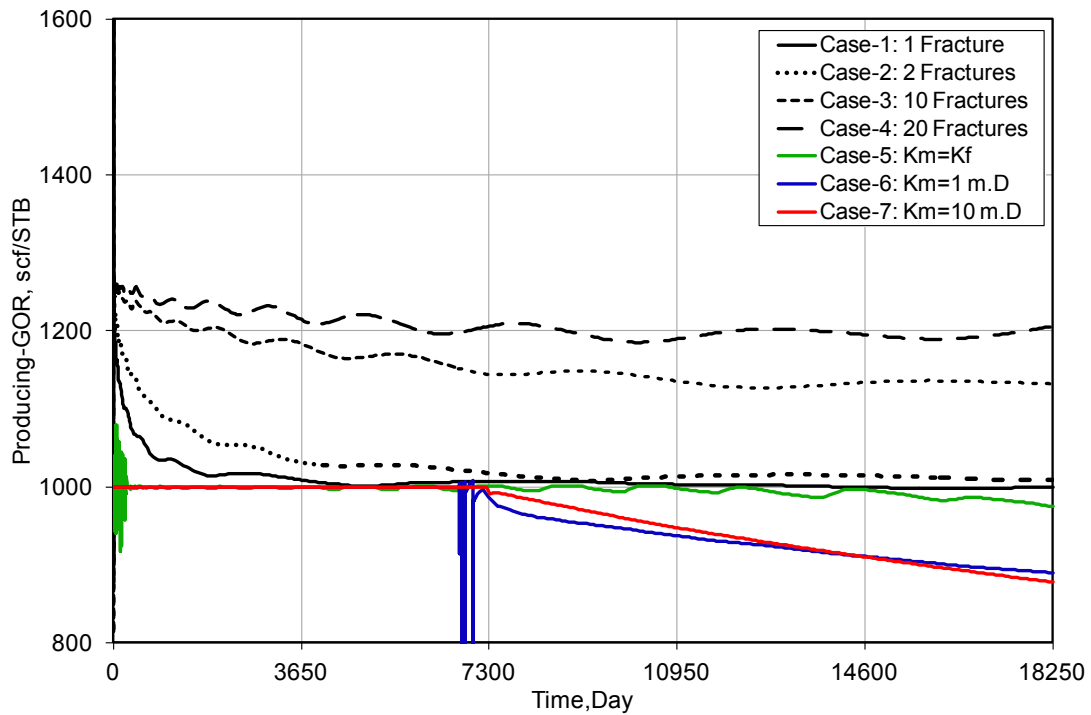


Fig. 4.4—Reservoir model producing gas-oil ratio profile of 7 cases by total revenue control, $GOR_i=1,000$ scf/STB.

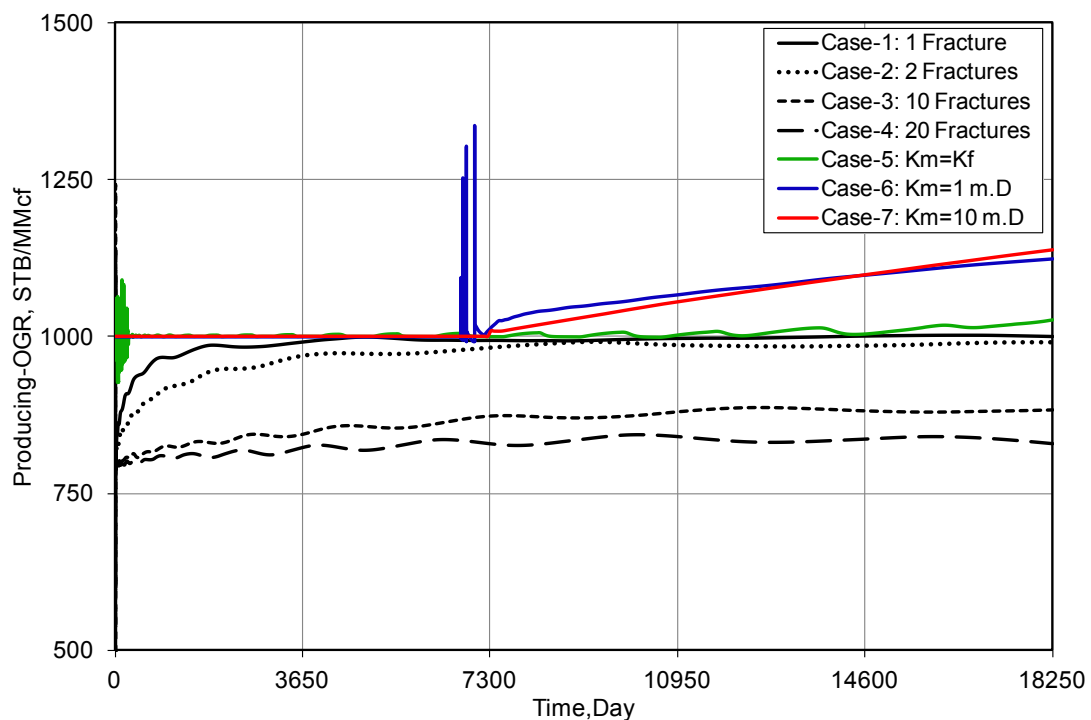


Fig. 4.5—Reservoir model producing oil-gas ratio profile of 7 cases by total revenue control, $r_s=1000$ STB/MMcf ($GOR_i=1,000$ scf/STB).

4.2 Cases of $GOR_i=3,000$ scf/STB

Initial gas-oil ratio of 3,000 scf/STB represents the fluid type of volatile oil. 7 cases are designed to compare their production performance under the total revenue control. **Table 4.3** lists the simulation optimal results of reservoir matrix permeability (k_m) and fracture permeability (k_f) combination. In the cases of 1, 2, 3 and 4, the fracture performs as a positive factor which improved the reservoir permeated capacity. However, the fracture in the cases 6 and 7 plays as a negative factor to limit the conductivity between reservoir matrix and horizontal well.

| Table 4.3—SIMULATION OPTIMAL RESULTS BY REVENUE CONTROL, $GOR_i=3,000$ scf/STB | | | | |
|--|-----------------|-------------|-------------|--|
| Case No. | Fracture-Number | k_m mD | k_f mD | |
| 1 | 1 | 0.025120 | 100000 | |
| 2 | 2 | 0.007236 | 100000 | |
| 3 | 10 | 0.000341 | 100000 | |
| 4 | 20 | 0.000087 | 100000 | |
| 5* | 1 | 0.125237 | 0.125237 | |
| 6 | 1 | 1 | 0.025621 | |
| 7 | 1 | 10 | 0.025010 | |

* $k_m=k_f$, fractures are not required to get 10 MMcf/day for the first 10 days cumulative production

Fig. 4.6 shows the 50-year cumulative revenue of each case. The cumulative revenue in all cases is same after the first 10 days' production. These profiles also indicate that high-permeability reservoir will yield larger revenue compared with low-permeability reservoir after a long time production (50 years).

The 50-years production profiles of gas and oil rate are shown in **Figs. 4.7 – 4.8**. In the high-permeability models ($k_m=1$ mD and $k_m=10$ mD), production keeps steady for the first 3 years. However, the production plateau in the low-permeability model is much shorter, less than one day. **Figs. 4.9 – 4.10** show the plot of producing gas-oil ratio and oil-gas ratio respectively. As seen in the ratio plot, the ratio stays at a stable level over the duration of 50 years of production.

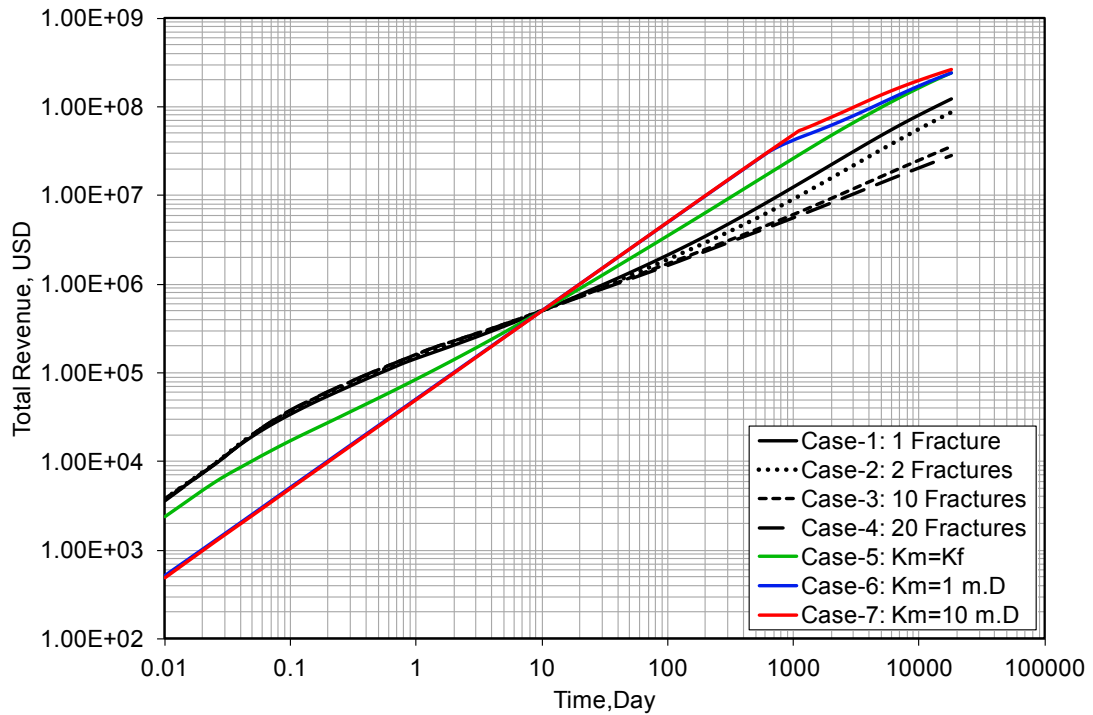


Fig. 4.6—Simulation well cumulative revenue of 50 years production of 7 cases, $GOR_i=3,000 \text{ scf/STB}$.

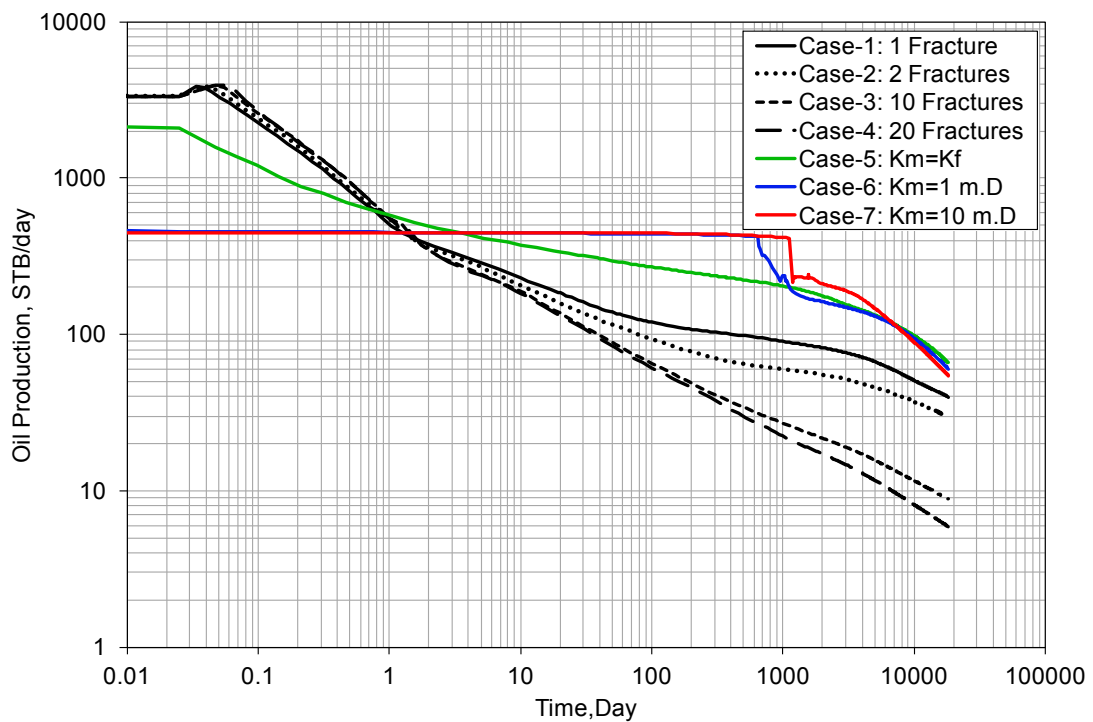


Fig. 4.7—Simulation well oil production profile of 7 cases by total revenue control, $GOR_i=3,000 \text{ scf/STB}$.

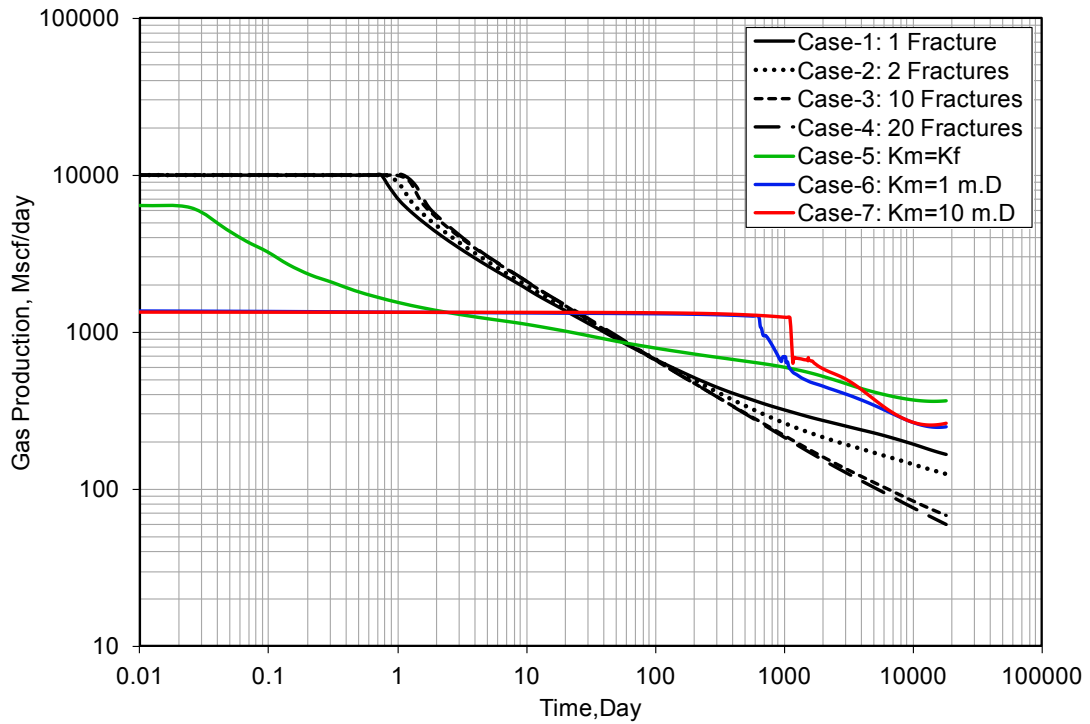


Fig. 4.8—Simulation well gas production profile of 7 cases by total revenue control, $GOR_i=3,000$ scf/STB

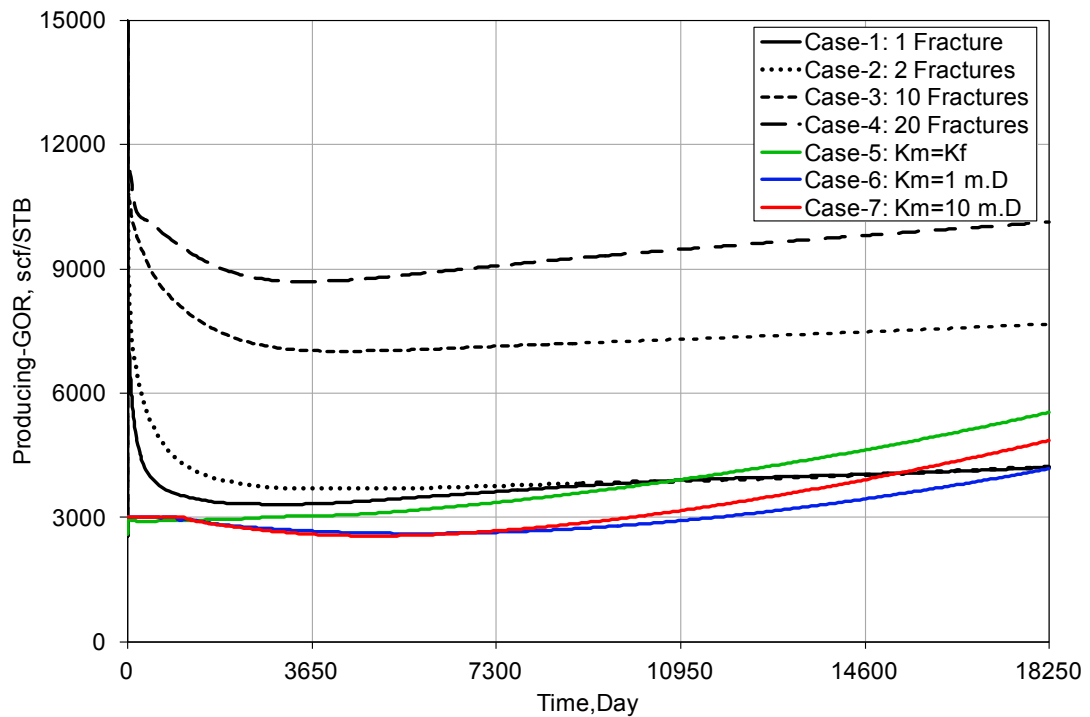


Fig. 4.9—Reservoir model producing gas-oil ratio profile of 7 cases by total revenue control, $GOR_i=3,000$ scf/STB.

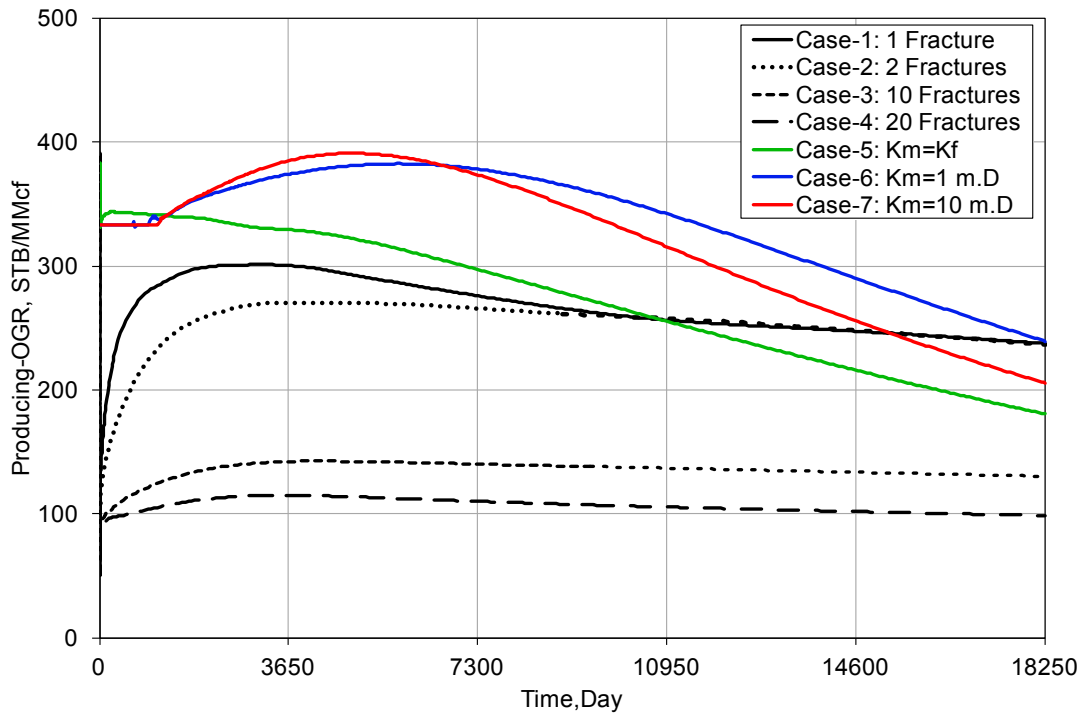


Fig. 4.10—Reservoir model producing oil-gas ratio profile of 7 cases by total revenue control, $r_s=333$ STB/MMcf ($GOR_i=3,000$ scf/STB).

4.3 Cases of $GOR_i=4,587$ scf/STB

Initial gas-oil ratio of 4,587 scf/STB represents the fluid type of near critical oil. 7 cases with specified reservoir permeability combination are simulated to obtain their optimal value under the total revenue constraint. The optimal results are shown in **Table 4.4**. These 7 cases include 4 cases of low-matrix-permeability reservoir and 2 cases of high-matrix-permeability reservoir, which represent the unconventional reservoir and conventional reservoir respectively. The critical case with identical permeability in matrix and fracture is also included in this study.

Fig. 4.11 shows the plot of 50-year production cumulative revenue. In general, high permeability reservoir will result large revenue after 50 years production. The production daily profile of oil and gas are shown in **Figs. 4.12 – 4.13**. Unlike the production profile of high permeability cases in $GOR_i=1,000$ scf/STB and $GOR_i=3,000$ scf/STB, there is no production plateau existing in these cases with $GOR_i=4,587$ scf/STB. The producing ratio of gas-oil and oil-gas were shown in the

Figs. 4.14 – 4.15. The ratio profile of $GOR_i=4,587$ scf/STB presents a typical trends for a near critical oil reservoir.

| Table 4.4—SIMULATION OPTIMAL RESULTS BY REVENUE CONTROL, $GOR_i=4,587$ scf/STB | | | |
|--|-----------------|-------------|-------------|
| Case No. | Fracture-Number | k_m mD | k_f mD |
| 1 | 1 | 0.043193 | 100000 |
| 2 | 2 | 0.011423 | 100000 |
| 3 | 10 | 0.000497 | 100000 |
| 4 | 20 | 0.000130 | 100000 |
| 5* | 1 | 0.348033 | 0.348033 |
| 6 | 1 | 1 | 0.163945 |
| 7 | 1 | 10 | 0.053445 |

* $k_m=k_f$, fractures are not required to get 10 MMcf/day for the first 10 days cumulative production

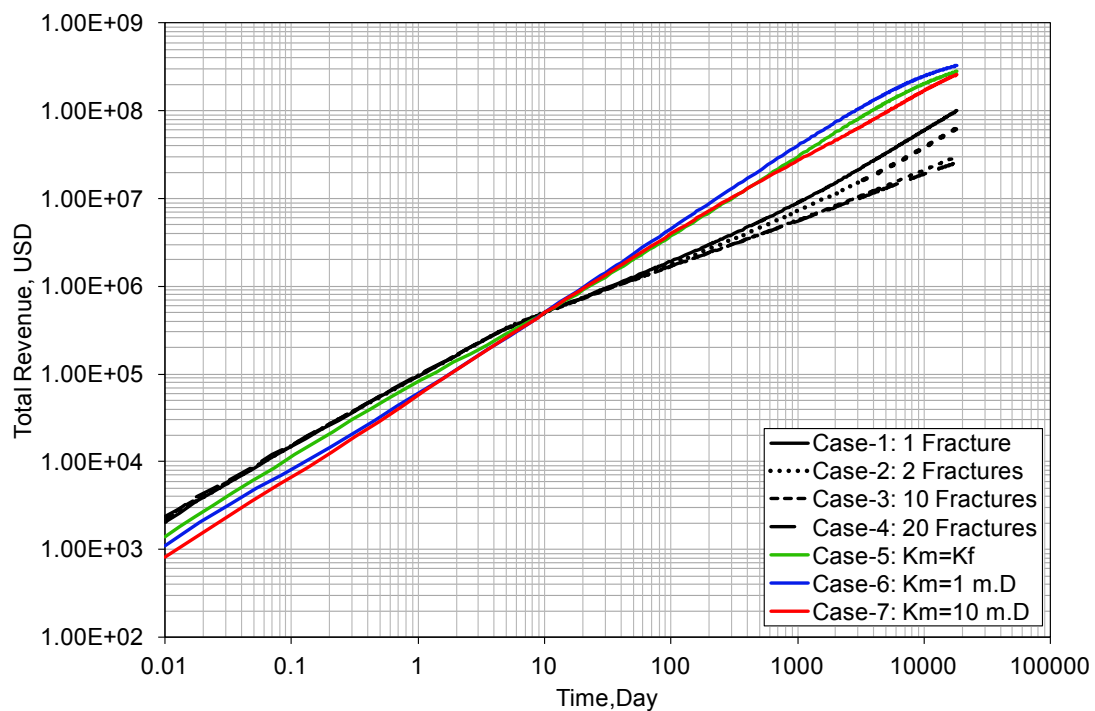


Fig. 4.11—Simulation well cumulative revenue of 50 years production of 7 cases, $GOR_i=4,587$ scf/STB.

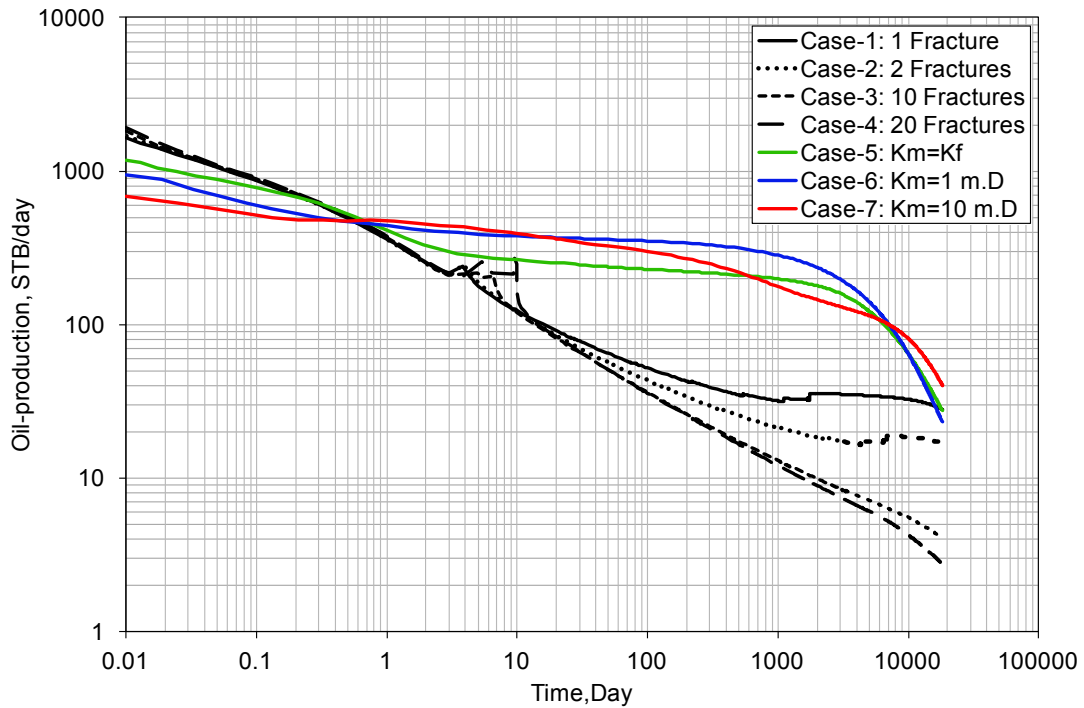


Fig. 4.12—Simulation well oil production profile of 7 cases by total revenue control, $GOR_i=4,587 \text{ scf/STB}$.

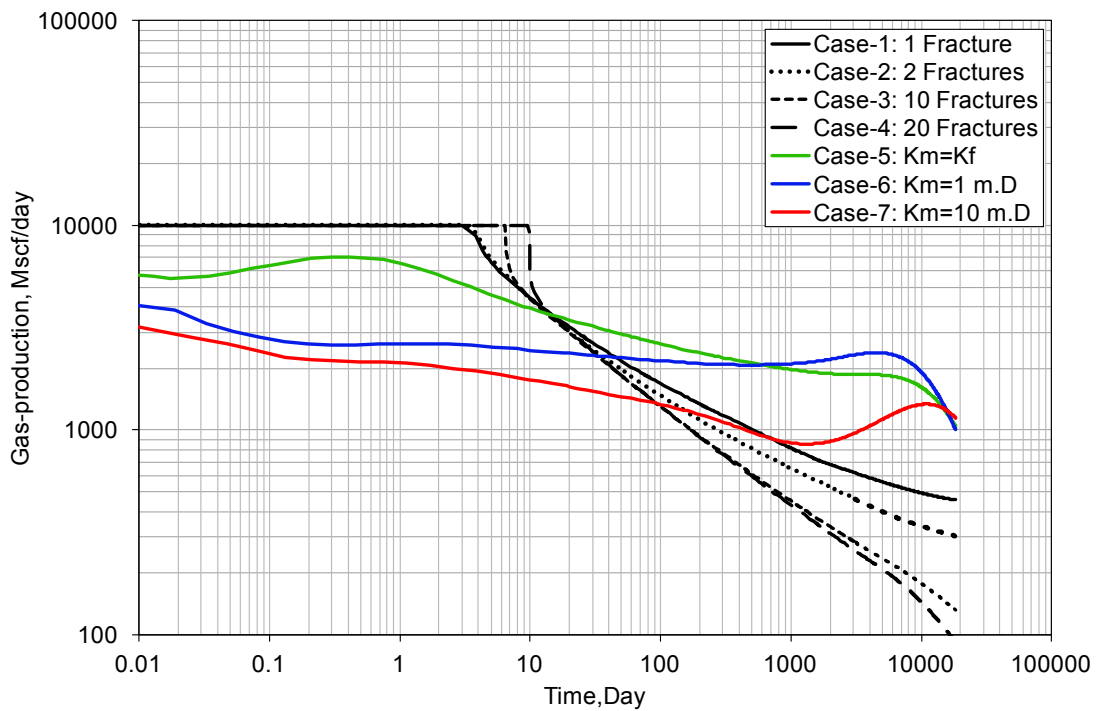


Fig. 4.13—Simulation well gas production profile of 7 cases by total revenue control, $GOR_i=4,587 \text{ scf/STB}$.

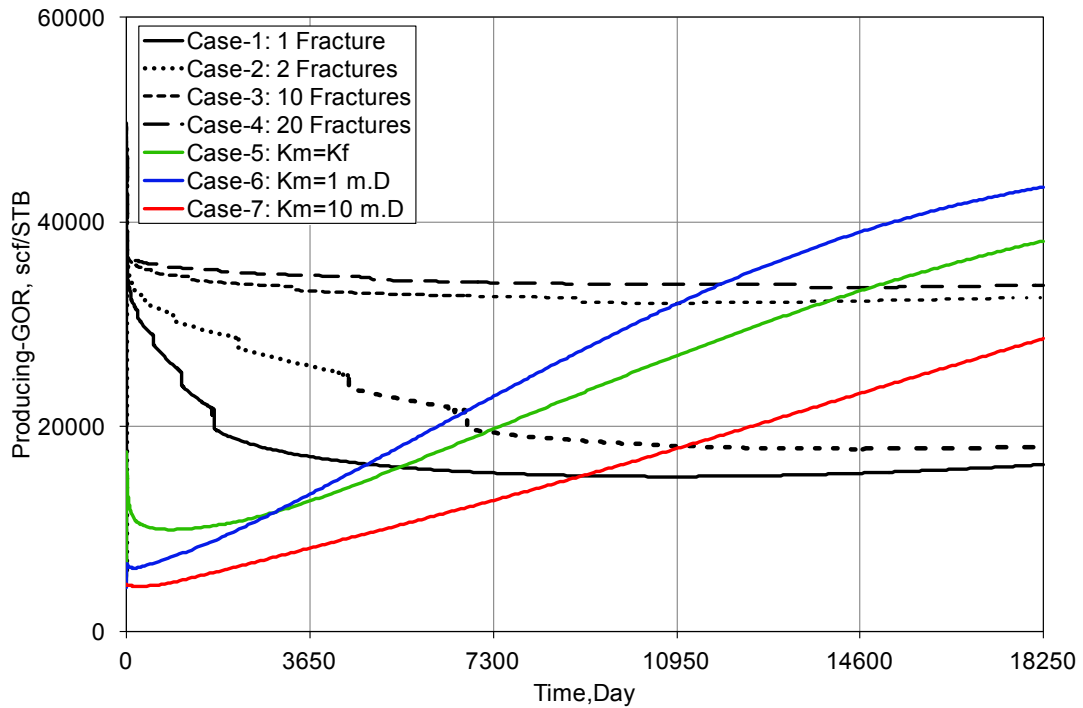


Fig. 4.14—Reservoir model producing gas-oil ratio profile of 7 cases by total revenue control, $GOR_i=4,587$ scf/STB.

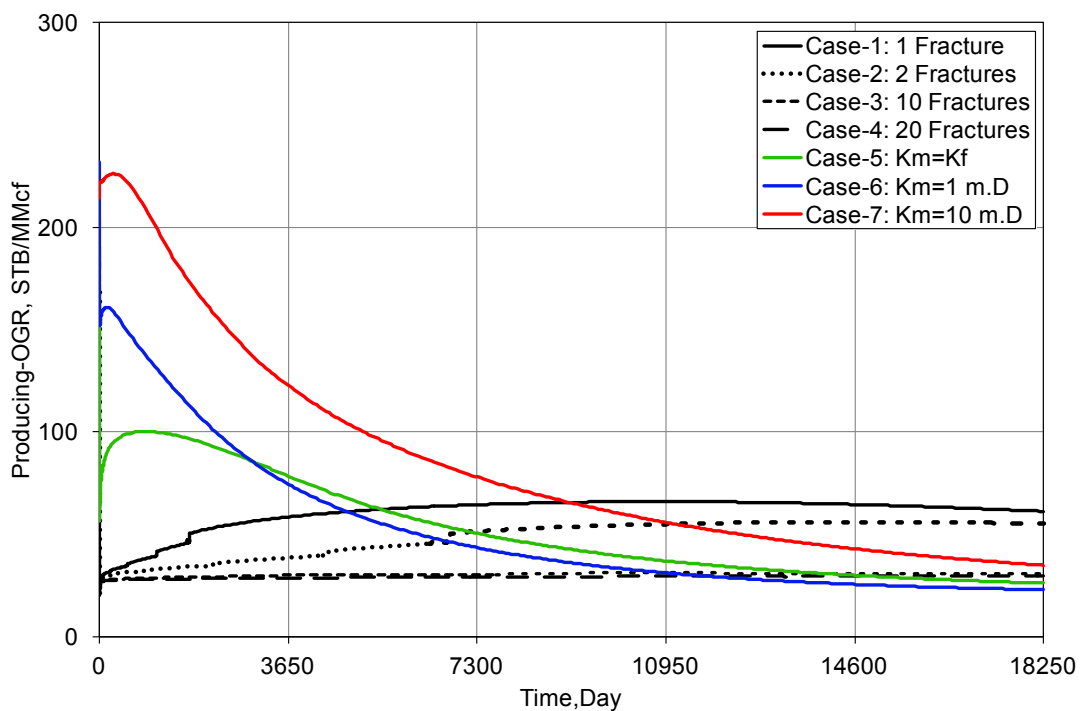


Fig. 4.15—Reservoir model producing oil-gas ratio profile of 7 cases by total revenue control, $r_s=218$ STB/MMcf ($GOR_i=4,587$ scf/STB).

4.4 Cases of $GOR_i=10,000$ scf/STB

The reservoir with an initial gas-oil ratio of 10,000 scf/STB represents the gas condensate reservoir. 7 cases with different permeability combination are run to obtain the revenue target. The optimal results of reservoir's parameters combination are shown in **Table 4.5**.

In all cases, the cumulative revenue of the first 10 days is same, 5×10^5 USD. And in general, the total revenue after 50 years production is high in the reservoir with high matrix permeability. The cumulative revenue profile of each case is shown in **Fig. 4.16**.

Figs. 4.17—4.18 show the well production profile of oil rate and gas rate. There is a 2—3 years production plateau existing in the cases of high matrix permeability ($k_m=1$ mD, 10 mD). However, the production's plateau in these cases of low matrix permeability lasted less than 10 days. The plots of producing gas-oil ratio and oil-gas ratio are given in **Figs. 4.19 – 4.20**. Simulation oscillation problem occurs in the case of $k_m=1$ mD, and more detailed analysis is included in **Appendix B**.

| Table 4.5—SIMULATION OPTIMAL RESULTS BY REVENUE | | | |
|--|-----------------|-------------|-------------|
| CONTROL: $GOR_i=10,000$ scf/STB | | | |
| Case No. | Fracture-Number | k_m mD | k_f mD |
| 1 | 1 | 0.017500 | 100000 |
| 2 | 2 | 0.004595 | 100000 |
| 3 | 10 | 0.000197 | 100000 |
| 4 | 20 | 0.000050 | 100000 |
| 5* | 1 | 0.159000 | 0.159000 |
| 6 | 1 | 1 | 0.032707 |
| 7 | 1 | 10 | 0.031466 |

* $k_m=k_f$, fractures are not required to get 10 MMcf/day for the first 10 days cumulative production

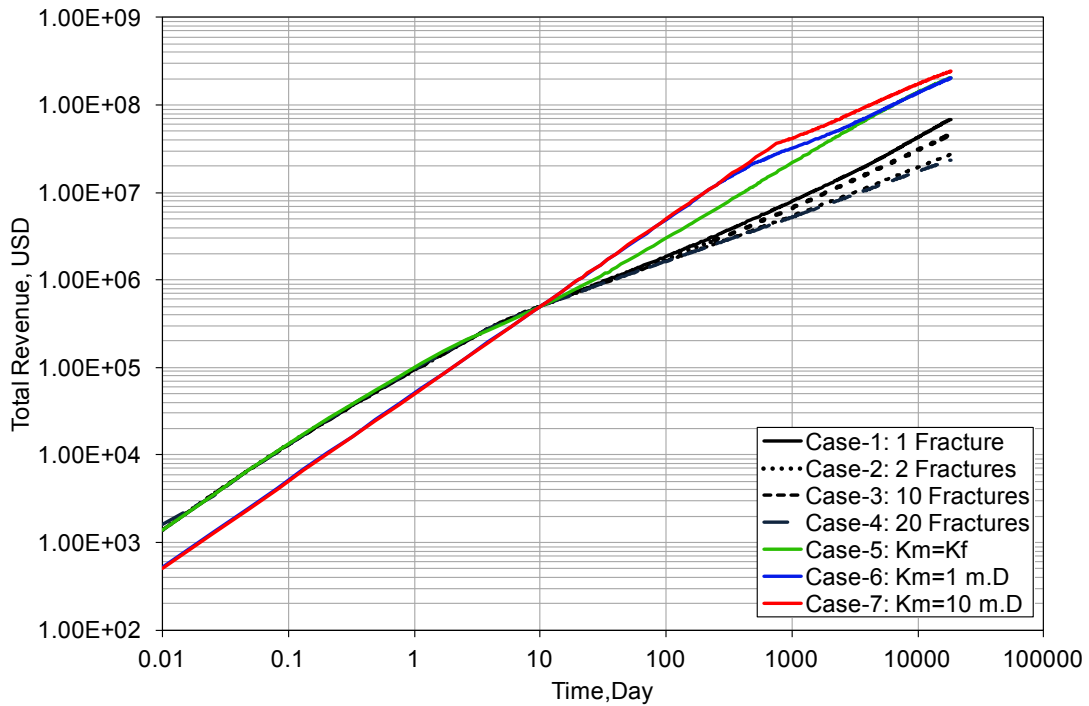


Fig. 4.16—Simulation well cumulative revenue of 50 years production of 7 cases, $GOR_i=10,000 \text{ scf/STB}$.

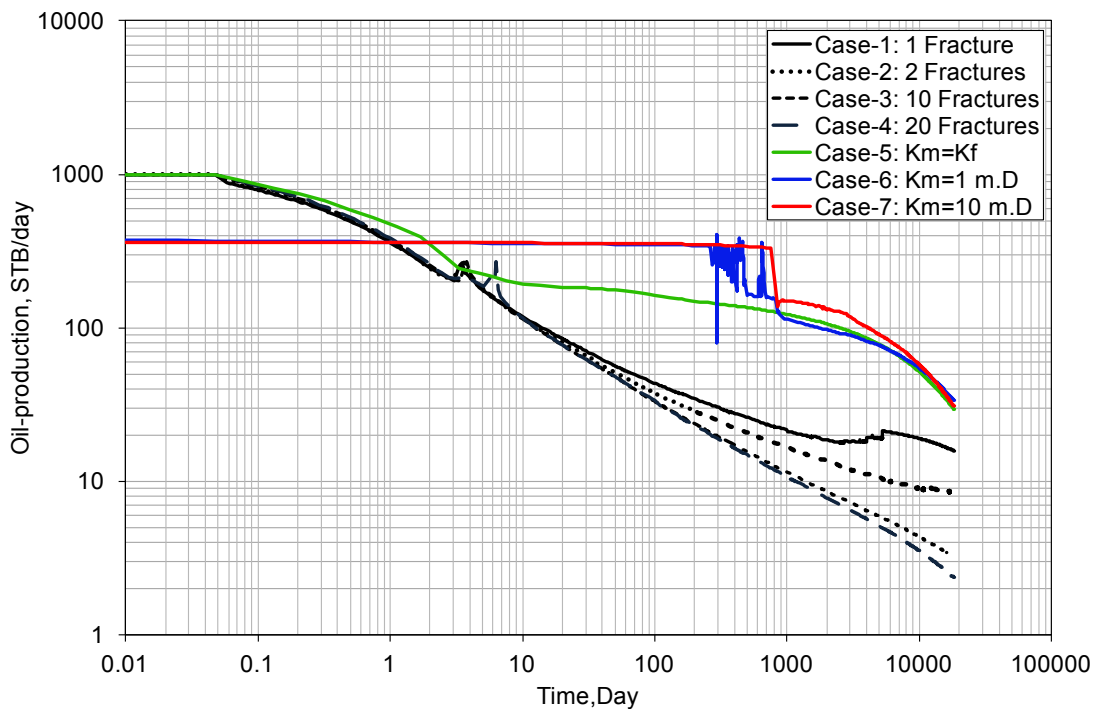


Fig. 4.17—Simulation well oil production profile of 7 cases by total revenue control, $GOR_i=10,000 \text{ scf/STB}$.

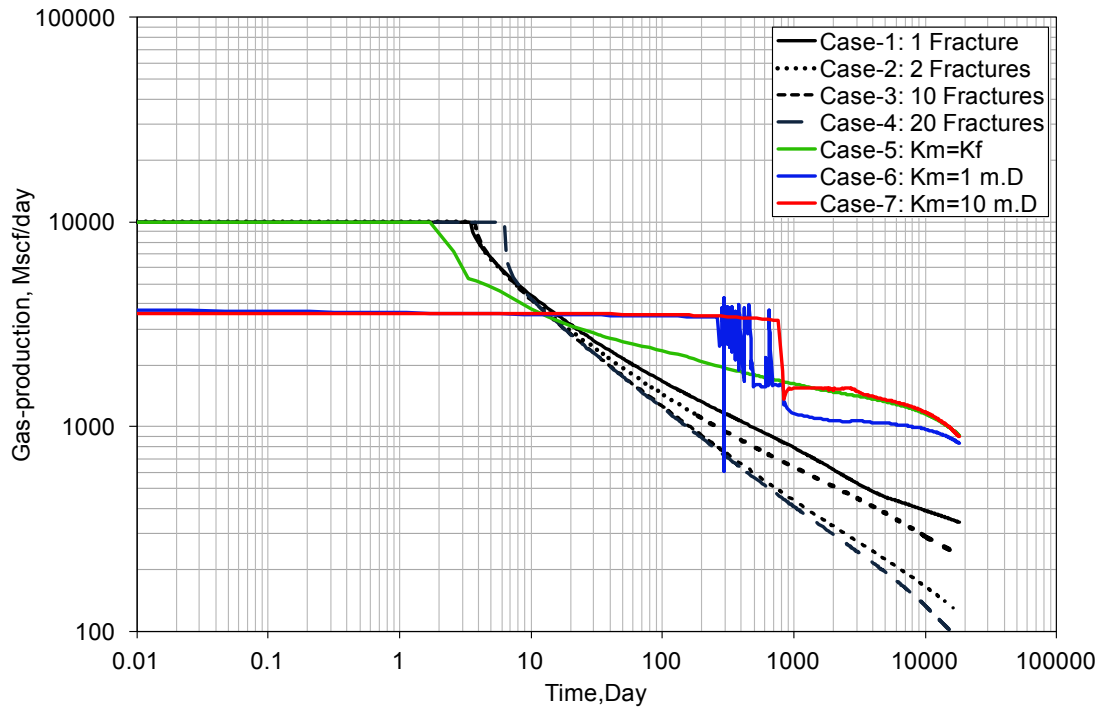


Fig. 4.18—Simulation well gas production profile of 7 case by total revenue control, $GOR_i=10,000$ scf/STB.

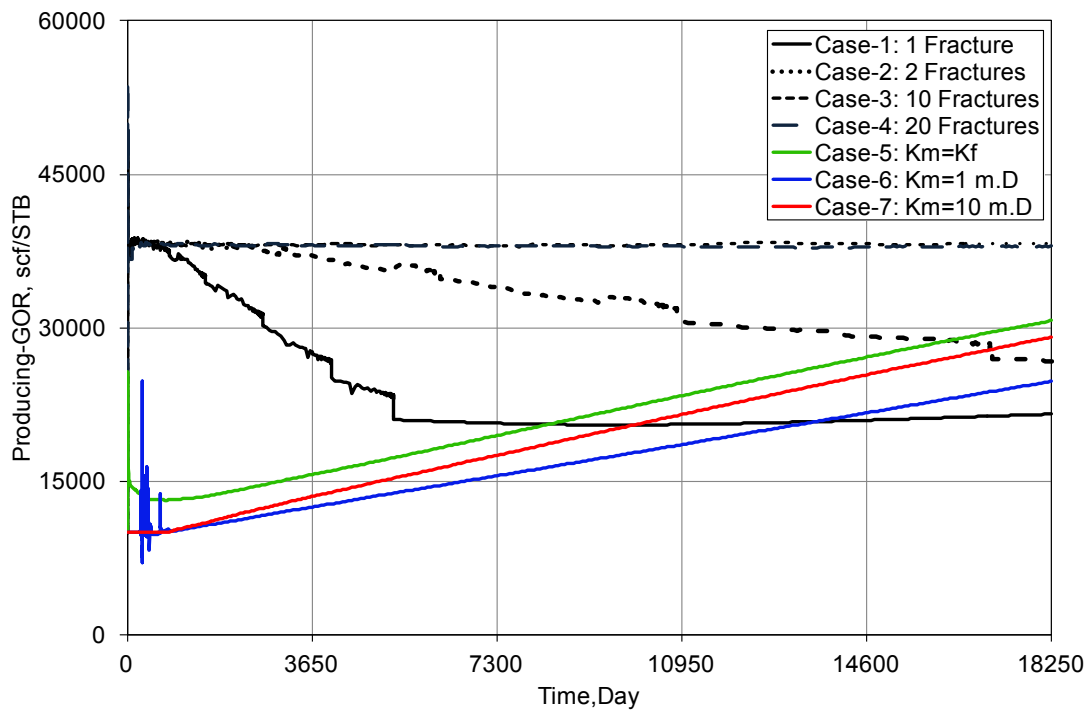


Fig. 4.19—Reservoir model producing oil-gas ratio profile of 7 cases by total revenue control, $GOR_i=10,000$ scf/STB.

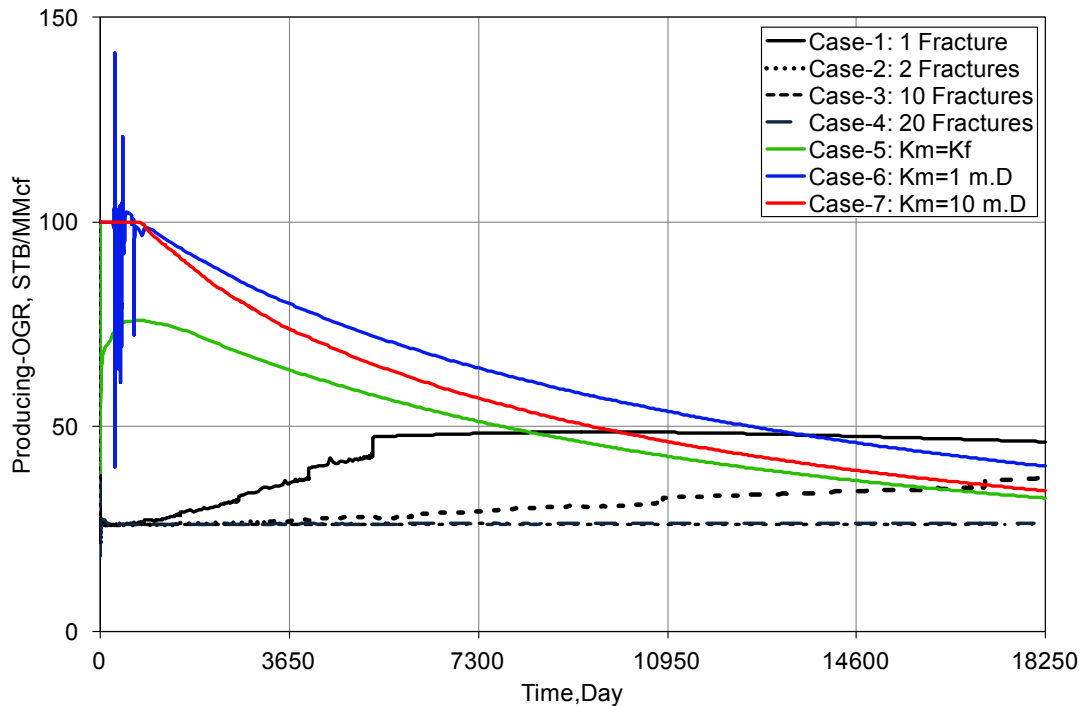


Fig. 4.20—Reservoir model producing oil-gas ratio profile of 7 cases by total revenue control, $r_s=100$ STB/MMcf($GOR_i=10,000$ scf/STB).

4.5 Cases of $GOR_i=100,000$ scf/STB

The gas-oil ratio of 100,000 scf/STB represents the fluid type of wet gas, which well production is gas with a small amount of liquid. 7 simulation cases with different permeability combination are run to present their production performances. **Table 4.6** lists the optimal results that reached the revenue standard of the first 10 days.

Fig. 4.21 shows the total revenue plot as a function of time. In the first 10 days, the total revenue of each case is similar, but the permeability has a significant impact on the revenue after this period. In general, high permeability in reservoir will result great total revenue after a 50-years production.

The shape of gas production profiles is similar with plot of oil production, which is shown in **Figs. 4.22 – 4.23**. The similar shape is result out of the fixed R_p and r_p over 50 years of production. The initial gas-oil ratio in simulator is higher than the maximum value of gas-oil ratio in the fluid model: 47,315 scf/STB. Under the influence of this limitation, the producing ratios of gas-oil and oil-gas is fixed to

47,315 scf/STB and 21.135 STB/MMscf respectively, which is shown in **Figs. 4.24 – 4.25**. This value of r_p is the minimum value of the r_s in the fluid model.

| Table 4.6—SIMULATION OPTIMAL RESULTS BY REVENUE CONTROL: $GOR_i=100,000$ scf/STB | | | |
|---|-----------------|-------------|-------------|
| Case No. | Fracture-Number | k_m mD | k_f mD |
| 1 | 1 | 0.014468 | 100000 |
| 2 | 2 | 0.004011 | 100000 |
| 3 | 10 | 0.000176 | 100000 |
| 4 | 20 | 0.000044 | 100000 |
| 5* | 1 | 0.116188 | 0.116188 |
| 6 | 1 | 1 | 0.060323 |
| 7 | 1 | 10 | 0.055708 |

* $k_m=k_f$, fractures are not required to get 10 MMcf/day for the first 10 days cumulative production

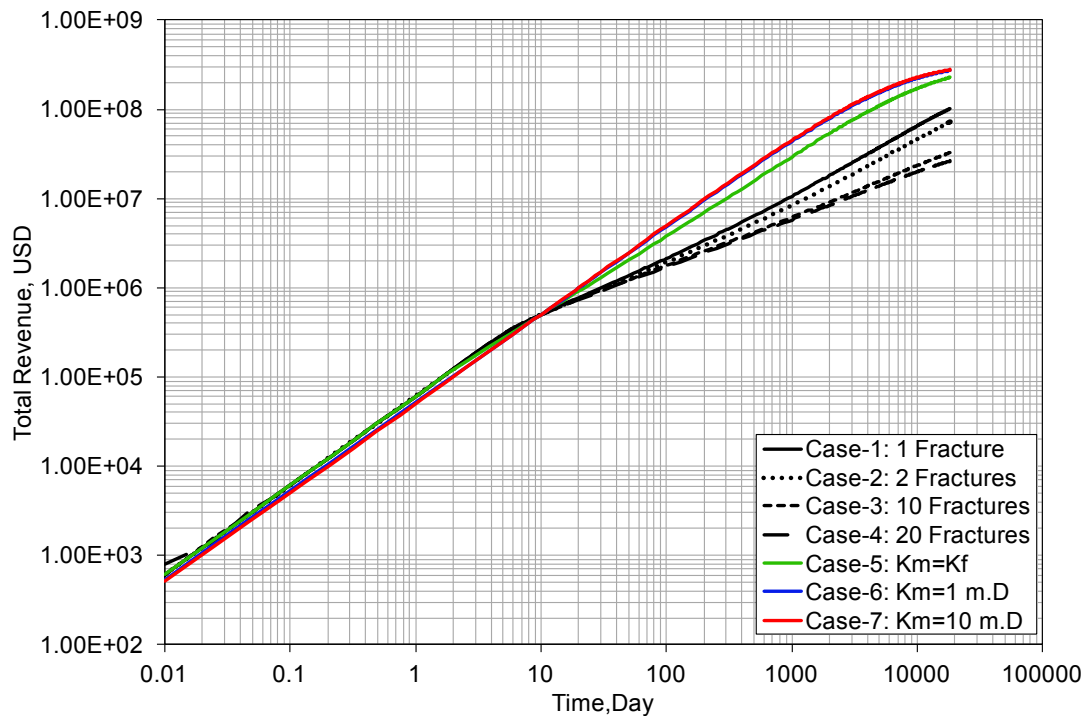


Fig. 4.21—Simulation well cumulative revenue of 50 years production of 7 cases, $GOR_i=100,000$ scf/STB.

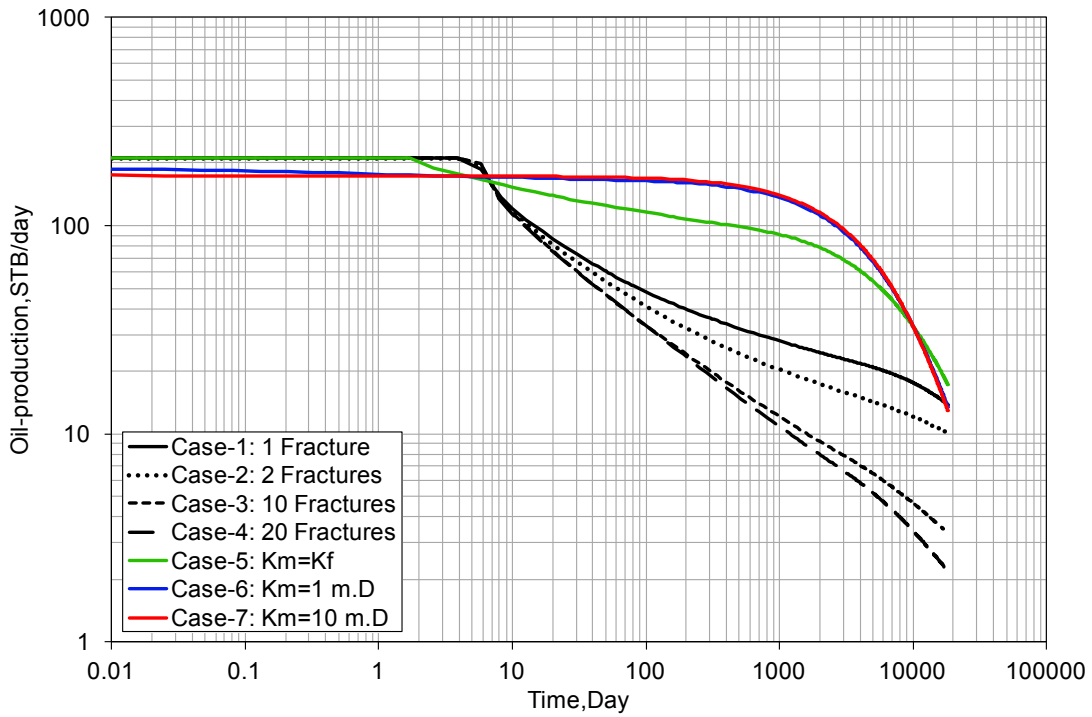


Fig. 4.22—Simulation well oil production profile of 7 cases by total revenue control, $GOR_i=100,000$ scf/STB.

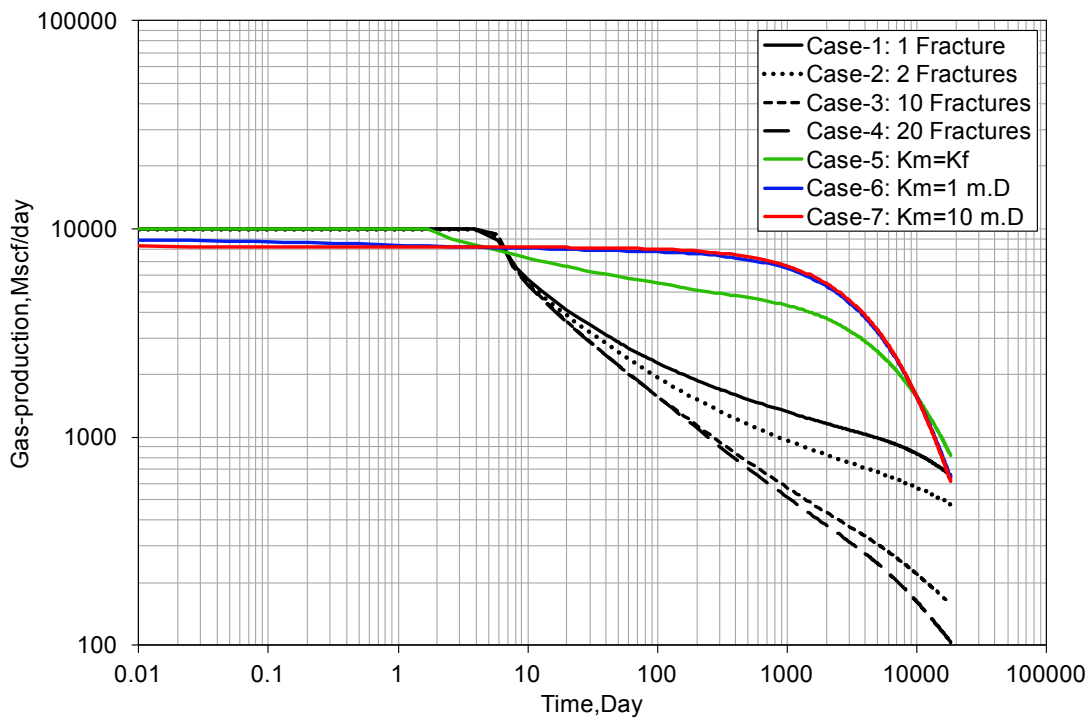


Fig. 4.23—Simulation well gas production profile of 7 cases by total revenue control, $GOR_i=100,000$ scf/STB.

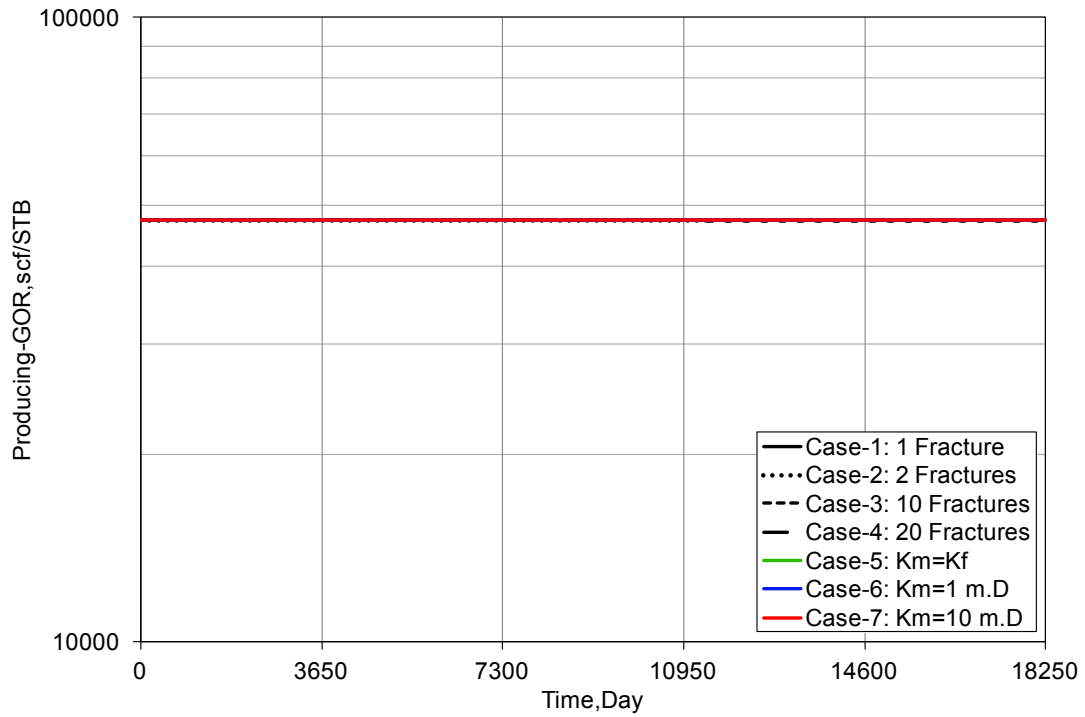


Fig. 4.24—Reservoir model producing gas-oil ratio profile of 7 cases by total revenue control, $GOR_i=100,000$ scf/STB.

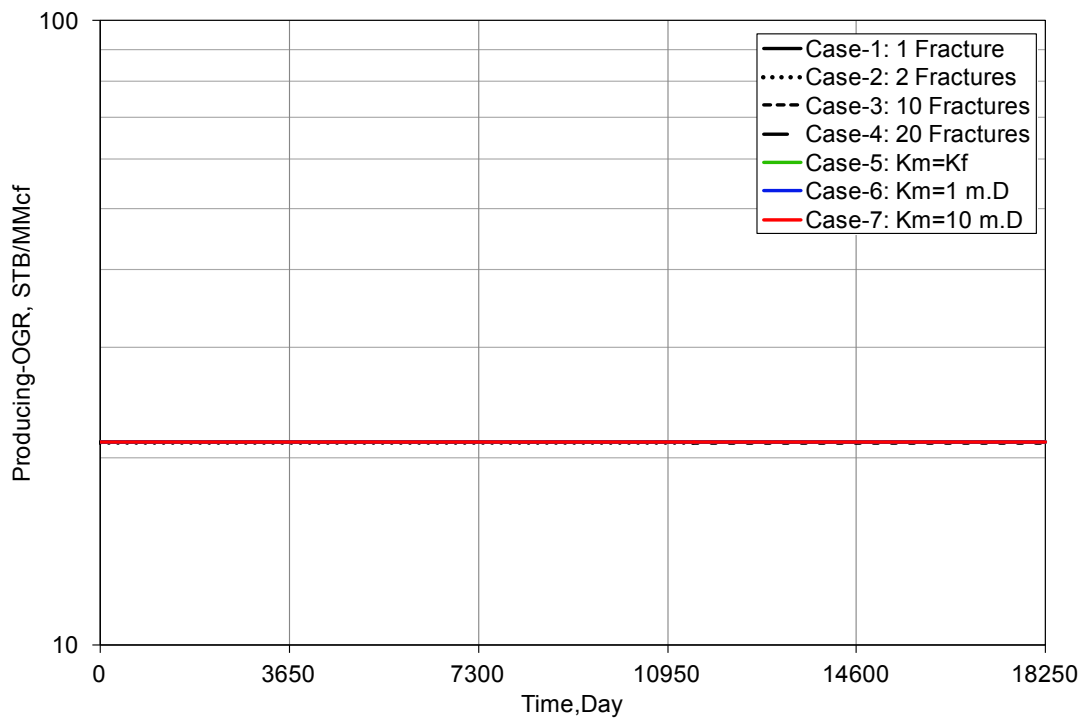


Fig. 4.25—Reservoir model producing oil-gas ratio profile of 7 cases by total revenue control, $r_s=21,135$ STB/MMcf($GOR_i=100,000$ scf/STB).

4.6 Revenue Control Summary

This section summarizes the main features of these simulation cases which controlled under total revenue of 5×10^5 USD in the first 10 days. 7 cases with different reservoir matrix permeability are studied, ranging from conventional reservoir to unconventional reservoir.

Comparing with the simulations which controlled by gas production rate, there are some similar features and also some differences in the simulation results. The phenomenon of oil-gas ratio keeping in stable level appears in all low permeability reservoir cases. However, the optimal results of permeability combination are significantly different. This is because simulation in this section is controlled by total revenue, which takes into account the production of gas and oil together. But the simulation in Chapter 3 is only considered the gas rate. The production rate relates to the fluid type, which is controlled by the initial gas-oil ratio (GOR_i).

On the condition of critical case, unlike the relation of permeability and GOR_i in the case of gas rate control, the relation under total revenue control is not unidirectional, which is shown in **Fig. 4.26**. This is influenced by the simulation is considered both oil and gas, and the price of products is different.

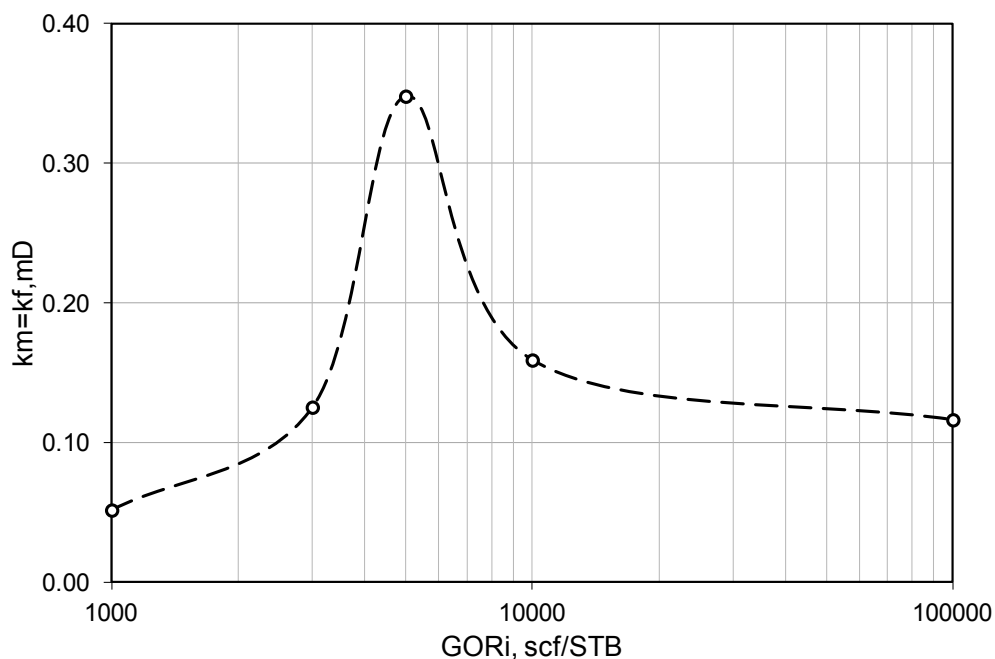


Fig. 4.26—Relation between reservoir permeability and initial gas-oil ratio, cases controlled by total revenue.

The optimal results of reservoir permeability are significantly affected by the initial gas-oil ratio. **Fig. 4.27** shows the revenue contribution from oil production in different fluids types. In the volatile oil reservoir ($GOR_i=1,000$ scf/STB), more than 90% of total revenue is from oil production. On the contrary, around 35% of total revenue is from oil production when reservoir fluid is wet gas ($GOR_i= 100,000$ scf/STB). The revenue contribution from oil production will vary in the near critical oil reservoir and gas condensate reservoir if reservoir permeability is changed.

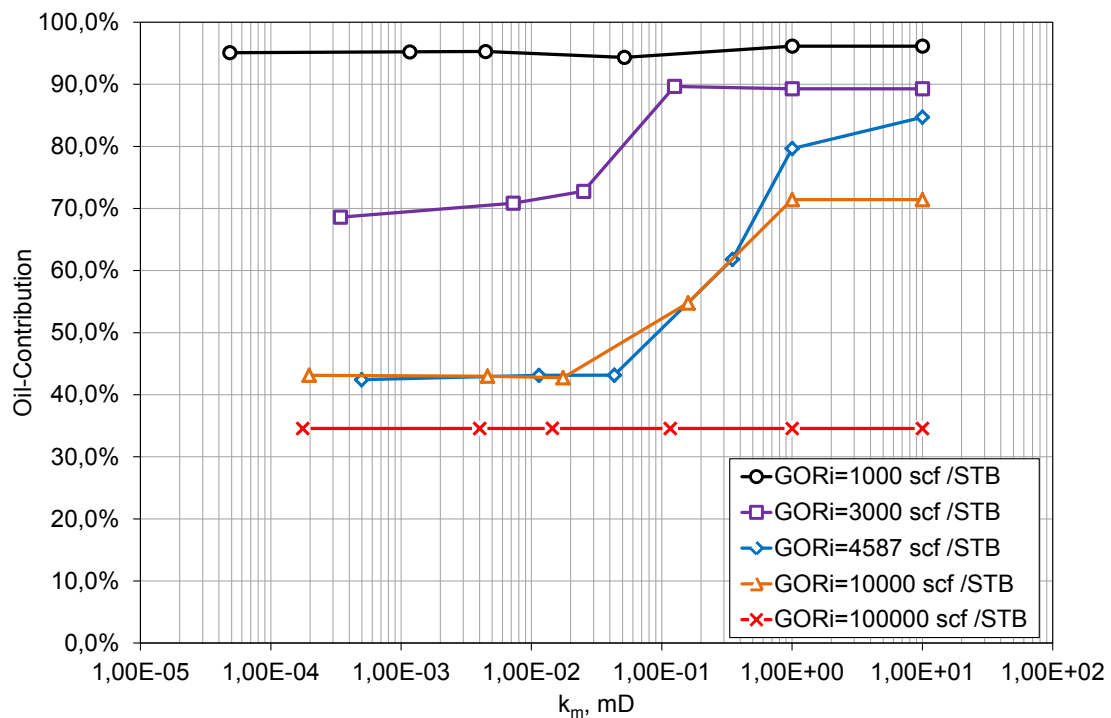


Fig. 4.27—Oil contribution to total revenue of the first 10 days in different initial gas-oil ratio

Chapter 5

Fractures Number and Reservoir Permeability Relation

This section presents the relation between the number of fractures and reservoir permeability when hydraulic fractures are used to stimulate the reservoir. The required number of fractures in the shale reservoir is calculated based on the analysis results.

5.1 Gas Rate Control

Table 5.1 lists the optimal results of the fractures number and reservoir permeability when the fracture permeability is fixed to 100,000 mD.

In low permeability reservoir, such as tight gas reservoir or shale reservoir, hydraulic fracturing treatment is required to obtain an economic production rate. The number of fractures is increased as matrix permeability reduced. **Fig. 5.1** shows the relation between the number of fractures and the reservoir matrix permeability when fixed the fracture permeability to 100,000 mD. There is a good agreement of linear correlation between fractures number and matrix permeability in log-log scale.

| Table 5.1—RELATION BETWEEN FRACTURES NUMBER AND RESERVOIR PERMEABILITY BY GAS RATE CONTROL, $k_f=100,000$ mD | | | | | |
|--|-------------------------|-----------------------|-----------------------|-----------------------|-----------------------|
| Fractures Number | Segment Spacing acre | GORi=1000 | GORi=3000 | GORi=4587 | GORi=10000 |
| | | scf/STB k_m^*,mD | scf/STB k_m^*,mD | scf/STB k_m^*,mD | scf/STB k_m^*,mD |
| 1 | 320 | 0.9245 | 0.2690 | 0.1100 | 0.0440 |
| 2 | 160 | 0.3000 | 0.0710 | 0.0298 | 0.0120 |
| 10 | 32 | 0.0165 | 0.0030 | 0.0013 | 0.0005 |
| 20 | 16 | 0.0043 | 0.0008 | 0.0003 | 0.0001 |

k_m^* : optimal result of matrix permeability when the fractures number and fluids type is fixed

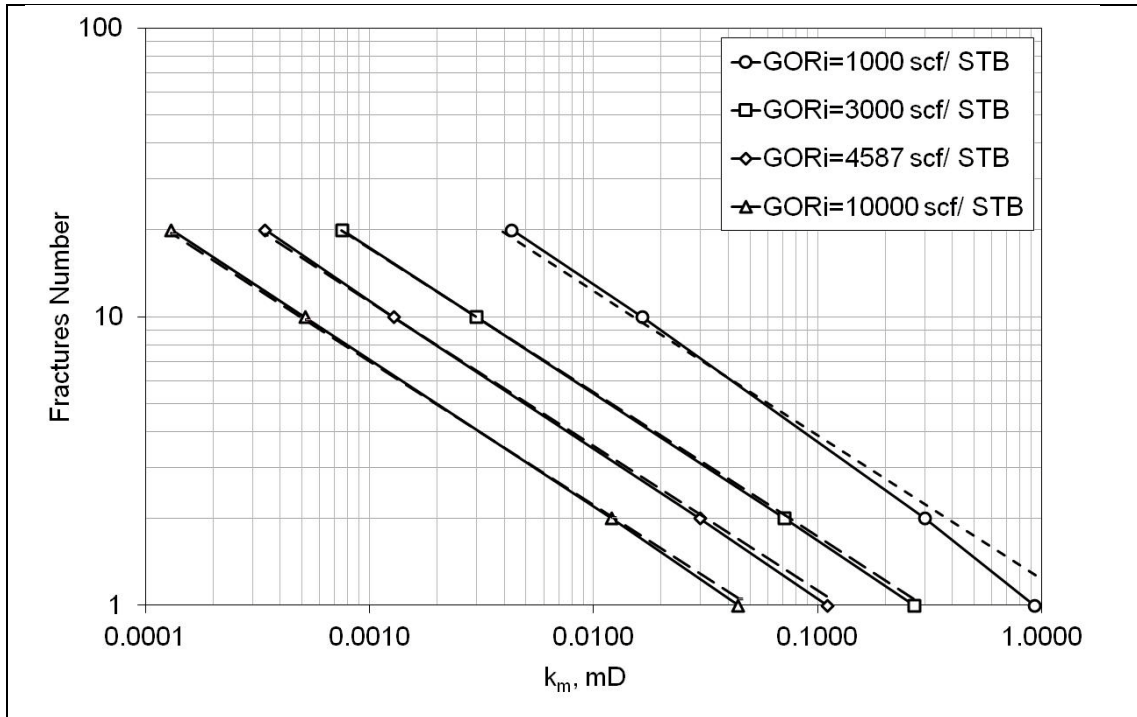


Fig. 5.1—Plot of fractures number in the function of reservoir matrix permeability, gas production control.

Equations between fractures number and matrix permeability are established for different reservoir fluids. The reservoir fluid system is defined by the initial gas-oil ratio (GOR_i). Dashed lines in **Fig. 5.1** show equation's plots of each fluid type:

$$\text{GOR}_i=1,000 \text{ scf/STB:} \quad N_f = \frac{1.2301}{\sqrt{k_m}} \quad (5.1)$$

$$\text{GOR}_i=3,000 \text{ scf/STB:} \quad N_f = \frac{0.5465}{\sqrt{k_m}} \quad (5.2)$$

$$\text{GOR}_i=4,587 \text{ scf/STB:} \quad N_f = \frac{0.3566}{\sqrt{k_m}} \quad (5.3)$$

$$\text{GOR}_i=10,000 \text{ scf/STB:} \quad N_f = \frac{0.2217}{\sqrt{k_m}} \quad (5.4)$$

In general, the relation between the fractures number and the reservoir matrix permeability is:

$$N_f = \frac{f(G, k_f, \text{GOR}_i, \text{Con}, \dots)}{\sqrt{k_m}} \quad (5.5)$$

Where:

$f(G, k_f, \text{GOR}_i, \text{Con}, \dots)$ is a function of fracture geometry, fracture permeability or conductivity, initial gas-oil ratio/reservoir fluids type, and simulation constraint, etc.

These equations can be used in the economic fractures number calculation when reservoir fluid type is specified. **Table 5.2** lists the calculation results in the shale reservoir range: 10^{-5} mD – 10^{-3} mD. Ignoring the revenue from oil production will lead to a big fractures number request in the oil type. This is unreasonable in times of high oil price.

| Fluid type | GOR _i | Fractures number(Integer Number) | | |
|---|------------------|----------------------------------|------------|-----------|
| Gas Condensate | 10000 | 70 | -----> 22 | -----> 7 |
| Near Critical Oil | 4587 | 113 | -----> 36 | -----> 11 |
| Volatile Oil B | 3000 | 173 | -----> 55 | -----> 17 |
| Volatile Oil A | 1000 | 389 | -----> 123 | -----> 39 |
| | | 1,00E-05 | 1,00E-04 | 1,00E-03 |
| Shale Reservoir, k_m, mD | | | | |

5.2 Revenue Control

In the simulations under total revenue control, production both from gas and oil were calculated to the total revenue. Total revenue of 5×10^5 USD was set as the economic standard of the simulation constraint. **Table 5.3** summarizes the optimal results of matrix permeability in terms of fractures number when the fracture permeability is fixed to 100,000 mD. The relation between the number of fractures and matrix permeability is shown in **Fig. 5.2**. There is a linear correlation in the log-log plot.

| Fractures Number | Segment Spacing acre | GOR _i =1000 scf/STB k _m *,mD | GOR _i =3000 scf/STB k _m *,mD | GOR _i =4587 scf/STB k _m *,mD | GOR _i =10000 scf/STB k _m *,mD | GOR _i =100000 scf/STB k _m *,mD |
|------------------|----------------------|--|--|--|---|--|
| 1 | 320 | 0.00444 | 0.02512 | 0.04319 | 0.01750 | 0.01447 |
| 2 | 160 | 0.00117 | 0.00724 | 0.01142 | 0.00460 | 0.00401 |
| 10 | 32 | 0.00005 | 0.00034 | 0.00050 | 0.00020 | 0.00018 |
| 20 | 16 | 0.00001 | 0.00009 | 0.00013 | 0.00005 | 0.00004 |

k_m*: optimal result of matrix permeability when the fractures number and fluids type is fixed

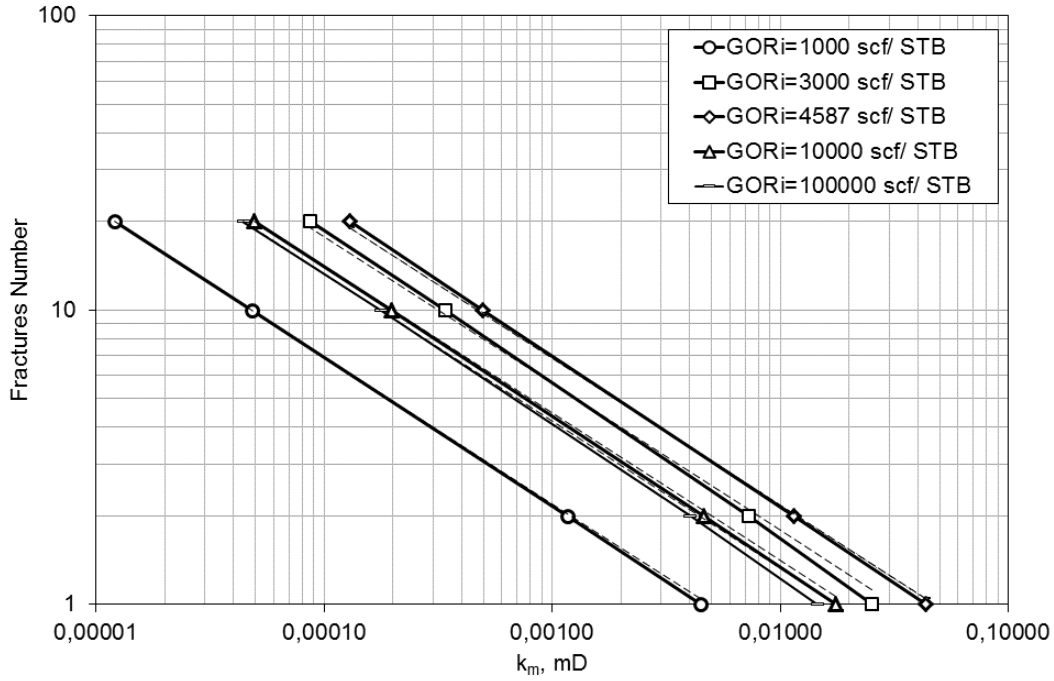


Fig. 5.2—Plot of fractures number in the function of reservoir matrix permeability, total revenue control.

Equations for each fluid system was generated based on the simulation results,

$$\text{GOR}_i=1,000 \text{ scf/STB:} \quad N_f = \frac{0.06936}{\sqrt{k_m}} \quad (5.6)$$

$$\text{GOR}_i=3,000 \text{ scf/STB:} \quad N_f = \frac{0.178}{\sqrt{k_m}} \quad (5.7)$$

$$\text{GOR}_i=4,587 \text{ scf/STB:} \quad N_f = \frac{0.217}{\sqrt{k_m}} \quad (5.8)$$

$$\text{GOR}_i=10,000 \text{ scf/STB:} \quad N_f = \frac{0.1407}{\sqrt{k_m}} \quad (5.9)$$

$$\text{GOR}_i=100,000 \text{ scf/STB:} \quad N_f = \frac{0.1326}{\sqrt{k_m}} \quad (5.10)$$

In general, same as the equation of (5.5), the relation between fractures number and matrix permeability is:

$$N_f = \frac{f(G, k_f, \text{GOR}_i, \text{Con}, \dots)}{\sqrt{k_m}} \quad (5.11)$$

Where:

$f(G, k_f, \text{GOR}_i, \text{Con}, \dots)$ is a function of fracture geometry, fracture permeability or conductivity, initial gas-oil ratio/reservoir fluids type, and simulation constraint, etc.

Table 5.4 gives the calculation results of required fractures number for shale reservoir which based on the generated equation. Numerically, the number of fractures in shale reservoir is much less than the results from gas rate control, particularly in the case of liquid rich reservoir, such as volatile oil and near critical oil. In the range of shale reservoir, the plot between fractures number and reservoir permeability reservoir is shown in **Fig. 5.3**. This plot can be used to fractures number evaluation if the reservoir's permeability and fluids type are known. Note that, all of this evaluation is based on the assumption of 5×10^5 USD total revenue in the first 10 days.

| Table 5.4—CALCULATION RESULTS OF FRACTURES NUMBER REQUEST BY GENERATED EQUATION, REVENUE CONTROL | | | | | | |
|---|------------------|--------------------------------------|--------|----------|--------|----------|
| Fluid type | GOR _i | Fractures number(Integer Number) | | | | |
| Wet Gas | 100000 | 42 | -----> | 13 | -----> | 4 |
| Gas Condensate | 10000 | 44 | -----> | 14 | -----> | 4 |
| Near Critical Oil | 4587 | 69 | -----> | 22 | -----> | 7 |
| Volatile Oil B | 3000 | 56 | -----> | 18 | -----> | 6 |
| Volatile Oil A | 1000 | 22 | -----> | 7 | -----> | 2 |
| | | 1,00E-05 | | 1,00E-04 | | 1,00E-03 |
| | | Shale Reservoir, k _m , mD | | | | |

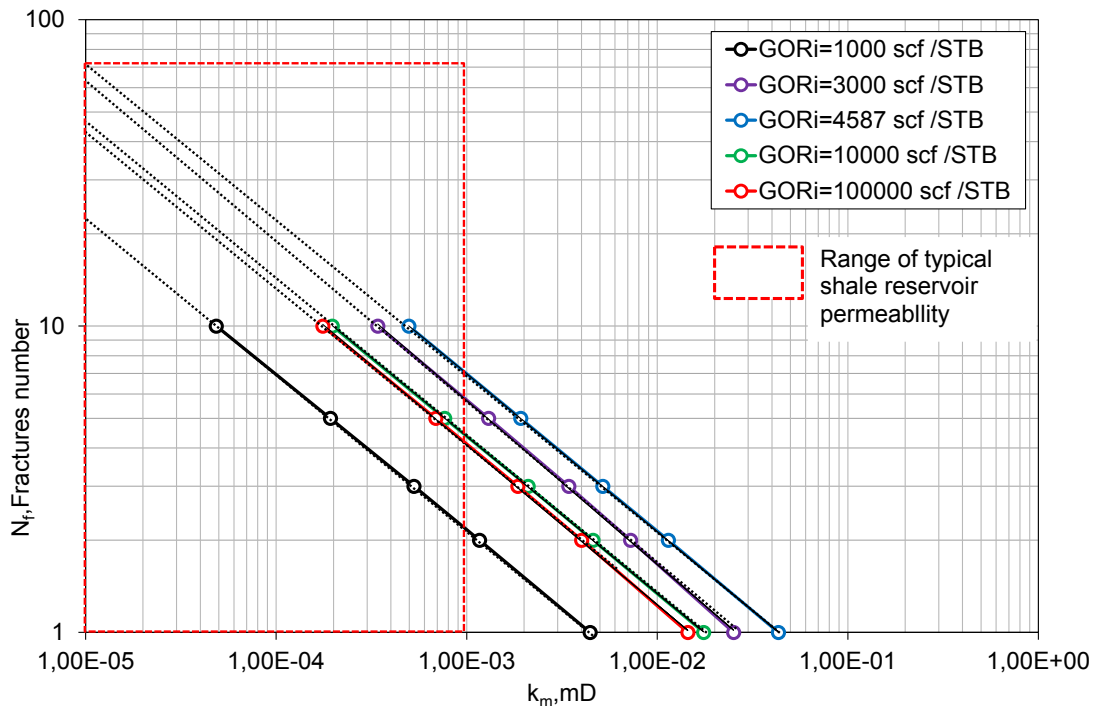


Fig. 5.3—Plot of fractures number and reservoir permeability when the fracture permeability fix to 100,000 mD and cumulative revenue of 5×10^5 USD.

Chapter 6

Production Performance Trends Study

This section presents the production performance variation trends from conventional reservoir to unconventional reservoir. The production from reservoir is not only the gas, but also petroleum liquid. Producing oil-gas ratio (r_p) is a precise parameter that is used to analyze the production performance of a liquid rich reservoir. A reservoir with initial gas-oil ratio of 4,587 scf/STB represents the near critical oil. In this part, the trends of producing oil-gas ratio are systematically studied, and the reservoir permeability ranges from high to ultra low. All of the results are based on numerical simulations.

Simulation models are designed with matrix permeability ranging from 10 mD to 10^{-5} mD. There are three combinations of matrix permeability and fracture permeability in the reservoir:

- High matrix permeability with low fracture permeability, fracture implemented as a damage factor which restricts the fluid flow from reservoir matrix to the well.
- Matrix permeability equal to fracture permeability, fracture on this condition is not contributing to the well's production.
- The fracture permeability is fixed to 100,000 mD together with low matrix permeability.

The optimal results from simulation are listed on **Table 6.1**. The value of fractures number is using an integer number, except the case when matrix permeability is closes to 0.1 mD.

The models are run to 50 years to compare their production performance of producing oil-gas ratio. Two concerns were expressed.

1, in the cases with high matrix permeability ($k_m=10$ mD, 5 mD and 1 mD), oil-gas ratio is high in the early stage and then decline during production period if the reservoir is developed by pressure depletion.

2, in the cases with low matrix permeability ($k_m=0.001$ mD, 0.0001mD and 0.00001mD), oil-gas ratio drops immediately and stays in a low level over the duration of 50-years-production period.

| Table 6.1—SIMULATION OPTIMAL RESULTS of CASE: GOR_i=4,587 scf/STB | | | |
|--|-------------------|------------------|-------|
| k_m, mD | | k_f, mD | N_f |
| 10 | | 0.0534 | 1 |
| 5 | | 0.0769 | 1 |
| 1 | | 0.1639 | 1 |
| 0.5 | | 0.2363 | 1 |
| 0.348 | | 0.348 | 0 |
| 0.12 | ≈ 0.1 | 100000 | 0.5* |
| 0.0114 | ≈ 0.01 | 100000 | 2 |
| 0.000988 | ≈ 0.001 | 100000 | 7 |
| 0.000092 | ≈ 0.0001 | 100000 | 23 |
| 0.0000094 | ≈ 0.00001 | 100000 | 75 |

* half length of standard fracture length, 100 ft

The variation tendency of oil-gas ratio from high permeability to low permeability is shown in **Fig. 6.1**. It indicates that more liquids can be extracted from the conventional reservoir (high permeability) by pressure depletion. The producing oil-gas ratios (r_p) in conventional reservoir will decline as the production continues. Liquids production out of gas in unconventional reservoir is low and keeps steady, particularly for the reservoir of permeability less than 0.001 mD.

As the reservoir is developed by pressure depletion, the average pressure of reservoir determines the quantity of energy stored in the reservoir. In low permeability reservoir, pressure depletion only occurs in the area that nearby the fracture, the reservoir average pressure keeps in a high level even after decades of production. That means the fluids in the area which is far away from the fracture are hard to flow to the wellbore. In contrast, the fluids in the high-permeability reservoir are much easier to flow from reservoir matrix to the fracture and to the wellbore. The average pressure of reservoir will drop a lot if the reservoir has been developed for some decades. **Fig. 6.2** presents a 10 years producing oil-gas ratio profile in terms of reservoir average

pressure. The plots in the cases of $k_m=5$ mD and 10 mD are close to each other, indicating a constant volume depletion (CVD) process. The ratios of oil-gas in the cases with matrix permeability less than 0.001 md ($k_m=0.001$ mD, 0.0001 mD and 0.00001 mD) remain in a low level. As introduced in Chapter 2, the initial reservoir pressure is 4,800 psia. After 10 years of production, the average pressure is reduced to 3,850 psia in the reservoir with matrix permeability of 1 mD. However, a constant pressure of 4,650 psia occurs in the reservoir with ultra low permeability ($k_m=0.00001$ mD). This is because the pressure drop is only happened in the area where around the fracture, or the drainage takes a long time to reach the segment's boundary.

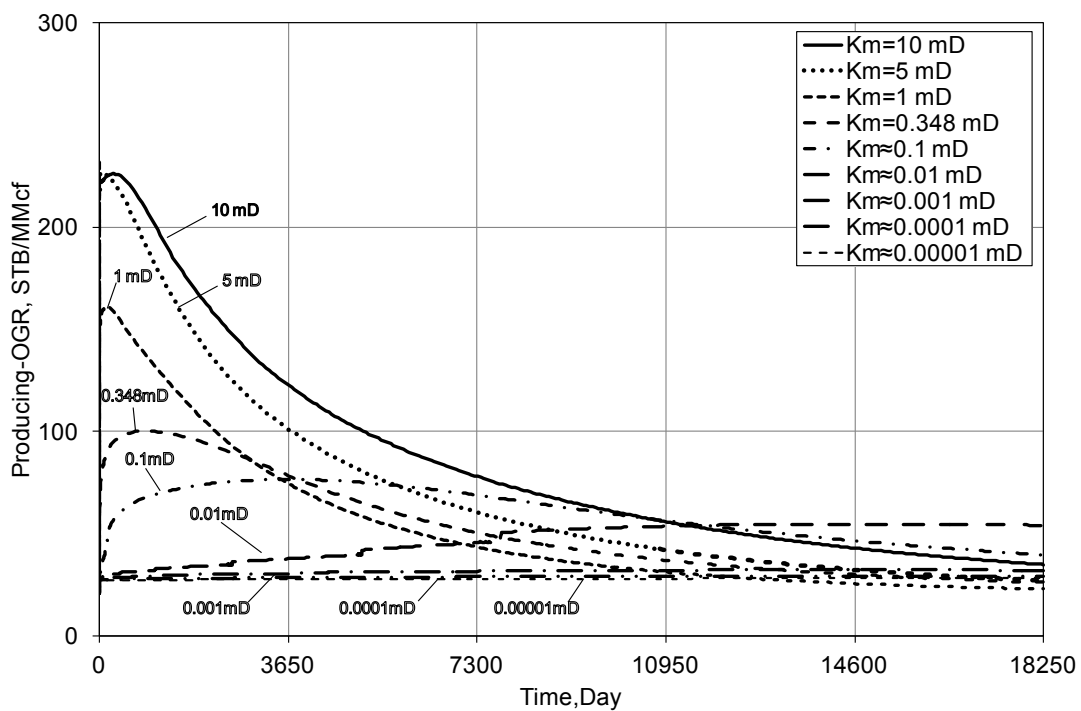


Fig. 6.1—Producing oil-gas ratio versus time, $r_s=218$ STB/MMcf ($GOR_i=4,587$ scf/STB).

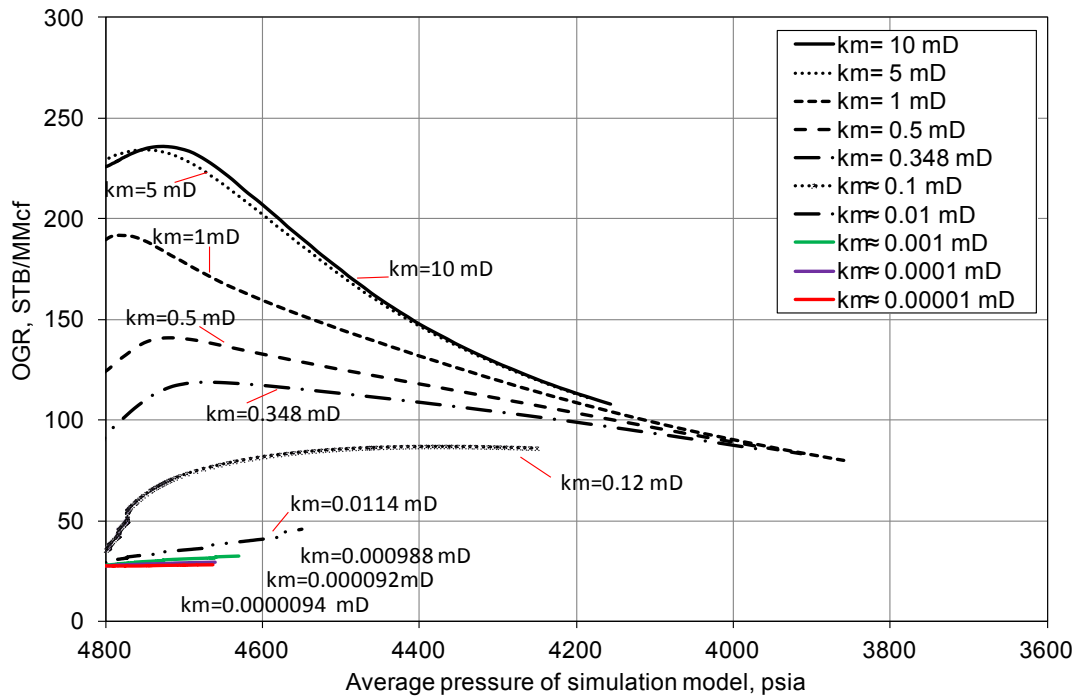


Fig. 6.2—Producing oil-gas ratio versus reservoir average pressure, $r_s = 218$ STB/MMcf ($GOR_i = 4,587$ scf/STB).

After a 10-year production, the gas recovery factor is 2.7% in the lowest permeability case. We find a good way/method to classify the conventional reservoir and unconventional reservoir based on the producing oil-gas ratio. The processes are:

1. Selecting the gas recovery factor of 2.7% as the standard.
2. All cases with different reservoir matrix permeability are run to meet this standard.
3. Plot r_s/r_p versus k_m (reservoir matrix permeability) when gas recovery factor reached 2.7% of each case.

The plot of r_s/r_p versus reservoir matrix permeability is shown in **Fig. 6.3**. The value of r_s/r_p represents the percentage of liquids production from the reservoir. In the high-permeability reservoir, the value of r_s/r_p is close or equal to 1, while in the low-permeability reservoir, the value of r_s/r_p is much higher. In this plot, three zones can be classified: conventional, transition, and unconventional. This classification is based on the well production performance and is related to reservoir fluid types. In this near critical oil system, reservoir permeability higher than 1 mD can be defined as the conventional reservoir, and reservoir with permeability less than 0.0001 mD is classified to unconventional reservoir, the reservoir with permeability between these two values is a transition zone. This method of classification is useful and practical in the industry. Note that, the standard of unconventional is significantly different

between dry gas reservoir and volatile oil reservoir. In the dry gas reservoir, the gas is easier to extract from the reservoir of 0.1 mD permeability, while in the volatile oil reservoir it becomes difficult of the same permeability value.

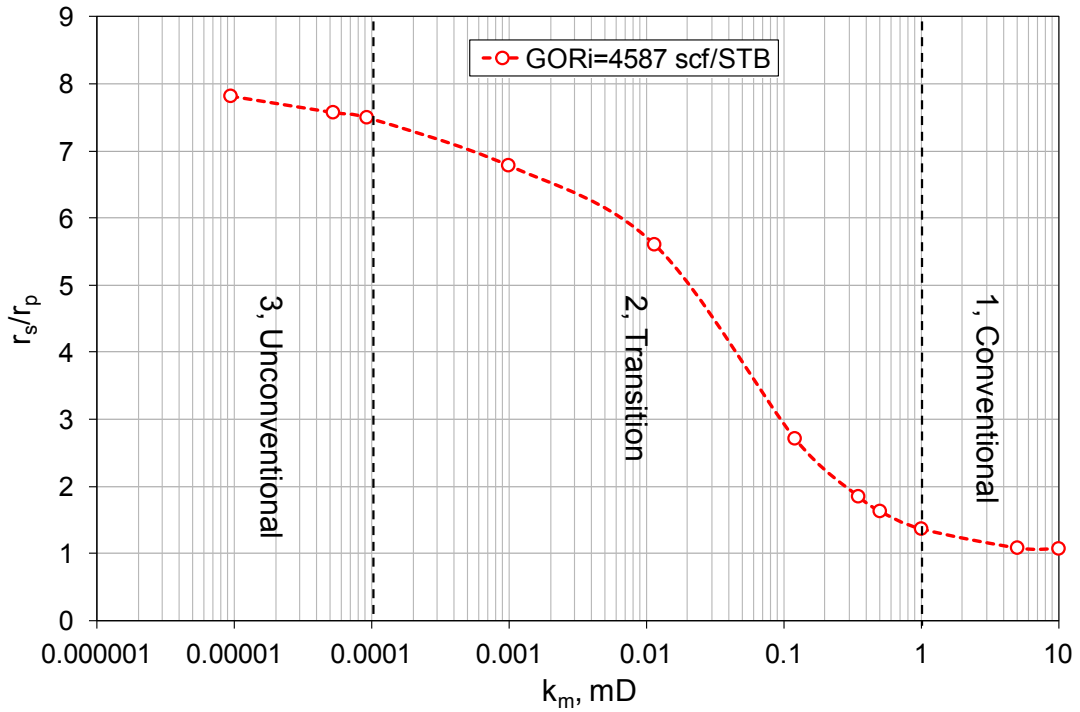


Fig. 6.3— r_s/r_p versus reservoir matrix permeability, and reservoir classification.

Chapter 7

Conclusion

Based on the ideal reservoir model, with a homogeneous layer and of constant parameters, numerical simulations were run in this study. Finally, the relation between fractures number and reservoir permeability are established. The trends of Production performance from conventional reservoir to unconventional reservoir were displayed as well.

1. With assumption of economic standards of either gas rate or total revenue, the required number of fractures will increase as the reservoir permeability decreases.
2. The reservoir with low permeability is developed economically with the help of hydraulic fracturing technology/treatment.
3. The relation between the number of fractures and reservoir permeability shows a linear correlation in the logarithm-logarithm coordinate system.
4. Less hydraulic fractures is required if the revenue of oil production is considered, particularly for the high liquid contents reservoir, such as volatile oil reservoir, near critical oil reservoir and liquid rich gas condensate reservoir.
5. The production performance ranging from the conventional reservoir to the unconventional reservoir is significantly affected by the reservoir permeability. In the conventional reservoir (high permeability), more liquid will be extracted from the reservoir and the producing ratio of oil-gas is declined as production. In the unconventional reservoir, the oil-gas ratio drops immediately and stays at a low level during the whole period of production.
6. Simulation oscillation problem only occurs in some cases of high permeability reservoir. This problem is caused by the model's gridding geometry and can be removed by changing the perforation location to the fracture's tip. A detailed analysis is included in **Appendix B**.

7. The plot of r_s/r_p versus reservoir permeability can be used to classify the zones of conventional, transition, and unconventional.

References

1. D.M.Anderson, M.Nobakht, S.Moghadam, and L.Mattar,Fekete Associates Inc.: *Analysis of production data from fracture shale gas wells*. SPE 131787.
2. Whitson, C.H. and Torp, S.B.: *Evaluating Constant Volume Depletion Data*. JPT(March,1983) 610;Trans AIME,275.
3. Waleed Fazelpour, Emerson/Roxar.: *Innovative Simulation Techniques to History Match Horizontal Wells in Shale Gas Reservoirs*. SPE Eastern Regional Meeting, 12-14 October 2010, Morgantown, West Virginia, USA. SPE 139114.
4. Cipolla, C. L., Lolon, E. P., Erdle, J. C., and Rubin, B. (2009). : *Reservoir Modeling in Shale-Gas Reservoirs*. SPE Eastern Regional Meeting, Charleston, West Virginia, USA. SPE 125530.
5. Brage Rugstad Knudsen.: *A Numerical Study of Fracture Geometry and Gridding in Shale Gas Reservoir models*. September 5, 2011
6. Golan, M. and Whitson, C.H.: *Well Performance*, Prentice-Hall, New York (1985).
7. Ge, J., Ghassemi, A.: *Permeability Enhancement in Shale Gas Reservoirs after Stimulation by Hydraulic Fracturing*. 45th U.S. Rock Mechanics / Geomechanics Symposium, June 26 - 29, 2011, San Francisco, California

Appendix A

SENSOR Input Deck

```
TITLE
  Simulate gas/oil flow in shale reservoir.
  Treat horizontal multi-frac well using vertical cartersian model
  - 1 mile x 1 mile area, with different farctures based on different
  reservoir matrix permeability.
  - ignore gravity.
  - initial GOR=4587 scf/STB
  - reservoir thickness h=200 ft, half-fracture length yf=200 ft.
ENDTITLE
```

```
GRID 81 74 1
RUN
CPU
IMPLICIT
D4
```

```
MAPSFILE P SG SO SW KX
MAPSPRINT P SG SO SW KX
```

```
C      Bwi cw      denw visw cr      pref
MISC 1      3.0E-6 62.4 0.5  4.0E-6 6000
```

```
C -----
C I_CELLS          81
C J_CELLS          74
C K_CELLS          1
C DEPTH           10000
C SYM_ELEMENTS     2
C -----
```

```
C -----
C Cell width along wellbore
C -----
```

```
DELX XVAR
```

| | | | | | | | | |
|---------|---------|---------|---------|---------|---------|---------|---------|---------|
| 27.8751 | 21.9888 | 17.3455 | 13.6827 | 10.7934 | 8.51416 | 6.71626 | 5.29801 | 4.17924 |
| 3.29673 | 2.60057 | 2.05141 | 1.61822 | 1.27651 | 1.00695 | 0.79432 | 0.62658 | 0.49427 |
| 0.3899 | 0.30756 | 0.24262 | 0.19138 | 0.15097 | 0.11909 | 0.09394 | 0.0741 | 0.05846 |
| 0.04611 | 0.03638 | 0.02869 | 0.02263 | 0.01785 | 0.01408 | 0.01111 | 0.00876 | 0.00691 |
| 0.00545 | 0.0043 | 0.00339 | 0.00268 | 0.01 | 0.00268 | 0.00339 | 0.0043 | 0.00545 |
| 0.00691 | 0.00876 | 0.01111 | 0.01408 | 0.01785 | 0.02263 | 0.02869 | 0.03638 | 0.04611 |
| 0.05846 | 0.0741 | 0.09394 | 0.11909 | 0.15097 | 0.19138 | 0.24262 | 0.30756 | 0.3899 |
| 0.49427 | 0.62658 | 0.79432 | 1.00695 | 1.27651 | 1.61822 | 2.05141 | 2.60057 | 3.29673 |
| 4.17924 | 5.29801 | 6.71626 | 8.51416 | 10.7934 | 13.6827 | 17.3455 | 21.9888 | 27.8751 |

```
C -----
C Cell width away from wellbore
C -----
```

```
DELY YVAR
```

| | | | | | | | | |
|--------|--------|---------|---------|---------|---------|--------|--------|--------|
| 164.52 | 96.855 | 57.0189 | 33.5672 | 19.7611 | 11.6334 | 6.8487 | 4.0318 | 2.3736 |
| 1.3973 | 0.8226 | 0.4843 | 0.2851 | 0.1678 | 0.0988 | 0.0582 | 0.0342 | 0.0202 |

| | | | | | | | | |
|--------|--------|---------|---------|---------|---------|---------|---------|--------|
| 0.0119 | 0.0070 | 0.0026 | 0.0032 | 0.0040 | 0.0051 | 0.0064 | 0.0080 | 0.0101 |
| 0.0127 | 0.0159 | 0.0200 | 0.0251 | 0.0315 | 0.0396 | 0.0497 | 0.0625 | 0.0785 |
| 0.0986 | 0.1239 | 0.1556 | 0.1955 | 0.2456 | 0.3086 | 0.3876 | 0.4870 | 0.6117 |
| 0.7685 | 0.9654 | 1.2128 | 1.5236 | 1.9141 | 2.4046 | 3.0208 | 3.7949 | 4.7673 |
| 5.9890 | 7.5237 | 9.4517 | 11.8738 | 14.9165 | 18.7390 | 23.5410 | 29.5736 | 37.152 |
| 46.672 | 58.633 | 73.6577 | 92.5331 | 116.245 | 146.034 | 183.457 | 230.469 | 289.53 |
| 363.72 | 456.93 | | | | | | | |

```

C -----
C Porosity
C -----
POROS CON
  0.059

```

```

MOD
41 41 1 20 1 1 = 0.3

```

```

C -----
C Permeability
C -----
KX CON
  8.953e-05

```

```

MOD
41 41 1 20 1 1 = 100000

```

```

KY EQUALS KX
KZ EQUALS KX

```

```

C -----
C Depth
C -----
DEPTH CON
  10000

```

```

C -----
C Thickness
C -----
THICKNESS CON
  200

```

```

C -----
C Relperm
C -----
KRANALYTICAL 1
  0.2 0.2 0.2 0.1      ! Swc Sorw Sorg Sgc
  1 0.5 1              ! krw(Sorw) krg(Swc) kro(Swc)
  2.5 2.5 2 3 1 0.2   ! nw now ng nog (nwg Swcg)

```

```

C -----
C Black oil table
C -----

```

| | | | | | | | | | | | | | | | | | | | | | | | | | | | | | | |
|-----------|-----|-----|------|------|------|------|------|------|------|------|------|------|------|------|------|------|------|------|------|------|------|------|------|------|------|------|------|------|------|------|
| BLACKOIL | 1 | 26 | 30 | SRK | | | | | | | | | | | | | | | | | | | | | | | | | | |
| PRESSURES | 100 | 500 | 1000 | 1200 | 1400 | 1600 | 1800 | 2000 | 2200 | 2400 | 2600 | 2800 | 2900 | 3000 | 3100 | 3200 | 3300 | 3400 | 3600 | 3800 | 4000 | 4200 | 4400 | 4600 | 4800 | 4825 | 5500 | 6000 | 6500 | 7000 |

```

RESERVOIR FLUID
0.00000000
0.00009032
0.00028785
0.72443534
0.09995367
0.04329560

```

0.01200208
 0.01612318
 0.00799159
 0.00604448
 0.01486822
 0.01338211
 0.01085318
 0.00878513
 0.00723370
 0.00595599
 0.00490595
 0.00404363
 0.00333555
 0.00275400
 0.00227619
 0.00188340
 0.00156027
 0.00129424
 0.00107500
 0.00089414
 0.00074477
 0.00062126
 0.00051899
 0.00043420
 0.00235598

SEPARATOR
 440 104
 14.70 60.0

ENDBLACKOIL

C -----
 C Fluid Properties
 C -----

PVTEOS SRK
 250 ! Reservoir temperature (deg F)

| CPT | MW | TC | PC | ZCRIT | SHIFT | AC | PCHOR |
|------|---------|---------|---------|---------|---------|---------|--------|
| H2S | 34.082 | 672.12 | 1299.97 | 0.28292 | 0.10153 | 0.09 | 80.1 |
| N2 | 28.014 | 227.16 | 492.84 | 0.29178 | -0.0009 | 0.037 | 59.1 |
| CO2 | 44.01 | 547.42 | 1069.51 | 0.27433 | 0.21749 | 0.225 | 80 |
| C1 | 16.043 | 343.01 | 667.03 | 0.2862 | -0.0025 | 0.011 | 71 |
| C2 | 30.07 | 549.58 | 706.62 | 0.27924 | 0.05894 | 0.099 | 111 |
| C3 | 44.097 | 665.69 | 616.12 | 0.2763 | 0.09075 | 0.152 | 151 |
| I-C4 | 58.123 | 734.13 | 527.94 | 0.28199 | 0.10952 | 0.186 | 188.8 |
| N-C4 | 58.123 | 765.22 | 550.56 | 0.27385 | 0.11028 | 0.2 | 191 |
| I-C5 | 72.15 | 828.7 | 490.37 | 0.27231 | 0.09773 | 0.229 | 227.4 |
| N-C5 | 72.15 | 845.46 | 488.78 | 0.26837 | 0.11947 | 0.252 | 231 |
| C6 | 83.676 | 921.53 | 473.57 | 0.244 | 0.13422 | 0.252 | 235.82 |
| C7 | 96.986 | 984.11 | 437.78 | 0.24284 | 0.14547 | 0.28777 | 267.77 |
| C8 | 110.671 | 1038.77 | 402.88 | 0.2409 | 0.15739 | 0.32768 | 300.61 |
| C9 | 124.134 | 1087.82 | 370.65 | 0.23727 | 0.17497 | 0.36975 | 332.92 |
| C10 | 137.435 | 1131.48 | 342.84 | 0.23464 | 0.19184 | 0.41118 | 364.84 |
| C11 | 150.672 | 1171.07 | 318.6 | 0.2317 | 0.20799 | 0.45208 | 396.61 |
| C12 | 163.837 | 1207.22 | 297.38 | 0.22867 | 0.2233 | 0.49235 | 428.21 |
| C13 | 176.92 | 1240.4 | 278.73 | 0.22619 | 0.23772 | 0.53195 | 459.61 |
| C14 | 189.918 | 1271.03 | 262.24 | 0.22366 | 0.25121 | 0.57085 | 490.8 |
| C15 | 202.824 | 1299.42 | 247.61 | 0.22116 | 0.26379 | 0.60905 | 521.78 |
| C16 | 215.636 | 1325.84 | 234.57 | 0.21908 | 0.27547 | 0.64654 | 552.53 |

| | | | | | | | |
|------|---------|---------|--------|---------|---------|---------|---------|
| C17 | 228.35 | 1350.51 | 222.89 | 0.21732 | 0.28628 | 0.68333 | 583.04 |
| C18 | 240.964 | 1373.64 | 212.41 | 0.21557 | 0.29626 | 0.71942 | 613.31 |
| C19 | 253.475 | 1395.37 | 202.95 | 0.21387 | 0.30547 | 0.75483 | 643.34 |
| C20 | 265.883 | 1415.85 | 194.39 | 0.21244 | 0.31394 | 0.78956 | 673.12 |
| C21 | 278.188 | 1435.21 | 186.63 | 0.21124 | 0.32173 | 0.82362 | 702.65 |
| C22 | 290.389 | 1453.54 | 179.56 | 0.21007 | 0.32889 | 0.85704 | 731.93 |
| C23 | 302.486 | 1470.94 | 173.1 | 0.20909 | 0.33545 | 0.88981 | 760.97 |
| C24 | 314.481 | 1487.49 | 167.18 | 0.20827 | 0.34148 | 0.92197 | 789.75 |
| C25 | 326.374 | 1503.27 | 161.75 | 0.20748 | 0.34699 | 0.95351 | 818.3 |
| C26+ | 422.424 | 1612.22 | 129.42 | 0.20385 | 0.37814 | 1.19607 | 1048.82 |

BIN

| | H2S | N2 | C02 | C1 | C2 | C3 | I-C4 | N-C4 | I-C5 | N-C5 | C6 | C7 | C8 | C9 | C10 | C11 | C12 | C13 | C14 | C15 | C16 | C17 | C18 | C19 | C20 | C21 | C22 | C23 | C24 | C25 | C26+ | | | | | | |
|------|------|------|------|----|----|----|------|------|------|------|----|----|----|----|-----|-----|-----|-----|-----|-----|-----|-----|-----|-----|-----|-----|-----|-----|-----|-----|------|--|--|--|--|--|--|
| H2S | 0 | | | | | | | | | | | | | | | | | | | | | | | | | | | | | | | | | | | | |
| N2 | 0 | 0 | | | | | | | | | | | | | | | | | | | | | | | | | | | | | | | | | | | |
| C02 | 0.08 | 0.02 | 0 | | | | | | | | | | | | | | | | | | | | | | | | | | | | | | | | | | |
| C1 | 0.07 | 0.06 | 0.12 | 0 | | | | | | | | | | | | | | | | | | | | | | | | | | | | | | | | | |
| C2 | 0.07 | 0.08 | 0.12 | 0 | 0 | | | | | | | | | | | | | | | | | | | | | | | | | | | | | | | | |
| C3 | 0.06 | 0.08 | 0.12 | 0 | 0 | 0 | | | | | | | | | | | | | | | | | | | | | | | | | | | | | | | |
| I-C4 | 0.06 | 0.08 | 0.12 | 0 | 0 | 0 | 0 | | | | | | | | | | | | | | | | | | | | | | | | | | | | | | |
| N-C4 | 0.06 | 0.08 | 0.12 | 0 | 0 | 0 | 0 | 0 | | | | | | | | | | | | | | | | | | | | | | | | | | | | | |
| I-C5 | 0.06 | 0.08 | 0.12 | 0 | 0 | 0 | 0 | 0 | 0 | | | | | | | | | | | | | | | | | | | | | | | | | | | | |
| N-C5 | 0.05 | 0.08 | 0.12 | 0 | 0 | 0 | 0 | 0 | 0 | 0 | | | | | | | | | | | | | | | | | | | | | | | | | | | |
| C6 | 0.03 | 0.08 | 0.12 | 0 | 0 | 0 | 0 | 0 | 0 | 0 | 0 | | | | | | | | | | | | | | | | | | | | | | | | | | |
| C7 | 0.03 | 0.08 | 0.1 | 0 | 0 | 0 | 0 | 0 | 0 | 0 | 0 | 0 | | | | | | | | | | | | | | | | | | | | | | | | | |
| C8 | 0.03 | 0.08 | 0.1 | 0 | 0 | 0 | 0 | 0 | 0 | 0 | 0 | 0 | 0 | | | | | | | | | | | | | | | | | | | | | | | | |
| C9 | 0.03 | 0.08 | 0.1 | 0 | 0 | 0 | 0 | 0 | 0 | 0 | 0 | 0 | 0 | 0 | | | | | | | | | | | | | | | | | | | | | | | |
| C10 | 0.03 | 0.08 | 0.1 | 0 | 0 | 0 | 0 | 0 | 0 | 0 | 0 | 0 | 0 | 0 | 0 | | | | | | | | | | | | | | | | | | | | | | |
| C11 | 0.03 | 0.08 | 0.1 | 0 | 0 | 0 | 0 | 0 | 0 | 0 | 0 | 0 | 0 | 0 | 0 | 0 | | | | | | | | | | | | | | | | | | | | | |
| C12 | 0.03 | 0.08 | 0.1 | 0 | 0 | 0 | 0 | 0 | 0 | 0 | 0 | 0 | 0 | 0 | 0 | 0 | 0 | | | | | | | | | | | | | | | | | | | | |
| C13 | 0.03 | 0.08 | 0.1 | 0 | 0 | 0 | 0 | 0 | 0 | 0 | 0 | 0 | 0 | 0 | 0 | 0 | 0 | 0 | | | | | | | | | | | | | | | | | | | |
| C14 | 0.03 | 0.08 | 0.1 | 0 | 0 | 0 | 0 | 0 | 0 | 0 | 0 | 0 | 0 | 0 | 0 | 0 | 0 | 0 | 0 | | | | | | | | | | | | | | | | | | |
| C15 | 0.03 | 0.08 | 0.1 | 0 | 0 | 0 | 0 | 0 | 0 | 0 | 0 | 0 | 0 | 0 | 0 | 0 | 0 | 0 | 0 | 0 | | | | | | | | | | | | | | | | | |
| C16 | 0.03 | 0.08 | 0.1 | 0 | 0 | 0 | 0 | 0 | 0 | 0 | 0 | 0 | 0 | 0 | 0 | 0 | 0 | 0 | 0 | 0 | 0 | | | | | | | | | | | | | | | | |
| C17 | 0.03 | 0.08 | 0.1 | 0 | 0 | 0 | 0 | 0 | 0 | 0 | 0 | 0 | 0 | 0 | 0 | 0 | 0 | 0 | 0 | 0 | 0 | 0 | | | | | | | | | | | | | | | |
| C18 | 0.03 | 0.08 | 0.1 | 0 | 0 | 0 | 0 | 0 | 0 | 0 | 0 | 0 | 0 | 0 | 0 | 0 | 0 | 0 | 0 | 0 | 0 | 0 | 0 | | | | | | | | | | | | | | |
| C19 | 0.03 | 0.08 | 0.1 | 0 | 0 | 0 | 0 | 0 | 0 | 0 | 0 | 0 | 0 | 0 | 0 | 0 | 0 | 0 | 0 | 0 | 0 | 0 | 0 | 0 | | | | | | | | | | | | | |
| C20 | 0.03 | 0.08 | 0.1 | 0 | 0 | 0 | 0 | 0 | 0 | 0 | 0 | 0 | 0 | 0 | 0 | 0 | 0 | 0 | 0 | 0 | 0 | 0 | 0 | 0 | 0 | | | | | | | | | | | | |
| C21 | 0.03 | 0.08 | 0.1 | 0 | 0 | 0 | 0 | 0 | 0 | 0 | 0 | 0 | 0 | 0 | 0 | 0 | 0 | 0 | 0 | 0 | 0 | 0 | 0 | 0 | 0 | 0 | | | | | | | | | | | |
| C22 | 0.03 | 0.08 | 0.1 | 0 | 0 | 0 | 0 | 0 | 0 | 0 | 0 | 0 | 0 | 0 | 0 | 0 | 0 | 0 | 0 | 0 | 0 | 0 | 0 | 0 | 0 | 0 | 0 | | | | | | | | | | |
| C23 | 0.03 | 0.08 | 0.1 | 0 | 0 | 0 | 0 | 0 | 0 | 0 | 0 | 0 | 0 | 0 | 0 | 0 | 0 | 0 | 0 | 0 | 0 | 0 | 0 | 0 | 0 | 0 | 0 | 0 | | | | | | | | | |
| C24 | 0.03 | 0.08 | 0.1 | 0 | 0 | 0 | 0 | 0 | 0 | 0 | 0 | 0 | 0 | 0 | 0 | 0 | 0 | 0 | 0 | 0 | 0 | 0 | 0 | 0 | 0 | 0 | 0 | 0 | 0 | | | | | | | | |
| C25 | 0.03 | 0.08 | 0.1 | 0 | 0 | 0 | 0 | 0 | 0 | 0 | 0 | 0 | 0 | 0 | 0 | 0 | 0 | 0 | 0 | 0 | 0 | 0 | 0 | 0 | 0 | 0 | 0 | 0 | 0 | 0 | | | | | | | |
| C26+ | 0.03 | 0.08 | 0.1 | 0 | 0 | 0 | 0 | 0 | 0 | 0 | 0 | 0 | 0 | 0 | 0 | 0 | 0 | 0 | 0 | 0 | 0 | 0 | 0 | 0 | 0 | 0 | 0 | 0 | 0 | 0 | 0 | | | | | | |

SEP 1
500 150
14.70 60.0

C -----
C Initialize
C -----

INITIAL

DEPTH GOR
10000 4587

PINIT 4800
ZINIT 10000

ENDINIT

C -----
C Trans. modification to fractures
C -----

MODIFY TX 1.0
40 40 20 20 1 1 * 1
41 41 20 20 1 1 * 1


```

C -----
C Define Wells
C -----
WELL
      I   J   K
PROD  41  1   1

BHP
PROD 500

WELLTYPE
  PROD MCF

PSM
C -----
C Define rate schedules.
C -----
RATE
  PROD 10000

MAPSFREQ 1
MAPSFILEFREQ 1

DT 0.01

TIME 10

TIME 365 30

TIME 2000 100

TIME 3650 365

TIME 7300 3650 ! Simulation time table can be edited as required.

END

```


Appendix B

Simulation Oscillation Problem Analysis

The simulation oscillation problem only occurs in the cases with high matrix permeability, which list on **Table Appendix B-1**. However, not all cases with high matrix permeability exists the simulation oscillation problem. Under the control either by gas rate or total revenue, fracture permeability is restricted to meet the constraint of gas rate or total revenue if its matrix permeability is higher than the reservoir permeability of critical case. In that cases, low-conductivity fracture play as a reservoir damage role which blocks the fluids flow from the reservoir's matrix to the horizontal wellbore.

| Case No. | Simulation Controlling type | GOR _i scf/STB | k _m mD | k _f mD |
|----------|-----------------------------|--------------------------|-------------------|-------------------|
| 1 | Gas rate | 3,000 | 5 | 0.1972 |
| 2 | Gas rate | 3,000 | 10 | 0.1923 |
| 3 | Gas rate | 10,000 | 5 | 0.0907 |
| 4 | Revenue | 1,000 | 0.051518 | 0.051518 |
| 5 | Revenue | 10,000 | 1 | 0.032707 |

The problem of oscillation is caused by model's gridding structure, which finest grids system nearby the fracture tip (41, 20, 1). But the producer is locates at the joint of wellbore and fracture (41, 1, 1), the grids size around producer is not gradual grow in y direction. In high matrix permeability cases, the fracture permeability is reduced to limit the well's production, and the fracture works as a damage factor for production.

In order to remove the simulation oscillation problem, well perforation location is relocated to the fracture tip (41, 20, 1), which is show in **Fig. Appendix B-1**. This relocation of perforation makes the grids nearby producer changed gradually and all of the smallest grids are close to the perforation grids. Take the case of GOR_i=3,000 scf/STB and with 5 mD reservoir matrix permeability as the example, the simulation

oscillation problem exists in the early 200 days if the producer is perforated at the joint. As seen in **Fig. Appendix B-2**, the oscillation problem in the early 200 days is omitted after we move the perforation location to the fracture tip. Two parameters are changed to meet the gas rate constraint: productivity index of well and the fracture permeability. In the case with matrix permeability is 5 mD, well's production index is changing from 0.07389 RB-CP/D-PSI to 200 RB-CP/D-PSI, and the fracture permeability is changed from 0.1792 mD to 0.242 mD.

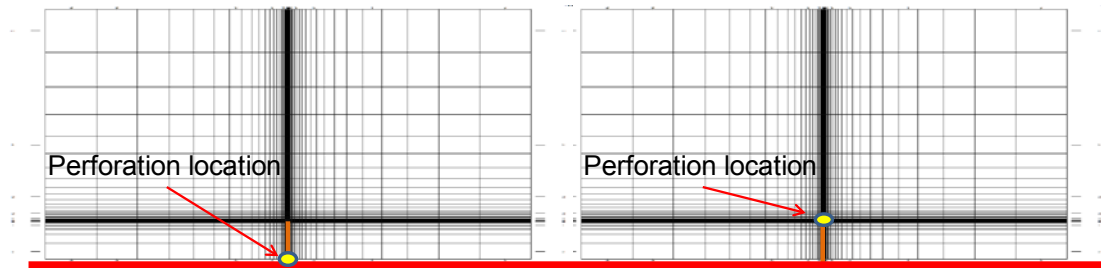


Fig. Appendix B-1—Relocation the well's perforation location from wellbore to fracture tip.

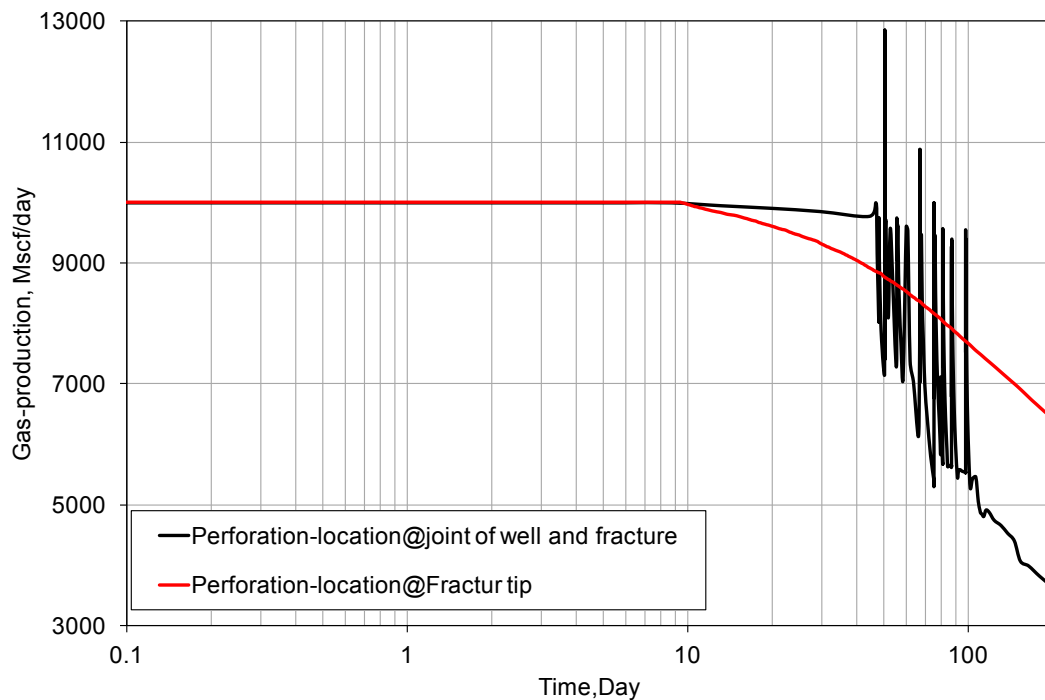


Fig. Appendix B-2—Comparison of simulation results between two cases with different perforation location.

In summary, the simulation oscillation problem only exists in some cases with high matrix permeability and can be resolved by changing the perforation position. However, the productivity index and fracture permeability need to be changed as well.